



Project No. 608930

FP7-SMARTCITIES-2013

OPTimising Hybrid Energy grids for smart cities

WP3 Monitoring and System Analysis

Deliverable 3.3.2

Comparison of weather forecast methods and evaluation of sophisticated climate data for the demonstration sites

M. Schroedter-Homscheidt, E. Borg, N. Killius, D. Jahncke,
S. Jung, M. Kosmale, L. Kraus, F. Renke, F. Schnell, H.-H. Vajen (DLR)
with contribution from H. Ruf (HS Ulm)

Version:	1.0
Due Date:	29 Feb 2016
Submission Date:	29 Feb 2016
Lead Coordinator:	DLR

Copyright

@ Copyright 2013-2016 The OrPHEuS Consortium

Consisting of

Coordinator	WIP – Renewable Energies (WIP)	Germany
Participants	Hochschule Ulm (HSU)	Germany
	Stadtwerke Ulm GmbH (SWU)	Germany
	Technische Universität Wien (TUW-EEG)	Austria
	Austrian Institute of Technology (AIT)	Austria
	Deutsches Zentrum für Luft- und Raumfahrt e.V. (DLR)	Germany
	NEC Europe Ltd. (NEC)	UK
	Lulea Tekniska Universitet (LTU)	Sweden
	Skellefteå Kraft (SKR)	Sweden

This document may not be copied, reproduced, or modified in whole or in part for any purpose without written permission from the OrPHEuS Consortium. In addition to such written permission to copy, reproduce, or modify this document in whole or part, an acknowledgment of the authors of the document and all applicable portions of the copyright notice must be clearly referenced.

All rights reserved.

This document may change without notice.

Deliverable Description

Abstract: The main scope of the Deliverable D3.3.2 (Task 3.3 Provisioning of sophisticated level of meteorological information, sub task ST 3.3.2) is to prepare a recommendation on additional meteorological information needed for different use cases. Several issues to be addressed had identified within the activities carried out during the 1st reporting in task 3.3 under the sub-task 3.3.1. Available meteorological data and forecasts are obtained. Ulm is a case for an electrical grid with an increasing amount of volatile renewable energies from photovoltaics while Skellefteå is dominated by a district heating system depending on air temperature and solar irradiance.

Key Words: ICT, smart cities, hybrid energy grid, energy saving, demonstrations, smart grid, energy control, monitoring

Document History

Version	Date	Authors	Description
0.1	2015-11-30	DLR	D3.3.2 Draft of deliverable
0.2	2016-02-17	DLR	Version for internal review
0.3	2016-02-28	DLR	Final Version
1.0	2016-03-11	WIP	Final Revision

Dissemination Level

Dissemination Level		
PU	Public	X
PP	Restricted to other program participants (including the Commission Services)	
RE	Restricted to a group specified by the Consortium (including the Commission Services)	
CO	Confidential, only for members of the consortium (including the Commission Services)	

Executive Summary

The OrPHEuS project elaborates a Hybrid Energy Network Control System for Smart Cities implementing novel cooperative local grid and inter-grid control strategies for the optimal interactions between multiple energy grids by enabling simultaneous optimization for individual response requirements, energy efficiencies and energy savings as well as coupled operational, economic and social impacts. Starting from existing system setups in two cities, enhanced operational scenarios are demonstrated for today's market setup, as well as for future market visions.

The main scope of the Deliverable D3.3.2 (Task 3.3 Provisioning of sophisticated level of meteorological information, sub task ST 3.3.2) is to prepare a recommendation on additional meteorological information needed for different use cases. Several issues to be addressed had identified within the activities carried out during the 1st reporting in task 3.3 under the sub-task 3.3.1. Available meteorological data and forecasts are obtained. Ulm is a case for an electrical grid with an increasing amount of volatile renewable energies from photovoltaics while Skellefteå is dominated by a district heating system depending on air temperature and solar irradiance.

Each chapter in this report covers a specific stakeholder need as being discussed with project partners. We cover the following application areas in our analysis:

- Modeling and nowcasting of solar irradiance for Ulm
- Solar variability on the regional level at DEMMIN
- Understanding failures in heat demand modeling on the whole infrastructure level in Skellefteå
- Understanding outliers in heat demand modeling on sub-grid level in Skellefteå
- Dealing with non-perfect and real forecasts for technical system modeling
- Meteorological forecasts for business case development and economic system modeling

Each chapter summarizes and updates shortly the information given in D3.3.1 on stakeholders and their needs, the user system, and user requirements with respect to meteorological information.

Based on this knowledge of the user system, a sophisticated level of meteorological information is defined. This consists of a review on available meteorological information, on what needs to be investigated to address the stakeholder's requirements, and what kind of meteorological data or forecasts can be obtained by the partners with help of DLR. This review is done from the perspective from the point of view of a hybrid energy grid stakeholder.

It has to be noted that this does not include the actual delivery of meteorological forecasts to partners – such an approach would be typically illegal according to each national meteorological service's data policy rules. Nevertheless, DLR is investigating especially the access to forecast data sets being available e.g. in the research departments without being available to the partners on the standard data flows. Also, DLR helped with questions occurring when getting meteorological data (e.g. reading routines, geographical grids, meaning of meteorological terms).

Overall, this deliverable contributes to the Scientific and Technical Objective (STO) No. 2 and especially the 'evaluation of sophisticated level of meteorological information'.

Administrative Overview

Task Description

Task 3.3 and especially sub task 3.3.2 investigates the necessary weather parameters for different application areas being investigated in OrPHEuS. It reviews the existing state of the art of information. Options for extended or more sophisticated meteorological information are discussed with focus on the demonstration site assessments. The activities in sub task 3.3.2 can afterwards be used in WPs 3, 4 and 5.

Relation to the Scientific and Technological Objectives

PKI No.	Objective/expected result	Indicator name	STO	Deliverable	MS	Expected Progress		
						Year 1	Year 2	Year 3
5	Description of the meteorology and identification of improvement potentials and information gaps at the demo sites	Meteorology and ID of improvements	STO2	D3.3.2				Draft M27 Final M30
7	Definition of sophisticated level of meteorological information	Meteorological information	STO2	D3.3.2				Draft M27 Final M30
20	Comparison of weather forecast methods	Comparison	STO2	D3.3.2				Draft M27 Final M30

Relations to activities in the Project

Relations to other activities in the project:

- Inputs:
 - Site description as provided in WP2.
 - D2.1 'Report on technical, economical and social patterns of energy service provision'
 - D2.2 'Report on multi-dimensional framework for smart hybrid energy network analyses'
 - D2.3 'Use cases'
 - D3.3.1 'Description of the meteorology and identification of improvement potentials and information gaps at demonstration site'
 - D3.4.2 'Validation of Metrics for the Comprehension of real-life data with virtual information'
 - D4.2 on scenario definition
 - D5.2 'Algorithms for cooperative control strategies for hybrid energy networks'

- **Outputs:**

Partners in WP3 will use the outcomes for their own analysis.

Partners in WP4 and WP5 can use the outcomes for a realistic design of use cases based on available/accessible meteorological information.

Partners in WP7 can use the information given for their assessment.

- **Explain how possible feedback from previous EC review is addressed.**

The previous EC review accepted D3.3.1 and the work undertaken as presented. Therefore, there is no additional feedback from EC taken into account. The DOW is still the valid basis.

Terminologies

Definitions

Historical observation: measured data for a certain past period

Near real time observation: measured data for the current point in time

Historical forecast: forecast at a certain time in the past

(Near real time) forecast: forecast in the current point in time

Nowcasting: Forecast with a very short time horizon of a few hours

Calibration of models = model tuning

Parameter = description of a system characteristic

Variable = state of a system

Abbreviations

CAMS	Copernicus Atmosphere Monitoring Service
CET	Central European Time
CHP	Combined Heat and Power plant
COSMO	Consortium for Small-Scale Modelling
COSMO-DE	Local model run by COSMO, covering Germany and parts of surrounding countries.
COSMO-DE- EPS	Like COSMO-DE, but Ensemble Prediction.
COSMO-EU	Like COSMO-DE, but covering whole Europe and with coarser resolution.
DEMMIN	Durable Environmental Multidisciplinary Monitoring Information Network – demo site located in northeastern Germany
DLR	Deutsches Zentrum für Luft- und Raumfahrt e.V. – German

	Aerospace Centre.
DWD	The German Meteorological Service (Deutscher Wetterdienst)
ECMWF	European Centre for Medium-Range Weather Forecasts
ENS	ECMWF forecast ensemble.
EPS	Ensemble Prediction System
ERA	ECMWF Re-Analysis.
EweLine	Development of innovative weather and power forecast models for the grid integration of weather dependent energy sources. A DWD project to develop NWP for special renewable energy purposes.
GHI	Global Horizontal Irradiance, measured in W/m ²
GLAMEPS	Grand Limited Area Ensemble Prediction System. Ensemble NWP run at SMHI.
H2G	Heat to Grid
HarmonEPS	Ensemble Prediction System based on HARMONIE.
HARMONIE	Hirlam Aladin Regional/Mesoscale Operational NWP In Europe.
HIRLAM	High Resolution Limited Area Model
HSU	Hochschule Ulm.
MACC-II	Monitoring Atmosphere and Climate. 2 nd period of the project.
MS	Milestone.
MSG	Meteosat Second Generation.
NCEP	National Centers for Environmental Prediction. Parts of the US National Weather Service.
NEC	NEC Europe Ltd.
NWP	Numerical Weather Prediction.
QC	Quality Control.
R&D	Research and Development department.
SCENES	Operational scheme from EUMETSAT to derive cloud information from satellite images.
SEVIRI	Spinning Enhanced Visible and Infrared Imager. Main instrument carried by the MSG satellites.
SKR	Skellefteå Kraft AB
SMHI	The Swedish Meteorological and Hydrological Institute.
SSRD	Solar Surface Radiation
STO	Scientific & Technological Objective.
SWU	Stadtwerke Ulm/Neu-Ulm Netze GmbH
TERENO	Terrestrial Environmental Observatories
TUW-EEG	Technische Universität Wien.
UTC	Universal Time, Coordinated.
WMO	World Meteorological Organization.
WP	Work Package.

Table of Contents

1.	Introduction.....	11
1.1	Purpose of the Document	11
1.2	Scope of the Document.....	11
1.3	Structure of the Document	11
2	Application area – Modeling of solar irradiance for Ulm	12
2.1	Stakeholders and their needs.....	12
2.1.1	User system	12
2.1.2	User requirements.....	12
2.1.3	Demo site.....	12
2.1.4	Relevant use cases and control problems	12
2.2	Developments performed	13
2.2.1	Grid status modeling	13
2.2.2	Set up satellite processing for the nowcasting scheme	13
2.2.3	Evaluation of COSMO-DE.....	15
3	Application area – Solar sub-grid/pixel variability on the regional level at DEMMIN.....	18
3.1	Stakeholders and their needs.....	18
3.1.1	User system	18
3.1.2	User requirements.....	19
3.1.3	Demo site.....	19
3.1.4	Relevant use cases and control problems	19
3.2	Work performed.....	19
3.2.1	DEMMIN study site.....	19
3.2.2	Setup of additional stations.....	21
3.2.3	Data preparation	26
3.2.4	Satellite-based structural characterization of DEMMIN sites	30
3.2.5	Satellite-based variability characterization	37
3.2.6	Ground observation variability.....	41
4	Application area – Understanding failures in heat demand modeling on the whole infrastructure level in Skellefteå.....	43
4.1	Stakeholders and their needs.....	43
4.1.1	User system	43
4.1.2	User requirements.....	43
4.1.3	Demo site.....	44
4.1.4	Relevant use cases and control problems	44

4.2	Work performed.....	44
4.2.1	Study rationale	44
4.2.2	Evaluation of SMHI/ECMWF forecast accuracy for Skellefteå	45
4.2.3	Assessment of SKR measurements and measurement sites (including Balderskolan) .	50
4.2.4	Study on meteorological Parameters influencing heat demand in Skellefteå	54
4.2.5	Study on failures in temperature predictions in Skellefteå.....	63
5	Application area – Understanding outliers in heat demand modeling on sub-grid level in Skellefteå	66
5.1	Stakeholders and their needs.....	66
5.1.1	User system	66
5.1.2	User requirements.....	67
5.1.3	Demo site.....	67
5.1.4	Relevant use cases and control problems.....	67
5.2	Work performed.....	67
5.2.1	Set up additional measurement points.....	73
5.2.2	Differences in heat demand between the two borders of the river	73
6	Application area – Dealing with non-perfect and real forecasts for technical system modeling .	75
6.1	Stakeholders and their needs.....	75
6.1.1	User system	75
6.1.2	User requirements.....	75
6.1.3	Demo site.....	76
6.1.4	Relevant use cases and control problems.....	76
6.2	Work performed.....	76
6.2.1	ECMWF’s deterministic forecast	77
6.2.2	SMHI deterministic forecast.....	80
6.2.3	DWD deterministic forecast	82
6.2.4	Overview over the available models	85
6.3	Consultations NEC / TUW: getting temperature data for scenario basis.....	85
6.3.1	Dataset advices.....	86
6.3.2	Identification of winter cases	86
6.3.3	Advice for further possibilites	87
6.3.4	Interpolation of data to 15-min time resolution	87
7	Application area – Meteorological forecasts for business case development and economic system modeling	87
7.1	Description of use of meteorological information	87

7.1.1	Stakeholders and their needs.....	87
7.1.2	State of the art	92
7.2	Work performed.....	92
7.2.1	Ensemble data	92
7.2.2	ECMWF Ensemble data	97
7.2.3	SMHI ensemble forecast	98
7.2.4	DWD ensemble forecast.....	99
7.3	Consultations COSMO-DE-EPS for HSU	104
7.3.1	Data characteristic to be considered.....	104
7.3.2	Content COSMO-DE-EPS subset data	105
8	Conclusions.....	107
9	Bibliography.....	108
10	Disclaimer	111
11	Contacts.....	112

1. Introduction

1.1 Purpose of the Document

The OrPHEuS project elaborates a Hybrid Energy Network Control System for Smart Cities implementing novel cooperative local grid and inter-grid control strategies for the optimal interactions between multiple energy grids by enabling simultaneous optimization for individual response requirements, energy efficiencies and energy savings as well as coupled operational, economic and social impacts. Starting from existing system setups in two cities, enhanced operational scenarios are demonstrated for today's market setup, as well as for future market visions. The purpose of this document is to understand user needs and requirements and to couple this understanding to the knowledge of available information from the meteorological sector.

This document is mainly targeted at the OrPHEuS project partners who work either at the demonstration sites or prepare for technical or economic simulations of the demo sites.

Some application areas for meteorological information apply to both demo sites. Therefore, we have chosen an order by application area, together with giving reference where and for what use case each chapter has relevance.

1.2 Scope of the Document

The main scope of the document is to prepare a recommendation on additional meteorological information needed for different use cases. Several issues to be addressed had identified within the activities carried out during the 1st reporting in task 3.3 under the sub-task 3.3.1. Available meteorological data and forecasts are obtained. Ulm is a case for an electrical grid with an increasing amount of volatile renewable energies from photovoltaics while Skellefteå is dominated by a district heating system depending on air temperature and solar irradiance.

It has to be noted that this document and its underlying work package does not include the actual delivery of meteorological forecasts to partners – such an approach would be typically illegal according to each national meteorological service's data policy rules. Nevertheless, DLR is investigating especially the access to forecast data sets being available e.g. in the research departments without being available to the partners on the standard data flows. Also, DLR started to negotiate low-cost data access for partners and helped with technical questions occurring.

1.3 Structure of the Document

Each chapter in this report covers a specific stakeholder need as being discussed with project partners. We cover the following application areas in our analysis:

- Modeling and nowcasting of solar irradiance for Ulm
- Solar sub-grid/pixel variability on the regional level at DEMMIN
- Understanding failures in heat demand modeling on the whole infrastructure level in Skellefteå
- Understanding outliers in heat demand modeling on sub-grid level in Skellefteå
- Dealing with non-perfect and real forecasts for technical system modeling
- Meteorological forecasts for business case development and economic system modeling

2 Application area – Modeling of solar irradiance for Ulm

2.1 Stakeholders and their needs

2.1.1 User system

There is the need for an increased knowledge in utilities about the investment for the grid planning due to rising decentralized energy input. Additionally, near real time information is needed for the operation of low voltage grids under larger solar shares.

The analysis of the influence of solar power in local electricity grids has generally been done so far only with grid models without real meteorological input. The quantification of realistic local levels of solar radiation values is still an ongoing open question. This applies mainly for the assessment of the grid status in a historical time series for grid planning purposes. Another requirement being expected in future a very short term forecast of solar radiation – which is also called a nowcasting system. This is related to the second unknown parameter, the actual load profile in an area with larger solar shares. Dealing with both unknowns appropriately, would improve an accurate grid planning and reduce operational risks. A method to couple satellite-based irradiances with the modeling of the electrical system has been derived in collaboration with HS Ulm.

2.1.2 User requirements

Parameters needed include

- Irradiance
- Ambient temperature
- Wind speed
- Snow cover

The spatial resolution is on the one hand the area average of a low voltage transformer as operated in the test area at the demo site. On the other hand, individual houses or large PV installations need to be covered with individual data.

Temporal resolution should be between 5 and 15 minutes.

Ambient temperature, wind speed, and snow cover is taken out of numerical weather prediction analysis or forecast fields. Here, we concentrate on irradiances from ground and satellite-based observations. Other project partners investigate control strategies based on the use of numerical weather prediction, which may serve as an additional source of irradiances.

2.1.3 Demo site

This application is of main interest for the Ulm demo site. In Skellefteå, the solar share is not significant enough to justify a short term forecasting (nowcasting) system.

2.1.4 Relevant use cases and control problems

Use cases: 2 (Single- vs. multi-utility generation and customer supply), 3 (Optimal asset management), 4 (Maximize remote self-generation), 6 (Special extreme situations)

Control setup 3 ('Green community')

2.2 Developments performed

2.2.1 Grid status modeling

A tool is being currently developed at HSU that allows the DSO to calculate the load flow and voltage at the low voltage transformer. Additionally, it quantifies the impact on low voltage distribution grids from a high penetration of photovoltaic power systems. The product is based on a roof potential analysis, satellite images and meteorological data in combination with the grid structure, the load profiles and the electricity consumption of households. A diagnosis tool uses irradiances from satellite and is compared against feed-in power measurements. A paper on 'Quantifying Residential PV feed-in power in low voltage grids based on satellite-derived irradiance data' by Ruf, Schroedter-Homscheidt, Heilscher and Beyer is under review at the Solar Energy journal (Ruf et al., 2015b). More details are described in Ruf et al. (2015a, also published as D3.4.2).

This development allows simulations of the grid status and the solar surplus based on historical irradiance time series as provided by CAMS/Heliosat-4 and assuming nowadays or future PV shares. It has been applied on real data and submitted to peer-review. Within respect to the OrPHEuS DOW this work has been completed fully.

2.2.2 Set up satellite processing for the nowcasting scheme

In order to derive solar irradiance for nowcasting, a separate satellite-based scheme (Fig. 2.1) is needed. Numerical weather prediction can be used for forecasting (as under investigation by other partners in OrPHEuS), but the nowcasting time range for the next 1-2 hours can't be covered by NWP methods.

HSU is operating already a satellite reception system, which acquires raw MSG SEVIRI satellite images in native EUMETSAT HRIT format.

For the estimation of surface solar irradiance from MSG, using physical models of radiative transfer, the atmospheric state must be a known prerequisite. While aerosols, water vapor and ozone forecasts will be taken in future from the publicly available Copernicus Atmosphere Monitoring Service (CAMS), clouds and snow information is retrieved in near-real-time from Meteosat Second Generation.

Cloud parameters are derived using the AVHRR Processing scheme Over cLOUDs Land and Ocean (APOLLO, Kriebel et al., 1989 and 2003) operated within the SCENES software. APOLLO discretizes all pixels into four different groups called cloud-free, fully cloudy, partially cloudy and snow/ice, before deriving physical properties. Within APOLLO, clouds are categorized into three layers according to their top temperature. Optically thin ice phase clouds (cirrus) are detected separately. In each fully cloudy pixel, cloud optical depth, liquid/ice water path and emissivity can be derived. Cloud optical depth is also interpolated to partially cloudy pixels. Additionally, cloud physical parameters deriving the overall situation e.g. with respect to scatteredness are derived. The APOLLO scheme has been updated scientifically towards a probabilistic cloud masking recently. In that process it was also transferred to linux- and Windows - based systems, which is a pre-requisite to run it on HS Ulm computers. The new scheme has been published recently (Klüser et al., 2015). H. Ruf obtained a short training on the use of APOLLO_NG already. The software will be transferred to HS Ulm.

Once all input data is available, irradiances can be derived with the Heliosat-4 scheme (chapter 9 in Espinar et al., 2014) and coupled with a nowcasting based on optical flow methods as e.g. implemented in Matlab libraries. The operationally used Heliosat-4 version of the Copernicus service has been recently validated thoroughly in Qu et al. (2015). DLR has set up a separate code to more easily transfer Heliosat-4 to partners like HS Ulm as the operational CAMS code is not easy accessible or transferable. The Heliosat-4 code version is made available as well.

For the actual nowcasting another additional module has been investigated which can be used as alternative for optical flow methods. For this purpose a nowcasting scheme as used for concentrating solar power plants in the South of Europe has been tested. Currently, the results are disappointing with respect to global irradiances.

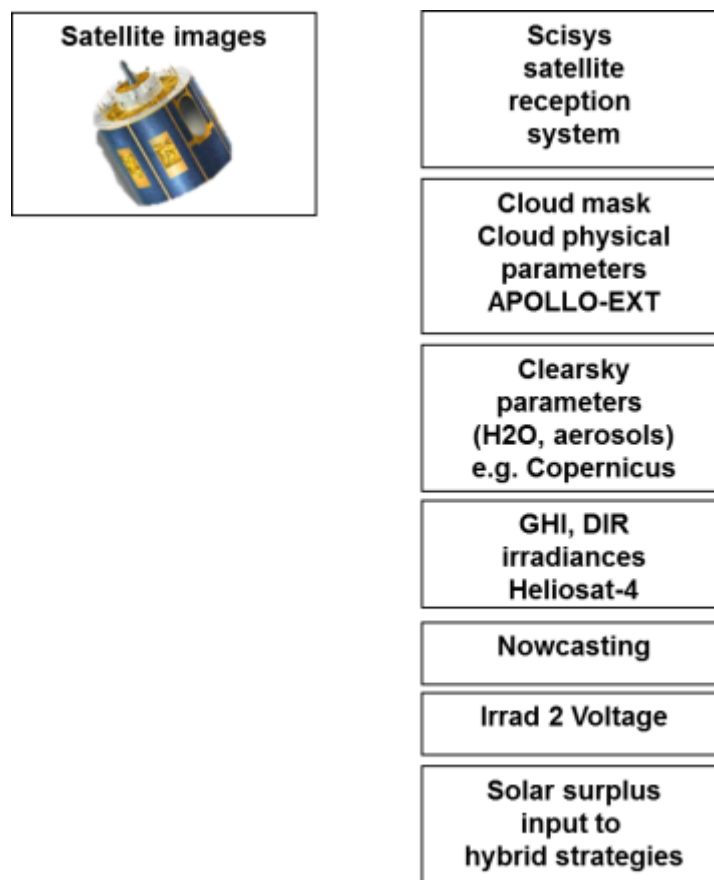


Fig. 2-1: Near real time satellite based nowcasting of solar irradiances and the solar surplus

Finally, the tool as described in Ruf et al. (2015) calculates voltage and finally solar surplus input for hybrid strategies. This approach allows the nowcasting of voltage and surplus solar energy. Currently, the nowcasting of the irradiances is still not working as good as expected.

It has to be noted, that Stadtwerke Ulm/Neu-Ulm Netze GmbH has declared the monitoring capability (section 2.2.1 and D3.4.2) as their highest priority as the use of nowcasting schemes is only expected once a change in the regulation/legislation will re-distribute the responsibility for the nowcasting to the DSO again. Such a change is expected but not existing at the moment.

2.2.3 Evaluation of COSMO-DE

HS Ulm has used the methodology of D3.4.2 and applied the simulation of PV feed-in-power to COSMO-DE forecasts for the period 10 April – 30 November 2014. We include the results here in D3.3.2.

Fig. 2-2 compares the day 1 forecasted (00 UTC run, 24 hours forecast lag, 15 min resolved) versus the measured GHI values for daytime values. For cloudy skies (low kc values given as blue colors), COSMO overestimates GHI strongly, while for clear sky (large kc values) it systematically underestimates. The RMSE is given as function of the day and for various spatial averaging of COSMO-DE. Various spatial smoothing methods for up to 5 and also for 49 grid boxes of the COSMO-DE forecasts have been tested. Results are given in Table 2-1. Differences of smoothing decisions are more visible in the GHI than in the PV feed-in power. For PV feed-in power both GHI and temperature are relevant and errors obviously compensate.

Table 2-1: Statistical measures for COSMO-DE evaluations

	COSMO-DE 00-UTC				MACC-RAD
	1x1	3x3	5x5	49x49	
ME [W/kWp]	48,9	48,6	48,7	52,5	48,4
RMSE [W/kWp]	147,7	146,1	144,5	140,1	114,3
STDV [W/kWp]	139,4	137,8	136,0	129,9	103,5

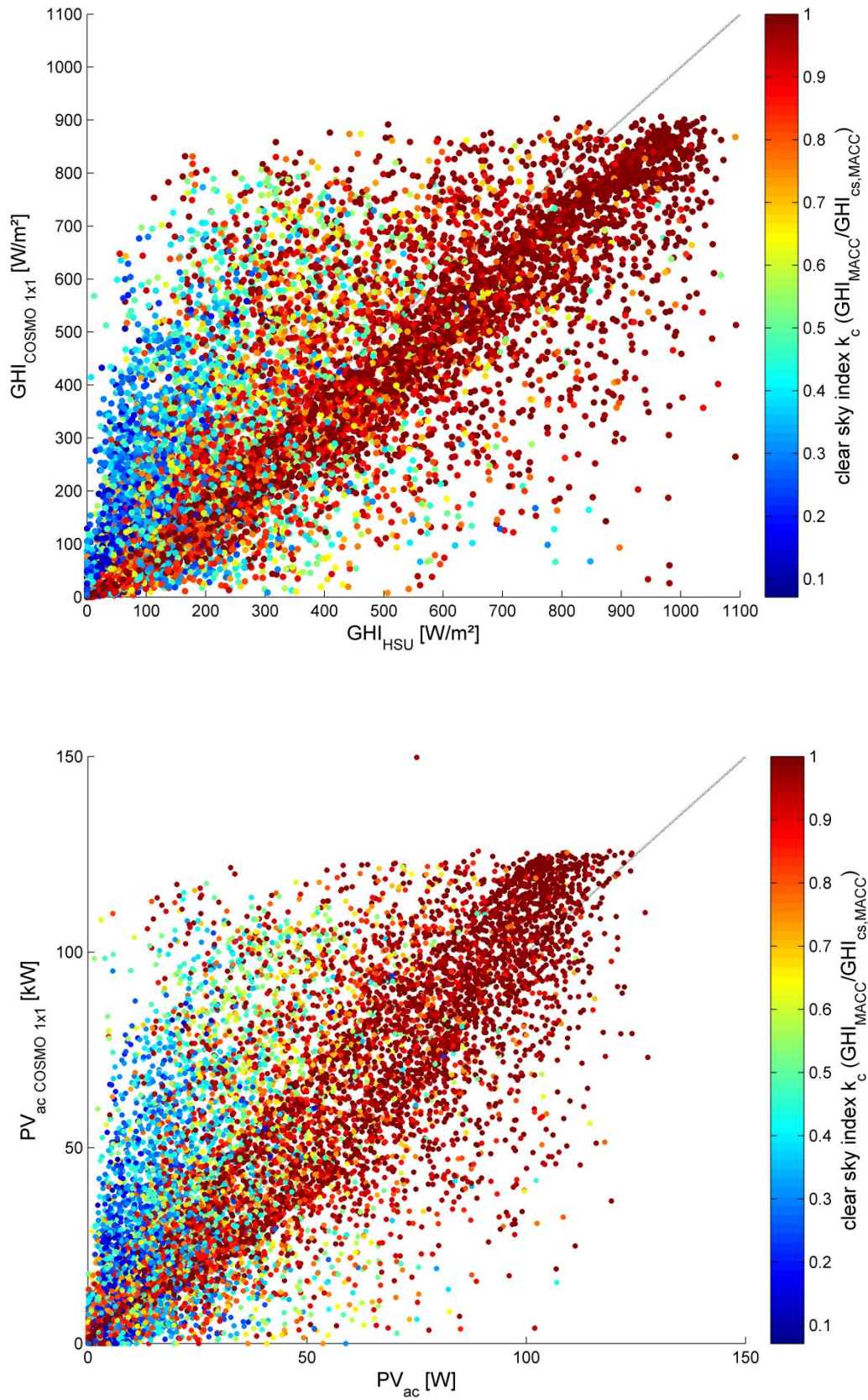


Fig. 2-2: Comparison of COSMO-DE based GHI vs. measured GHI at the HS Ulm location (upper) and for the feed-in power (lower panel)

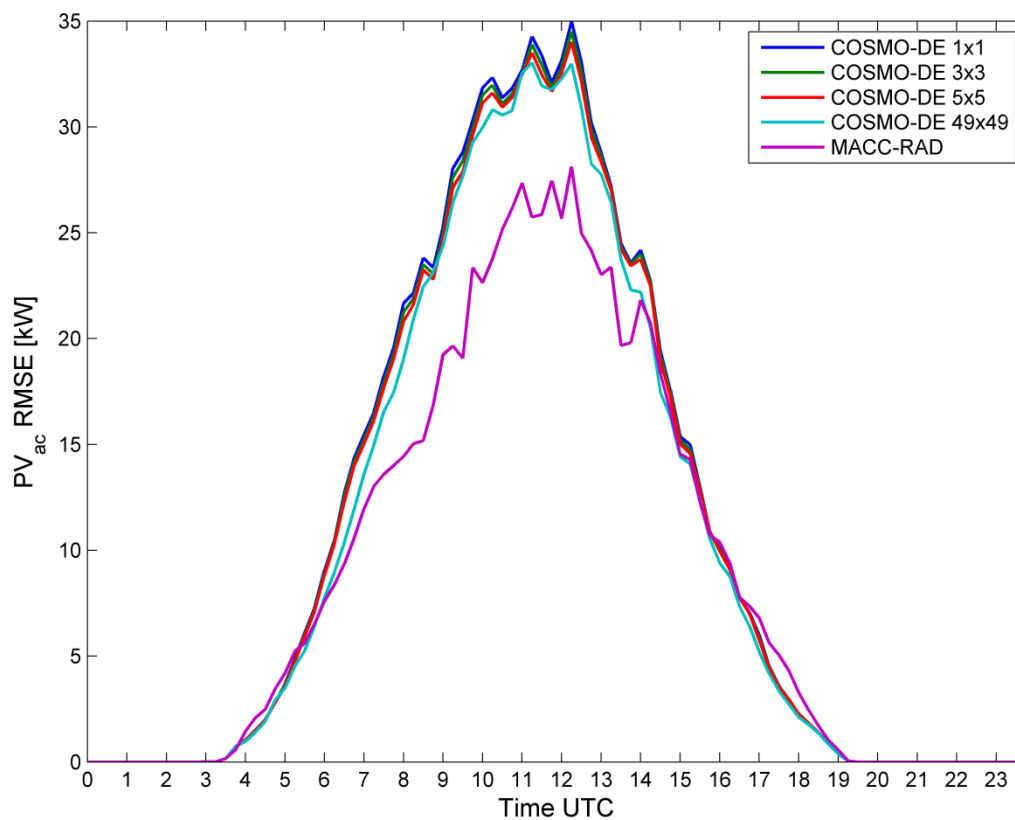
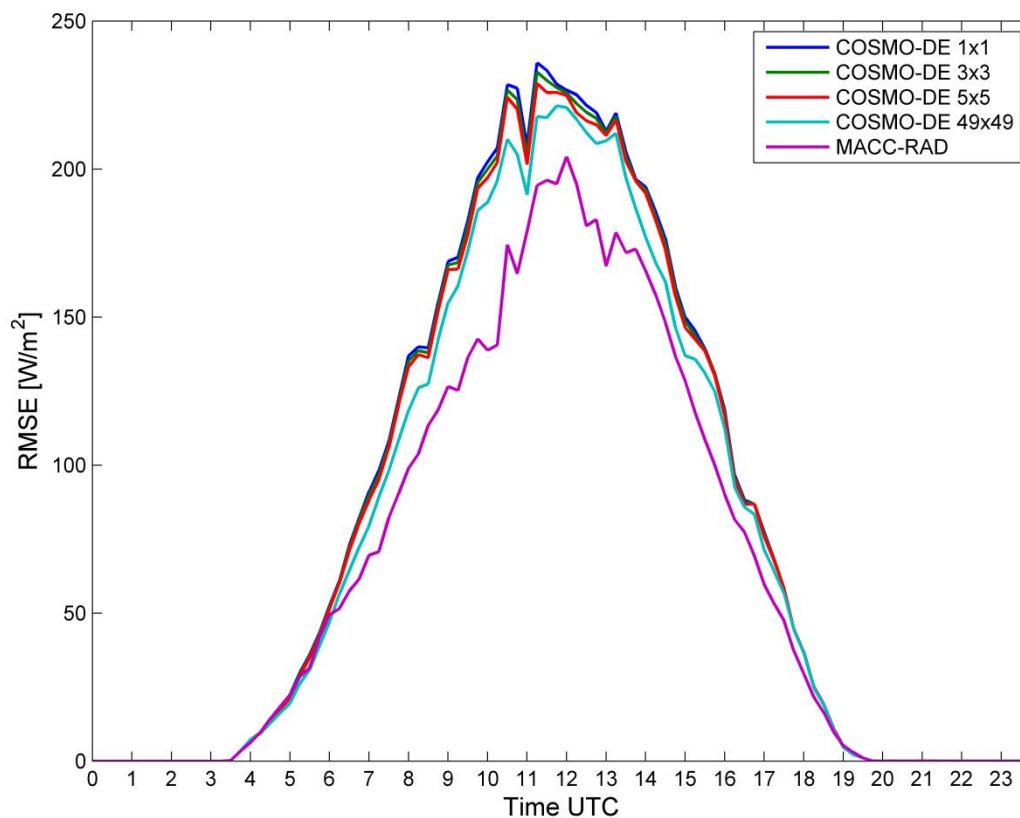


Fig. 2-3: Comparison of COSMO-DE based GHI RMSE vs. measured GHI RMSE at the HS Ulm location (upper) and for the feed-in power (lower panel)

3 Application area – Solar sub-grid/pixel variability on the regional level at DEMMIN

3.1 Stakeholders and their needs

3.1.1 User system

Stakeholders as SWU would like to model the photovoltaic production of each individual PV producer in their area. We know from spatially high resolving satellite imagery and also from personal experience, that clouds often have a size covering the area of e.g. a road and the houses around. Nevertheless, typical satellite-based solar irradiance time series are available on a typically 3x5 to 5x6 km² pixel scale. Fig. 3-1 illustrates the distribution of satellite pixels around an area of interest for OrPHEuS as a demo site.

Also, transformers in medium voltage or high voltage grids integrate the solar production on a similar scale. On the other hand, the spatial integration scale of low voltage transformers covers a smaller area and in the other extreme case, any ground based measurement system provides single point measurements only. Besides these two spatial ranges, we normally don't have any information. We don't know about the typical spatial variability inside a pixel or a transformer area. We only know that a highly variable temporal feature is observed reflecting an existing spatial variability. To investigate the typical pattern and strategies to assess this variability, measurements of neighboring pixels and inside a satellite pixel are needed.

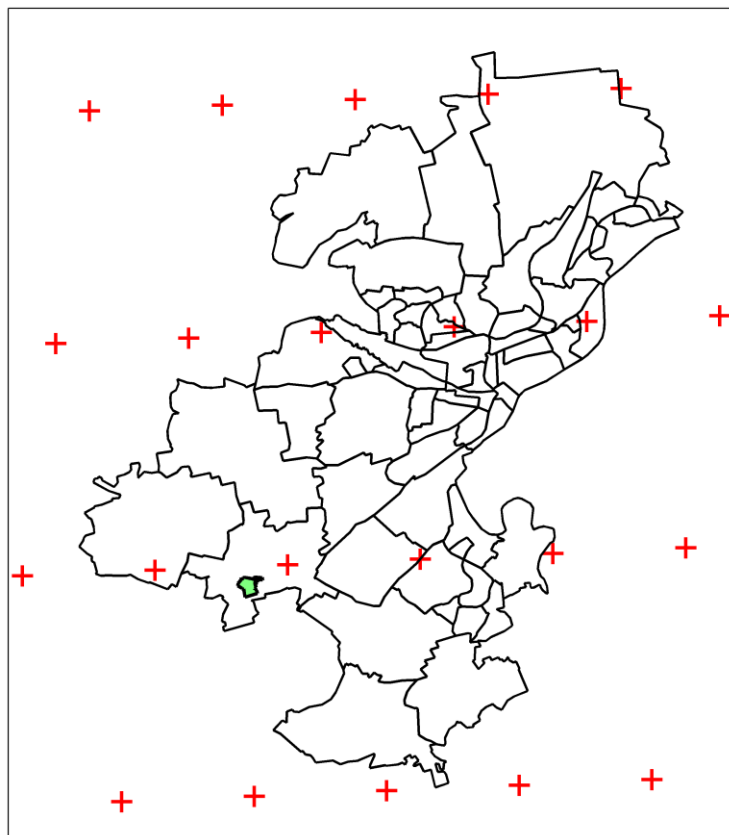


Fig 3-1: Location of an Ulm demo site Einsingen (green) with the nearest satellite pixel center and the neighboring satellite pixel centers (red)

3.1.2 User requirements

Users require knowledge on how the GHI variability inside a forecast model grid box can be quantified.

3.1.3 Demo site

This application is of main interest for the Ulm demo site, but there is no suitable measurement network available in Ulm – therefore, the assessment will be done at the DEMMIN demo site. In Skellefteå, the solar share is not significant enough and the thermal inertia in heat demand control is too large - therefore, the sub-grid or sub-pixel variability is only of academic interest but not of practical usability for heat demand control projects.

3.1.4 Relevant use cases and control problems

Use cases: 2 (Single- vs. multi-utility generation and customer supply), 3 (Optimal asset management), 4 (Maximize remote self-generation), 6 (Special extreme situations)

Control setup 3 ('Green community')

3.2 Work performed

3.2.1 DEMMIN study site

The observatory DEMMIN (Durable Environmental Multidisciplinary Monitoring Information Network) is a durable Earth observation demo site of the Earth Observation Center inside DLR for the calibration and validation of remote sensing mission, sensors, data, and remote sensing based value added information products. The demo site has been established in 1999 closely linked to a cooperation of DLR and the IG Demmin, an association of local farmers.

The calibration and validation test site DEMMIN (Durable Environmental Multidisciplinary Monitoring Information Network) is located approx. 180 km north of Berlin in the federal state Mecklenburg-Western Pomerania. The upper left corner of the is 54°05'N, 12°42'E the lower right corner 53°41'N, 13°30'E (see fig. 3-2). The German lowland landscape is formed during the Pleistocene especially during the Pomeranian stage. The north-east of DEMMIN is dominated by a flat end moraine (Vorpommersches Flachland), whereas the south-east of the test site is dominated by the hilly ground moraine of Mecklenburg Lake District (Rückland der Mecklenburgischen Seenplatte). The altitudinal range within the test site is around 80 m with some slopes of considerable gradients (12°) along the Tollense River in the south eastern part of the test site (Borg et al., 2009).

The climate conditions are represented by long-term measurements by the DWD weather station Demmin (between 1961 and 1990, 53° 54 'north, 13° 01' east, height above NN: 17 m) and the climate station Teterow (53° 45 'north, 12° 37' east, height above NN: 46 m). Due to micro-relief, climate conditions may vary significantly on a local scale (Borg et al., 2009).

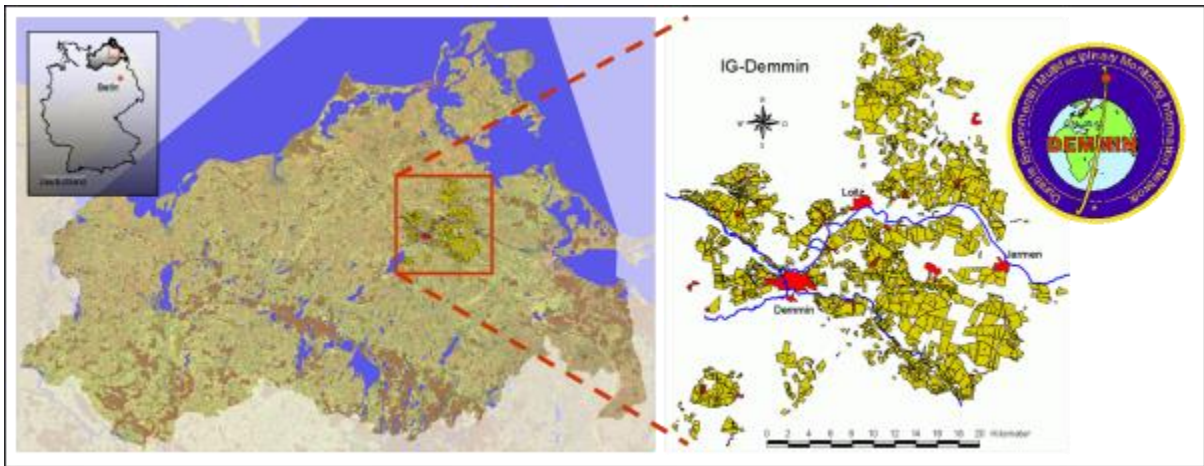


Fig. 3-2: Location of DEMMIN demo site (Borg et al., 2014)

A typical measurement station is shown in fig. 3-3. It allows the measurement of air temperature and air humidity, wind speed and direction, leaf wetness, up- and down-welling short-wave radiation, up- and down-welling long-wave radiation, rain, barometric pressure, soil moisture and soil temperature in different depth. The stations cover the complete test site, but they non-uniformly distributed on the test site. Objective of the chosen distribution of stations is the optimization of parameter measurements and data transfer as well as to guarantee the access to local weather conditions and its variability. The sample rate of the sensors is 900 sec. Every 15 minutes the measured samples are computed to a mean parameter value and transmitted automatically via 450 MHz telemetry to a receiving station and a data server.

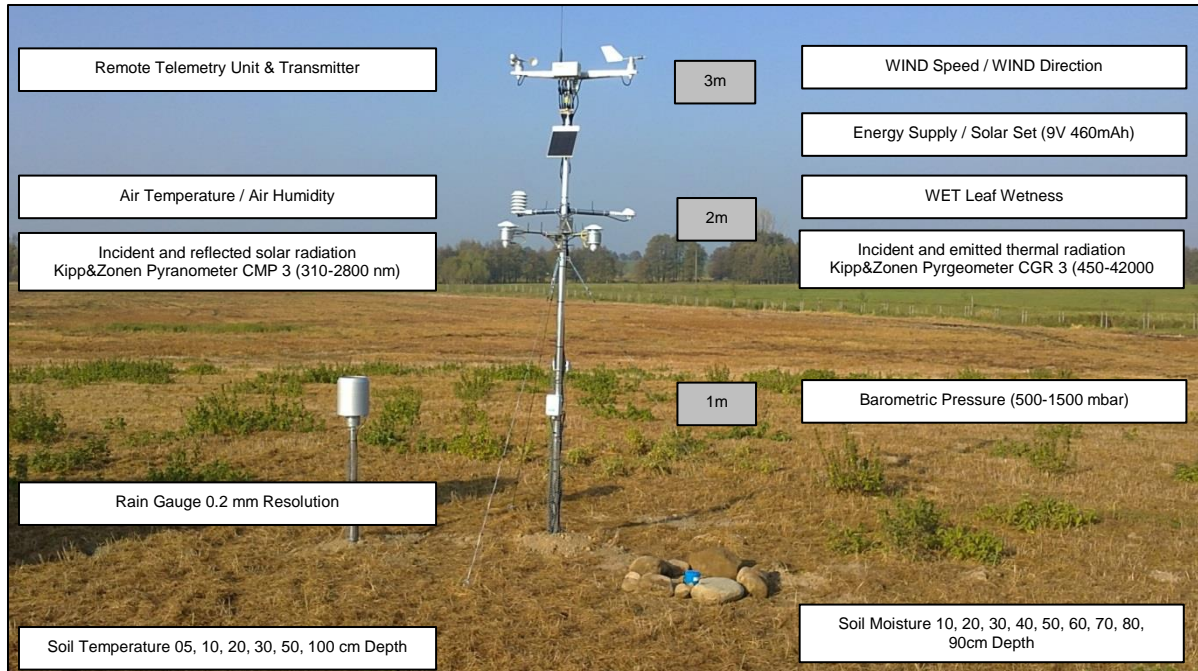


Fig. 3-3: Typical DEMMIN environmental measurement station and instrumentation

As mentioned before measurements are usually taken every 15 minutes, but for new stations this is increased to 1 min.

3.2.2 Setup of additional stations

For the OrPHEuS project the implemented environmental measuring system in the test site DEMMIN was modified in order to guarantee i) a stable data acquisition, ii) a secured and stable data transmission, and iii) a higher repetition rate of the measurement system. The pre-condition for the realization the project requirements were the installation of new equipment (e.g. 3 additional measurement stations). For the implementation of the complementary measurement stations the following investments were planned:

1. radio telemetry unit A 753 S4 Band III,
2. Kipp & Zonen pyranometer CMP-3,
3. Solar set 5 Watt as energy supply,
4. aluminum pillar, and
5. cables and fixing materials.



Fig. 3-4: Location of the implemented environmental measurement stations for measuring the radiation in a) Alt Plestlin, b) Böken, and c) Sassen.

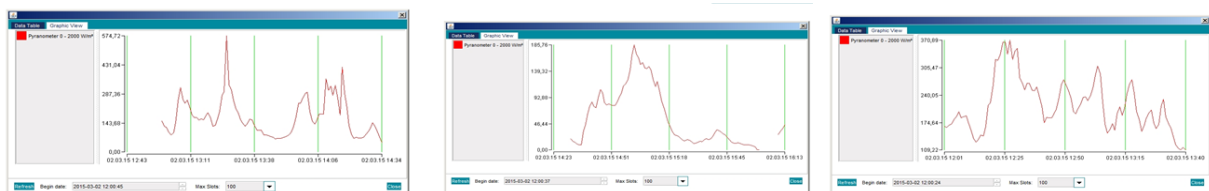


Fig. 3-5: Samples for measured time series of radiation in a) Alt Plestlin, b) Böken, and c) Sassen.

The following implementations were carried out:

1. For the implementation of 3 additional radiation stations (measurement sensors: Kipp & Zonen pyranometer CMP-3), optimal measurement locations were identified to complement the environmental measurement network DEMMIN. For this, measurements and optimization of the telemetry line between the measurement station and the basis station in order to enable a correct data acquisition and transmission.
2. Additional to step 1, the implementation of a separate telemetry gateway (radio telemetry unit A 753 S4 Band III) with a separate telemetry frequency was implemented for a secure transmission of radiation data to all other measured parameters.
3. The clock frequency of the separate environmental measurement system was increased from the standard of 15 minutes to 1 minute. This offer a higher information reactivity of the system to environmental changes as moving of clouds and cloud fields.
4. The realization of the higher measurement rate required a new energy concept for the measurement stations.

The fig. 3-4 a-c) shows the measurement stations in-situ, while Fig 3-5 provides sample data.

In fig. 3-6 the locations of the implemented complementary stations are represented. The telemetry lines between the measurement stations and the gateway are shown as green lines. In the center of the lines the gateway location can be seen.

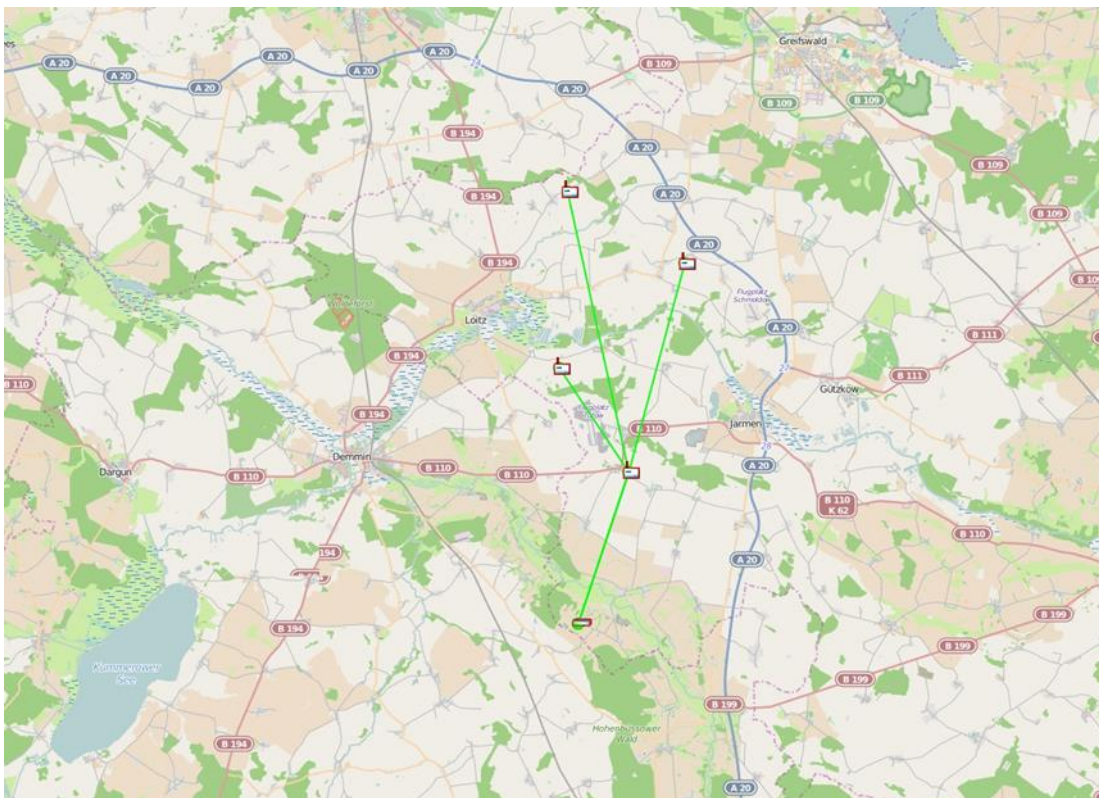


Fig. 3-6: Location of the measurement stations Alt Plestlin, Böken, and Sassen and the telemetry gateway.

Table 3-1: Table of characteristics of the used DEMMIN test site measurement stations, in red the new OrPHEuS sites

Pos.	Site	GPS	Closest MSG element (E to W, max 3712)	MSG pixel center LAT (°N)	Kipp&Zonen CM3 / CMP3	Kipp&Zonen CG3 / CGR 3	Start of Measurements	Availability of Data
		LON (°N) GPS LAT (°E)	Closest MSG line (S to N, max 3712)	MSG pixel center LON (°E)				
8	Alt Tellin	53.832769 13.257204	1589 3435	53.8281 13.2303	Upwards	-	20.06.2011	Ongoing
15	Beestland	53.925514 12.918089	1596 3437	53.9370 12.9137	Upwards	-	20.05.2014	Ongoing
11	Beggerow	53.501773 13.021490	1591 3430	53.5180 13.0214	Upwards	-	16.08.2013	Ongoing
12	Bentzin	53.958010 13.262559	1589 3437	53.9515 13.2741	Upwards	-	01.08.2013	Ongoing
6	Buchholz	53.827198 13.214191	1589 3435	53.8281 13.2303	Upwards Downwards	Upwards Downwards	04.06.2007 "	26.02.2014 "
7	Goermin	53.982808 13.257952	1590 3438	54.0113 13.2445	Upwards Downwards	Upwards Downwards	25.11.2004 "	04.02.2013 "
5	Kletzin	53.937318 13.157541	1591 3437	53.9474 13.1710	Upwards Downwards	Upwards Downwards	25.11.2004 "	Ongoing "
4	Medrow	53.986939 12.954075	1596 3438	53.9989 12.9351	Upwards Downwards	Upwards Downwards	24.11.2004 "	Ongoing "
9	Neu Tellin	53.859892 13.212109	1590 3436	53.8877 13.2007	Upwards	-	20.06.2011	Ongoing
3	Seedorf	53.950296 13.022384	1594 3437	53.9412 13.0166	Upwards Downwards	Upwards Downwards	24.11.2004 "	Ongoing "
10	Sommersdorf	53.789933 12.902111	1595 3435	53.8157 12.9224	Upwards	-	29.11.2011	Ongoing
1	Verchen	53.844454 12.933129	1595 3436	53.8773 12.9437	Upwards Downwards	Upwards Downwards	25.11.2004 "	Ongoing "
2	Warrenzin	53.908444 12.933145	1595 3437	53.9390 12.9651	Upwards Downwards	Upwards Downwards	25.11.2004 "	Ongoing "
20.	Wotenick	53.945578 12.987718	1595 3437	53.9390 12.9651	Upwards	-	06.05.2014	Ongoing
16	Alt Plestlin	53.947 13.193	1590 3437	53.9495 13.2226	Upwards Downwards	Upwards Downwards	24.06.2015 "	Ongoing "
4	Böken	53.995 13.29	1589 3438	54.0135 13.2962	Upwards Downwards	Upwards Downwards	24.06.2015 "	Ongoing "
8	Sassen	54.027 13.20	1591 3438	54.0093 13.1929	Upwards Downwards	Upwards Downwards	24.06.2015 "	Ongoing "

Table 3-2: Table of characteristic of the GFZ (German Research Centre for Geosciences Potsdam) measurement stations of the TERENO initiative hosted by the test site DEMMIN

Pos.	Site	GPS	Closest MSG element	MSG pixel	Kipp&Zonen CMP 3	Kipp&Zonen CGR 3	Start of Measurements	Availability of Data
		LON (°N)	(E to W, max 3712)	center LAT (°N)				
		LAT (°E)	(S to N, max 3712)	center LON (°E)				
16	Alt Plestlin	53.9416	1590	53.9495	Upwards	Upwards	25.01.2013	Ongoing
		13.2067	3437	13.2226	Downwards	Downwards	"	"
4	Böken	53.997152	1589	54.0135	Upwards	Upwards	18.10.2011	Ongoing
		13.312405	3438	13.2962	Downwards	Downwards	"	"
5	Groß Zastow	54.017045	1589	54.0135	Upwards	Upwards	18.10.2011	Ongoing
		13.273310	3438	13.2962	Downwards	Downwards	"	"
7	Groß Zetelwitz	54.040108	1591	54.0093	Upwards	Upwards	18.10.2011	Ongoing
		13.226967	3438	13.1929	Downwards	Downwards	"	"
20.	Heydenhof	53.8712	1589	53.8898	Upwards	Upwards	28.10.2012	Ongoing
		13.265	3436	13.2522	Downwards	Downwards	"	"
15	Karlshof	53.9217	1593	53.9430	Upwards	Upwards	25.01.2013	Ongoing
		13.0802	3437	13.0679	Downwards	Downwards	"	"
11	Kuntzow	53.96053	1588	53.9536	Upwards	Upwards	20.10.2011	Ongoing
		13.327784	3437	13.3256	Downwards	Downwards	"	"
18	Leppin	53.8934	1591	53.8856	Upwards	Upwards	11.01.2013	Ongoing
		13.1659	3436	13.1492	Downwards	Downwards	"	"
2	Mühlenkamp	53.988919	1591	54.0093	Upwards	Upwards	18.10.2011	Ongoing
		13.167381	3438	13.1929	Downwards	Downwards	"	"
12	Müssentin	53.914266	1588	53.8919	Upwards	Upwards	25.10.2011	Ongoing
		13.312933	3436	13.3036	Downwards	Downwards	"	"
14	Nielitz	54.0257	1593	54.0053	Upwards	Upwards	25.01.2013	Ongoing
		13.099	3438	13.0898	Downwards	Downwards	"	"
1	Passow	53.994773	1590	54.0113	Upwards	Upwards	18.10.2011	Ongoing
		13.234334	3438	13.2445	Downwards	Downwards	"	"
9	Rustow	53.958126	1593	53.9430	Upwards	Upwards	25.10.2011	Ongoing
		13.078658	3437	13.0679	Downwards	Downwards	"	"
3	Sanzkow	53.881050	1591	53.8856	Upwards	Upwards	18.10.2011	Ongoing
		13.124363	3436	13.1492	Downwards	Downwards	"	"
8	Sassen	54.015598	1591	54.0093	Upwards	Upwards	18.10.2011	Ongoing
		13.202466	3438	13.1929	Downwards	Downwards	"	"
19	Ueckeritz	53.9215	1590	53.9495	Upwards	Upwards	11.01.2013	Ongoing
		13.1932	3437	13.2226	Downwards	Downwards	"	"
13	Voelschow	53.8668	1588	53.8919	Upwards	Upwards	25.01.2013	Ongoing
		13.3117	3436	13.3036	Downwards	Downwards	"	"
17	Zarnekla	54.0027	1594	54.0031	Upwards	Upwards	22.01.2013	Ongoing
		13.0141	3438	13.0382	Downwards	Downwards	"	"
6	Zarrenthin	53.942591	1589	53.9515	Upwards	Upwards	11.10.2011	Ongoing
		13.285746	3437	13.2741	Downwards	Downwards	"	"
10	Zeitlow	53.951361	1592	53.9453	Upwards	Upwards	25.10.2011	Ongoing
		13.122220	3437	13.1195	Downwards	Downwards	"	"

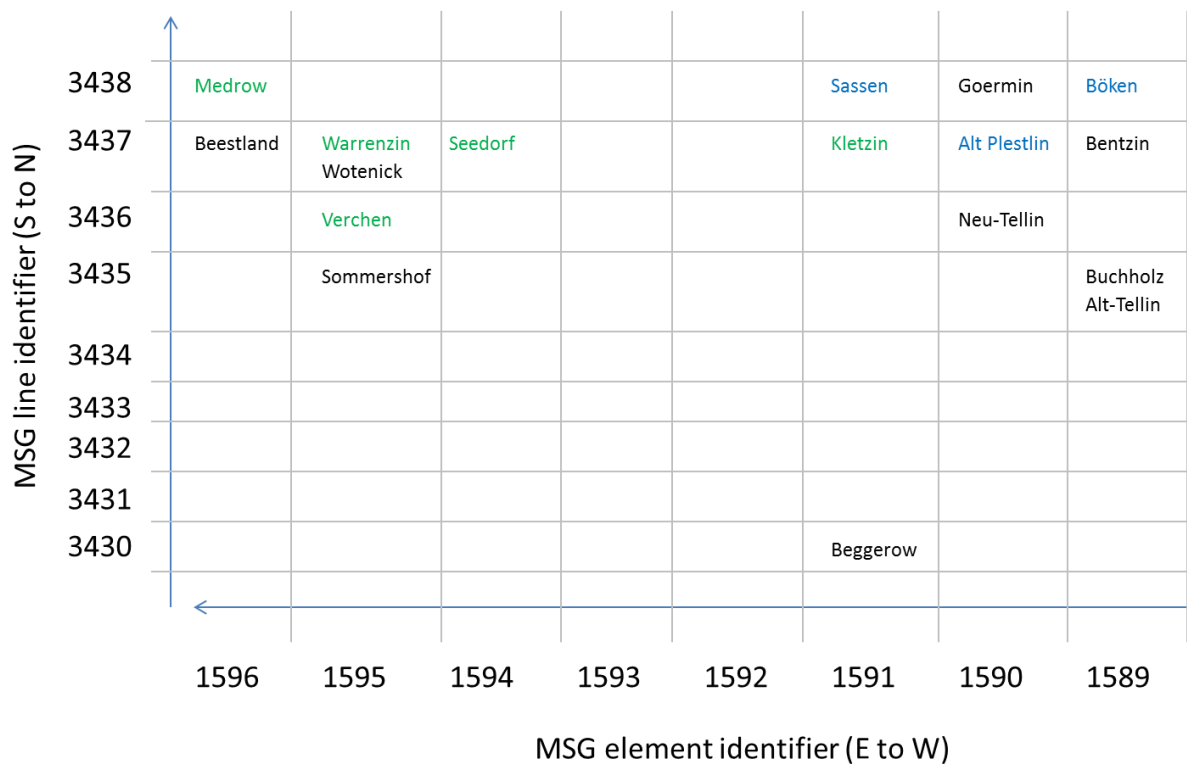
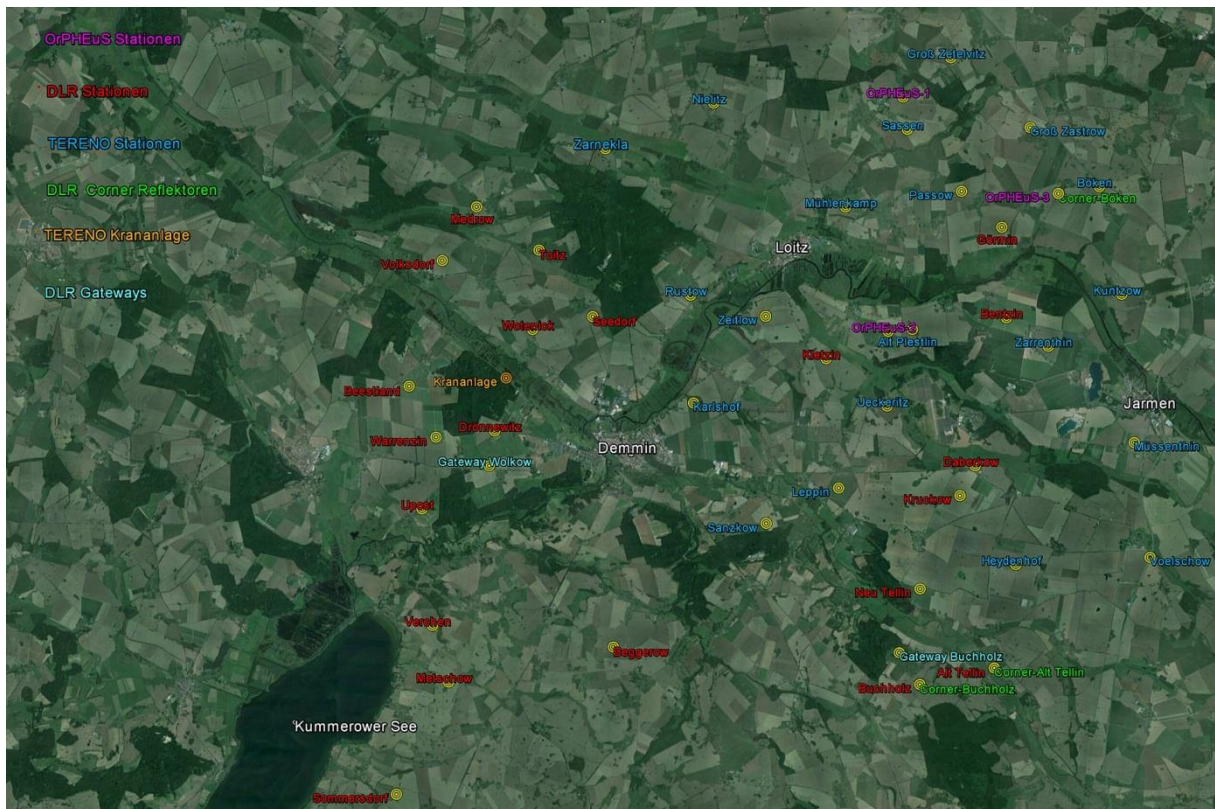


Fig. 3-7: Upper part: Location of the environmental measurement stations (yellow) within the large calibration and validation facility DEMMIN of DLR. In the map the TERENO environmental measurement stations of GFZ are included as they are hosted by DLR. MSG pixel centers (red) and data gateways (green) are also displayed. Lower part: MSG pixel grid and the location of all stations inside the MSG pixels - data with data before 2014 (green) and OrPHEuS stations (blue) are marked.

The characteristics of the environmental measurement stations within the test site DEMMIN are given in tab. 3-1 (DEMMIN) and in tab. 3-2 (TERENO). These TERENO stations of GFZ are hosted by the calibration and validation test facility DEMMIN of DLR. Beside the name of the location of each measurement station there GPS coordinates (LON (°N), LAT (°E)), the available measurement sensors, the start of the measurements, and the availability of data are given. To identify the measurement stations within the MSG pixels also the closest MSG elements and lines (E to W, max 3712; S to N, max 3712) and their GPS coordinates (LON (°N), LAT (°E)) are listed in tab. 3.2-1 and 3.2-2.

The location of the environmental measurement stations within the calibration and validation test site DEMMIN are shown in fig. 3-6. In addition to these stations the TERENO environmental measurement stations of the GFZ are included in the map. It becomes clear that the test field is area cover uniformly uncovered.

For the satellite imagery, two pixels with two stations exist: Warrenzin and Wotenick with overlapping measurements in May 2014 to August 2015 and Buchholz and Alt-Tellin with overlapping measurements from January 2014 to February 2015. For other stations, a large number of stations in neighboring satellite imagery pixels can be seen.

3.2.3 Data preparation

The applications of the OrPHEuS related solar energy analysis is based on the use of MESOR-format.

This format permits the data storage line by line in ASCII format, and it contains a header including defined information of a defined thesaurus. Additional to these, the MESOR-format permits an easy conversion into XML-format (Hoyer-Klick et al., 2008).

```
#MESOR V1.1 11.2007
#type sequenceOfRadiationValue
#unitName W/m^2
#valueType Global Horizontal Irradiance
#IPR.providerName DEMMIN
#IPR.providerURL http://demminweb.dlr.de
#IPR.timeSeriesTitle OrPHEuS_Beestland
#IPR.copyrightText DEMMIN
#location.latitude lat 53.926102
#location.longitude lon 13.921800
#location.height 0
#location.summarizationType 1h
#spectral.begin 310
#spectral.end 2800
#spectral.unit nm
#timezone UTC
#comment converted from ADCON original by txt2mesor
#comment converted at Fri Oct 02 08:28:36 2015
#comment by F.Renke at www.nz.dlr.de
#comment instrument 0 manufacturer KIPP
#comment instrument 0 CMP-3
#comment instrument 0 http://www.kippzonen.com/Product/11/CMP-3-Pyranometer
#comment instrument 0 sensitivity (5 ...15)*10E-6 V/W/m^2c
#comment missing data is -99.0
#channel Datum YYYY-MM-DD
#channel Zeit HH:MM
#channel GHI W/m^2
#begindata
2014-01-01 00:15 -99.0
2014-01-01 00:30 -99.0
2014-01-01 00:45 -99.0
2014-01-01 01:00 -99.0
2014-01-01 01:15 -99.0
...
```

#enddata

The operating measurement system of the DEMMIN test site is based on ADCON-Telemetry technology. In order to realize the data transfer controllable and cost-effective, transfer frequencies in the range between 400 to 500 MHz are used. But, since the amount of transferable data in the used frequency bands is limited, a relative simple format is used for data transmission in DEMMIN.

In the consequence, this format is not compatible to MESOR-format. Therefore, a data converter was developed, in order to make the DEMMIN-data available for the further investigations in the MESOR-format.

	01.01.2005, 00:15	2006-09-12, 2007-01-16	2007-01-17, 2008-03-04	2008-03-05, 2008-04-29	2008-04-30, 2008-11-12	2008-11-13, 2009-01-27	2009-01-28, 2009-05-10	2009-05-11, 2009-06-28	2009-06-29, 2013-07-23	2012-07-24, 2012-10-11	2012-10-12, 2013-10-01	2013-10-02, 2013-10-23	2013-10-24, 2013-12-31	01.01.2014, 00:15	25.03.2014, 09:15	06.05.2014, 15:00	19.02.2015, 20:00	19.02.2015, 13:30	24.06.2015, ~12:40	31.07.2015, 14:15	31.08.2015, 00:00	17.09.2015, 07:35
Kletzin																						
Medrow																						
Seedorf																						
Verchen																						
Warrenzin																						
Neutellin																						
Alt Tellin																						
Beestland																						
Beggerow																						
Bentzin																						
Buchholz																						
Goermin																						
Sommersdorf																						
Wotenick																						
Alt Plestlin (OrPHEuS2)																						
Boeken (OrPHEuS3)																						
Sassen (OrPHEuS1)																						

Fig. 3-8: Data availability of DEMMIN and new OrPHEuS stations

	2011-10			2012		2013-01			2014	2015	Ongoing
	2011-10-11	2011-10-18	2011-10-20	2011-10-25	2012-10-28	2013-01-11	2013-01-22	2013-01-25			
Zarrenthin											
Böken											
Groß Zastow											
Groß Zetelwitz											
Mühlenkamp											
Passow											
Sanzkow											
Sassen											
Kuntzow											
Müssentin											
Rustow											
Zeitlow											
Heydenhof											
Leppin											
Ueckeritz											
Zarnekla											
Alt Plestlin											
Karlshof											
Nielitz											
Voelschow											

Fig. 3-9: Data availability of DEMMIN TERENO stations

3.2.4 Satellite-based structural characterization of DEMMIN sites

First we have to check if there are major differences in weather patterns at the various stations in DEMMIN.

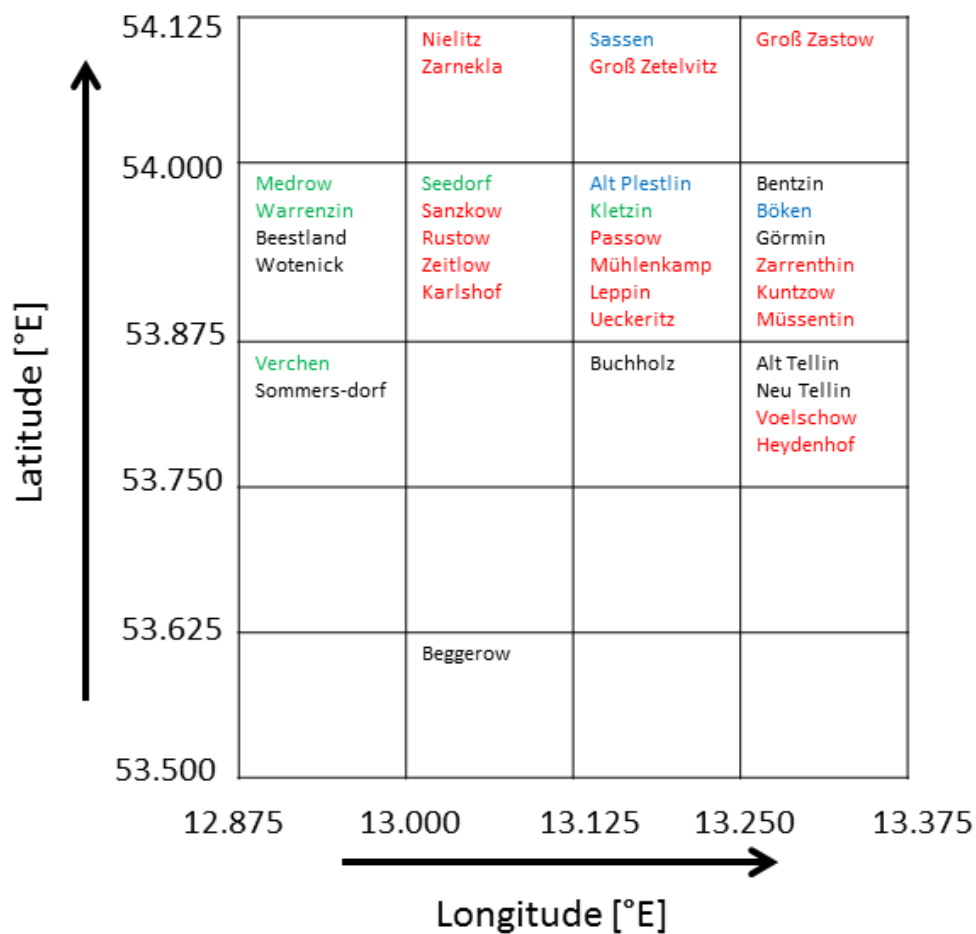


Fig. 3-10: Map of ECMWF grid boxes and the ground stations inside the grid box. Stations with data before 2014 (green), OrPHEu stations (blue), and TERENO stations (red) are marked.

Therefore, a number of stations have been compared with respect to their cloud patterns for a long-term statistic from 2004 to 2013. Methods to generate the cloud statistics are described in Wey and Schroedter-Homscheidt (2014).

For each ECMWF grid box (Fig 3-10) a single station has been used to reduce the number of stations but on the other hand to keep the variation over the region. Those are compared to Kletzin as an arbitrarily chosen reference station.

The number of clear and cloudy pixels is very similar (Fig. 3-11/3-12) for all locations. Also for all other cloud statistics the patterns are very similar, with exception of the two south-western stations Sommersdorf and Beggerow. Sommersdorf shows about 5% less thin cirrus cloud cases and about 2% more thick water-dominated clouds for both the lower and medium height atmosphere. Also in the variation of cloud situations over the month of the year, those two stations show a larger number both scattered and broken water cloud cases than the other stations. Sommersdorf and Beggerow are both in the vicinity of a larger lake. This may result in similar cloud patterns, which are consistent to each other and – as said – slightly different than the rest of the DEMMIN stations. Nevertheless, the cloud statistics over the months as well as the hours of the day remain constant at all stations.

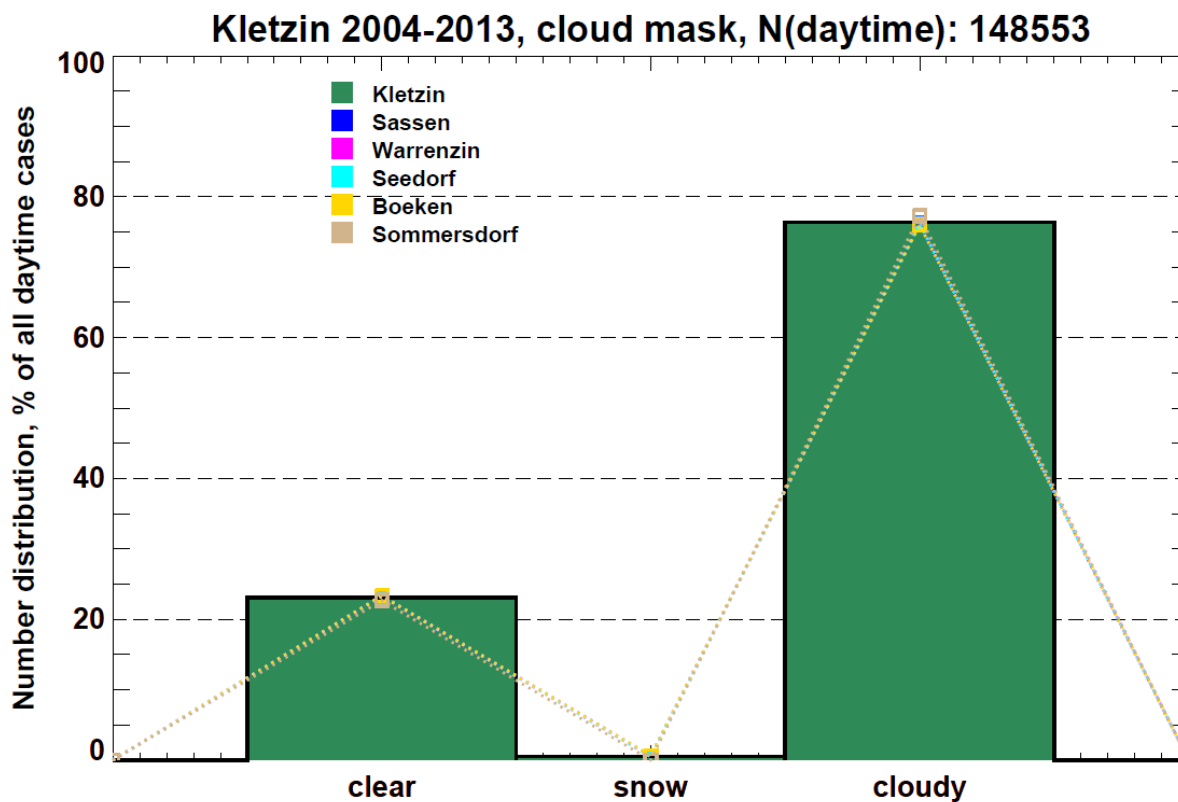


Fig. 3-11: Number distribution of clear, snowy and cloudy cases at Sassen, Warrenzin, Seedorf, Boeken, Sommersdorf with Kletzin as the reference (green).

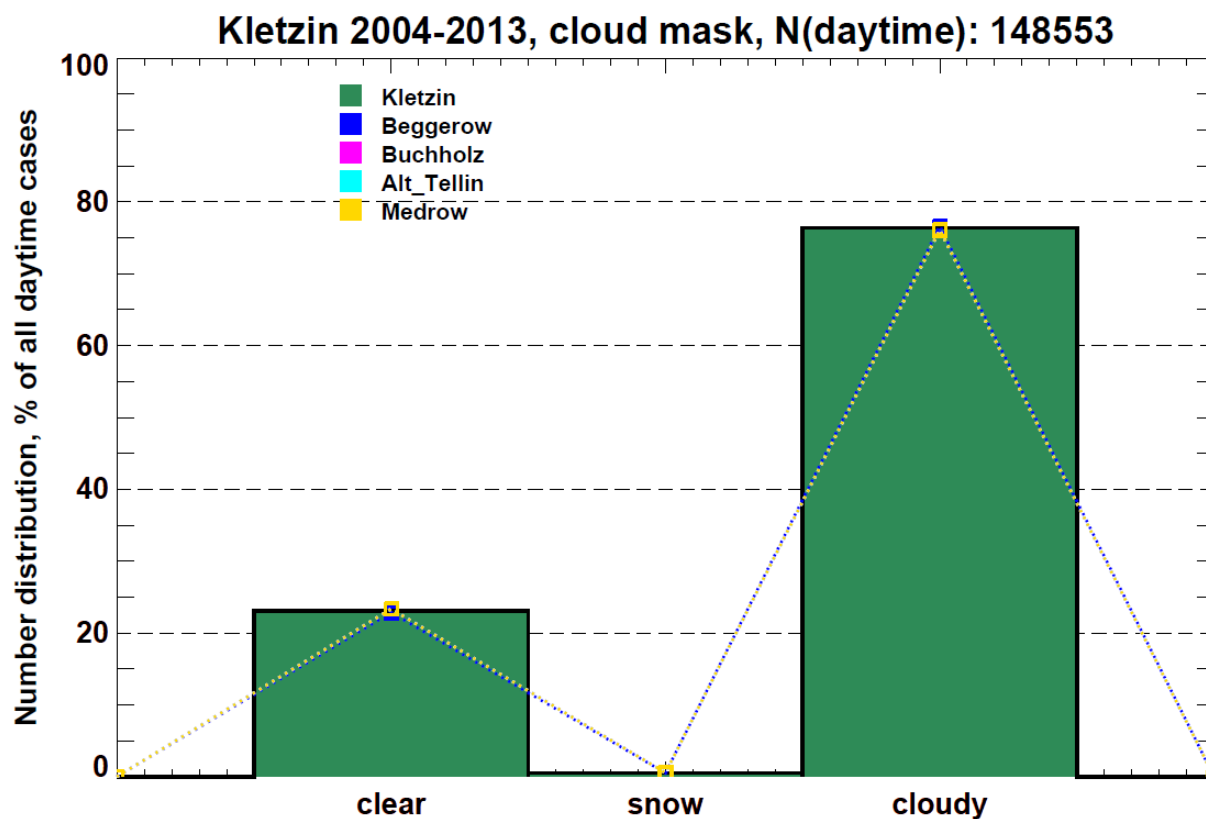


Fig. 3-12: Number distribution of clear, snowy and cloudy cases at Beggerow, Buchholz, Alt-Tellin, Medrow with Kletzin as the reference (green).

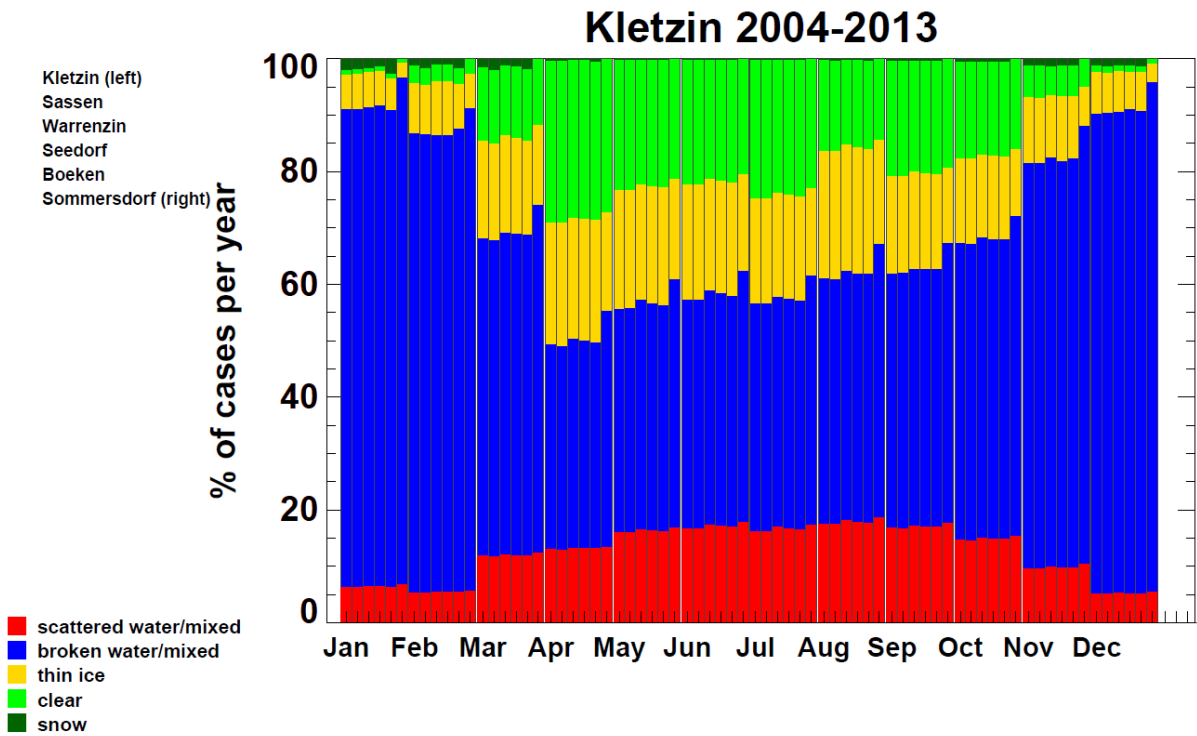


Fig. 3-13: Number distribution of scattered/broken/thin ice/clear and clear+snow conditions at Sassen, Warrenzin, Seedorf, Boeken, Sommersdorf with Kletzin as the reference (left) and over the month of the year.

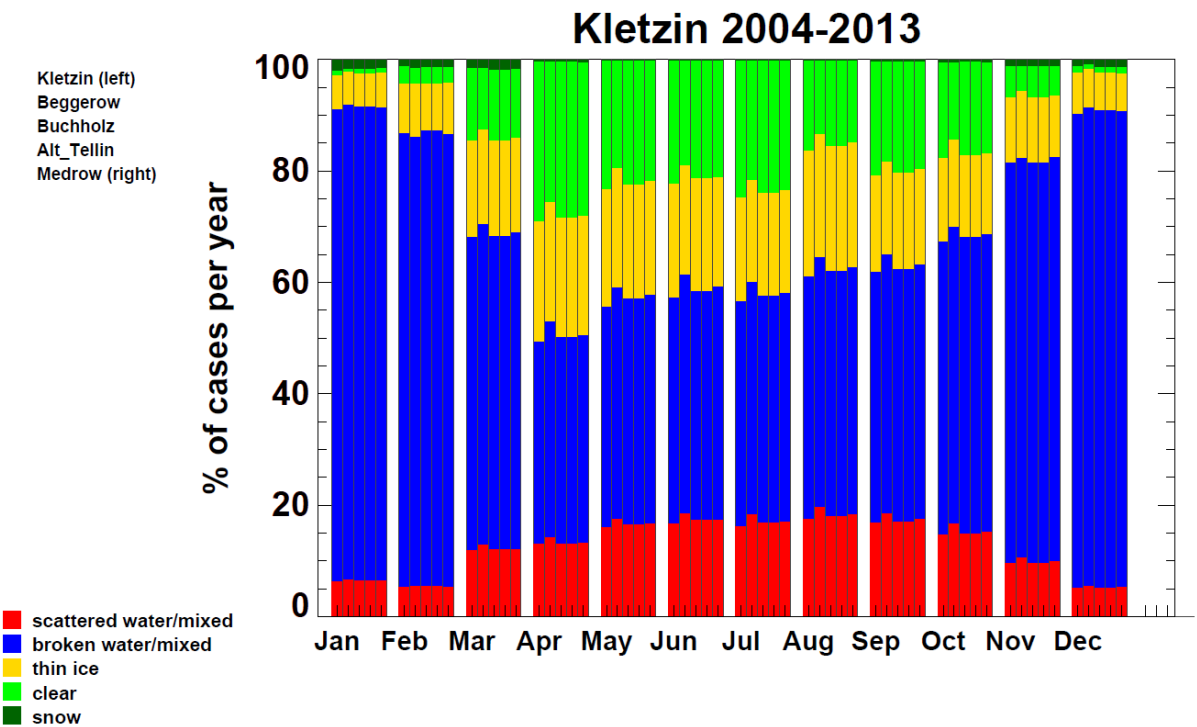


Fig. 3-14: Number distribution of scattered/broken/thin ice/clear and clear+snow conditions at Beggerow, Buchholz, Alt-Tellin, Medrow with Kletzin as the reference (green) and over the month of the year.

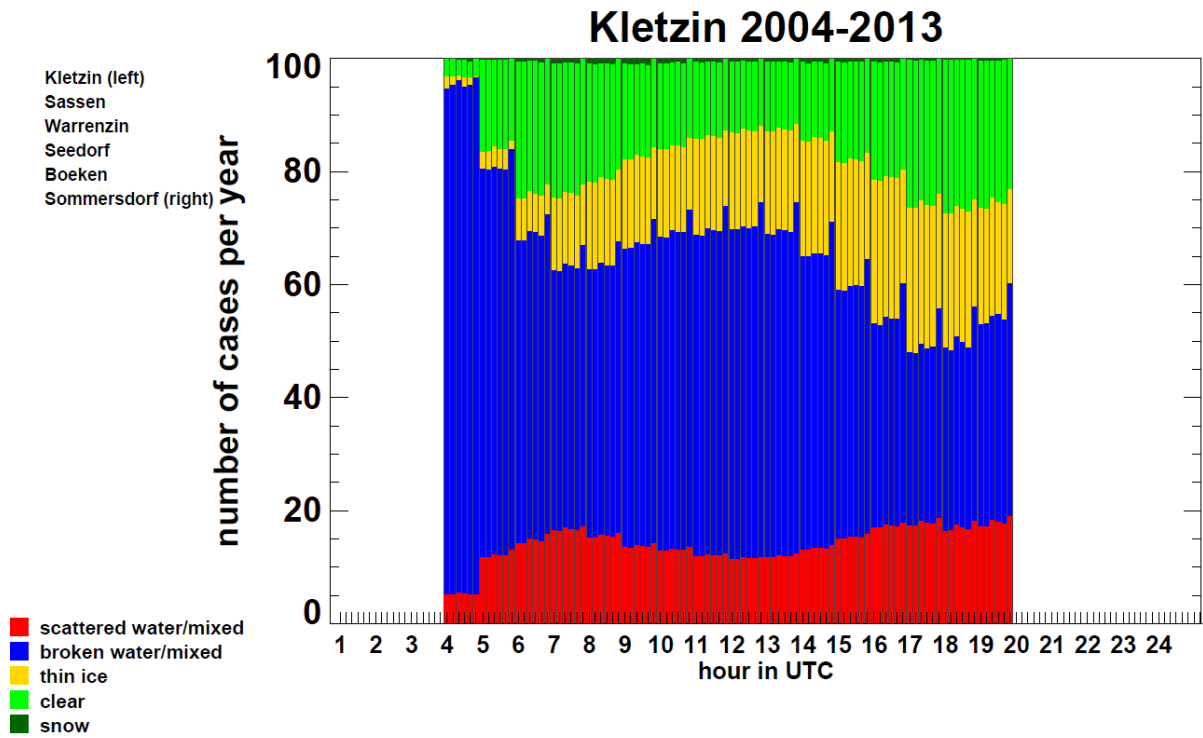


Fig. 3-15: Number distribution of scattered/broken/thin ice/clear and clear+snow conditions at Sassen, Warrenzin, Seedorf, Boeken, Sommersdorf with Kletzin as the reference (left) and over the time of the day.

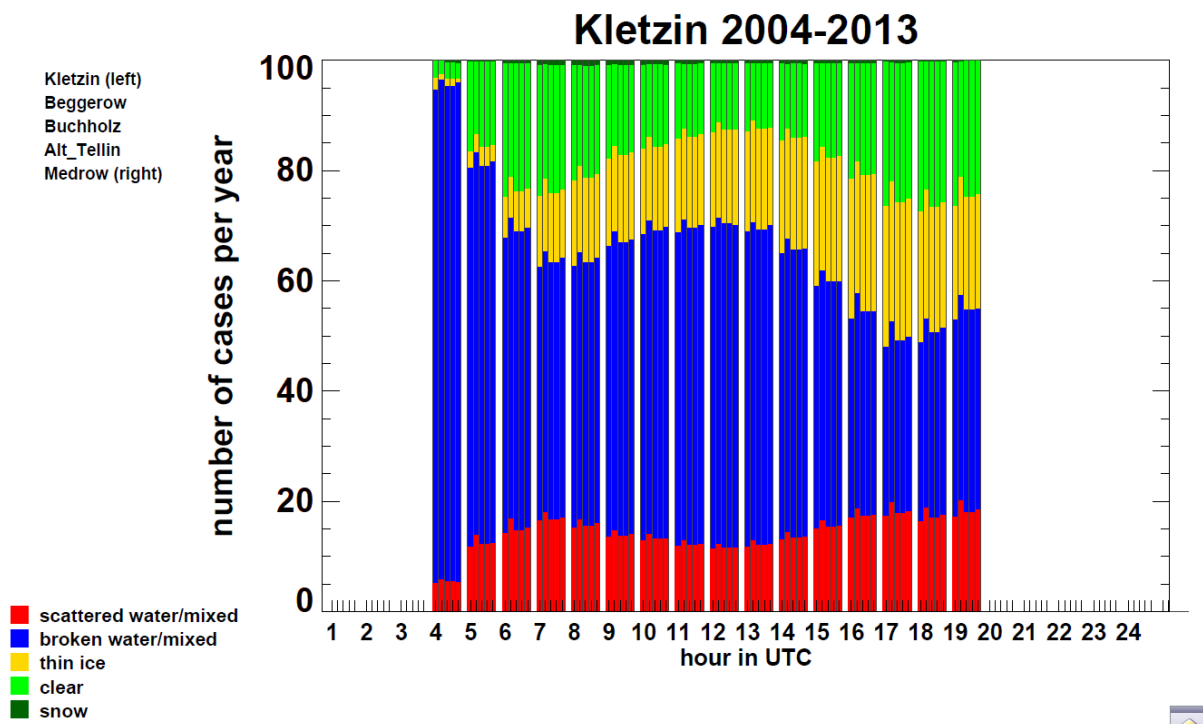


Fig. 3-16: Number distribution of scattered/broken/thin ice/clear and clear+snow conditions at Beggerow, Buchholz, Alt-Tellin, Medrow with Kletzin as the reference (green) and over the time of the day.

Therefore, we conclude that besides from these very small deviations, the DEMMIN site is very homogeneous in the distribution of the clouds on average in a long-term statistics over 10 years of satellite-based cloud observations. This is very welcome, as it shows that the DEMMIN observations are obtained in an area without large spatial trends. This is a prerequisite for any variability studies e.g. in NWP based forecast grid boxes.

Within OrPHEuS, we suggest to use DEMMIN ground observations to do further assessments of COSMO and ECMWF based numerical weather prediction. In a next group of figures 3-17 to 3-19 we assess the differences in cloud statistics at DEMMIN with Kletzin as the reference site (green) and the Ulm test site Einsingen (blue). This comparison is made for the years 2004 to 2012 as we have extracted Einsingen data previously only until 2012.

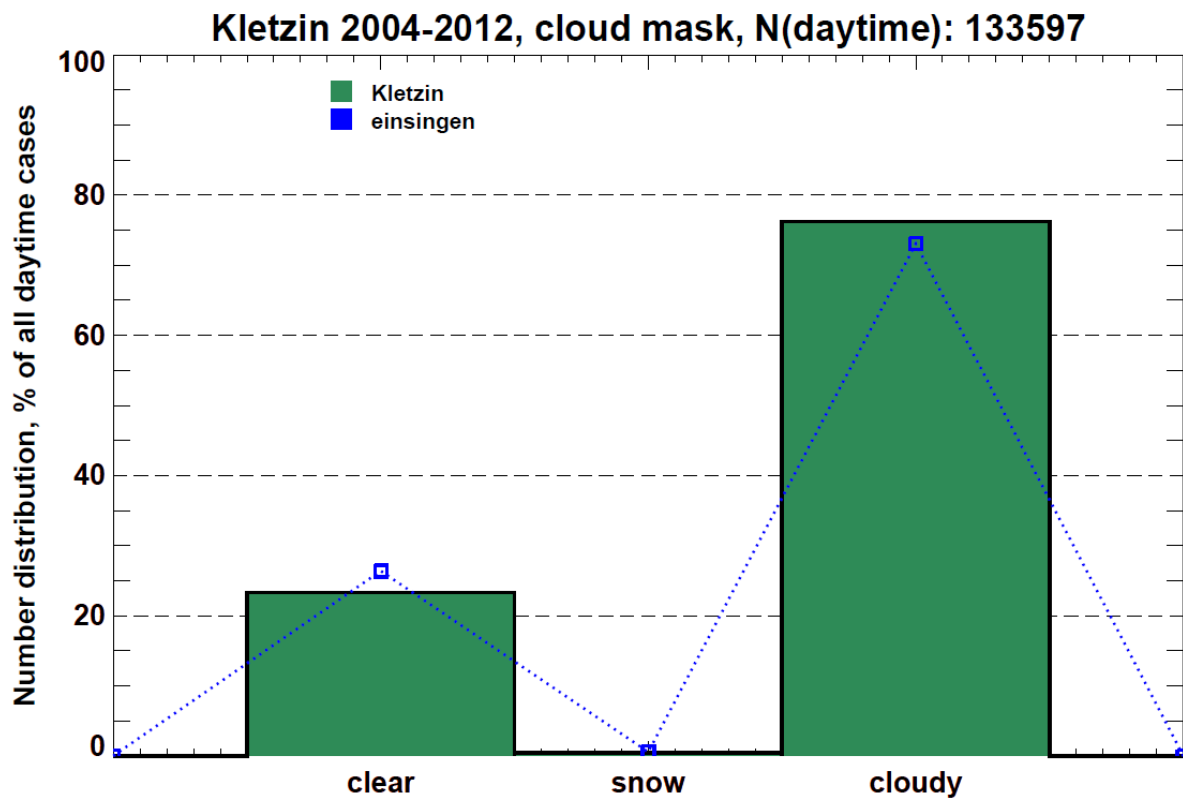


Fig. 3-17: Number distribution of clear, snowy and cloudy cases at Kletzin as the reference (green) compared to the Ulm Einsingen test site.

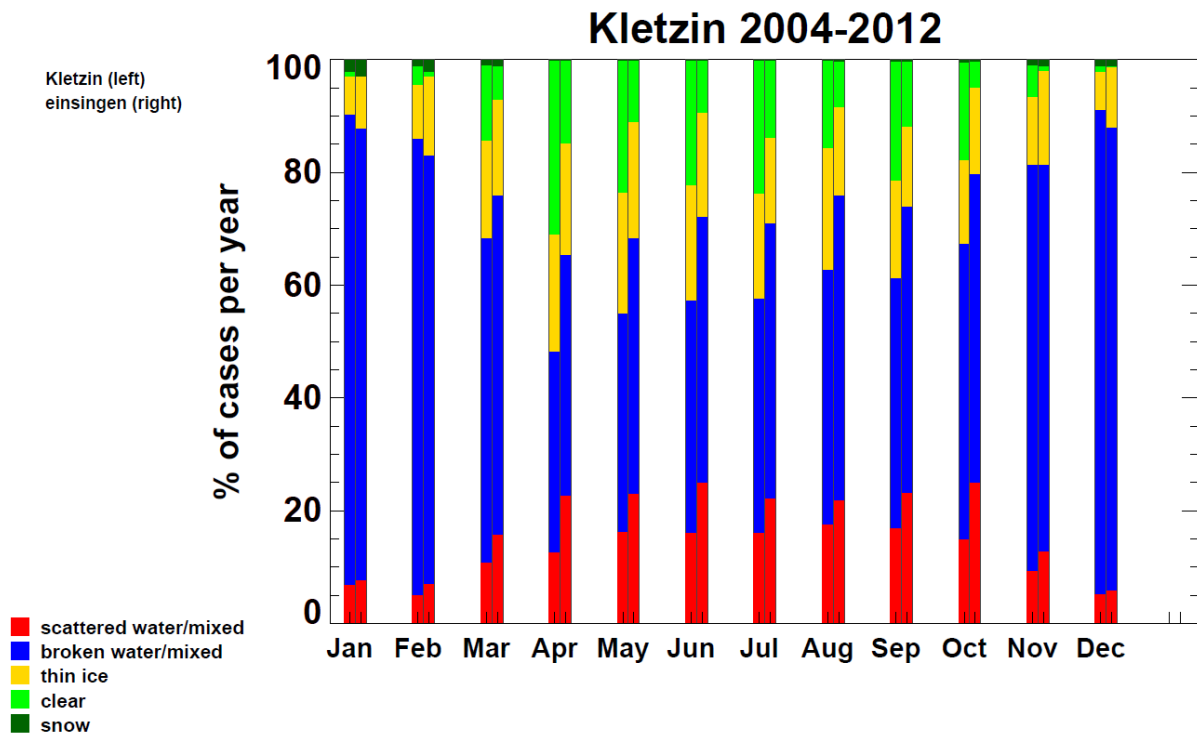


Fig. 3-18: Number distribution of scattered/broken/thin ice/clear and clear+snow conditions at Kletzin as the reference (green) compared to the Ulm Einsingen test site and over the month of the year.

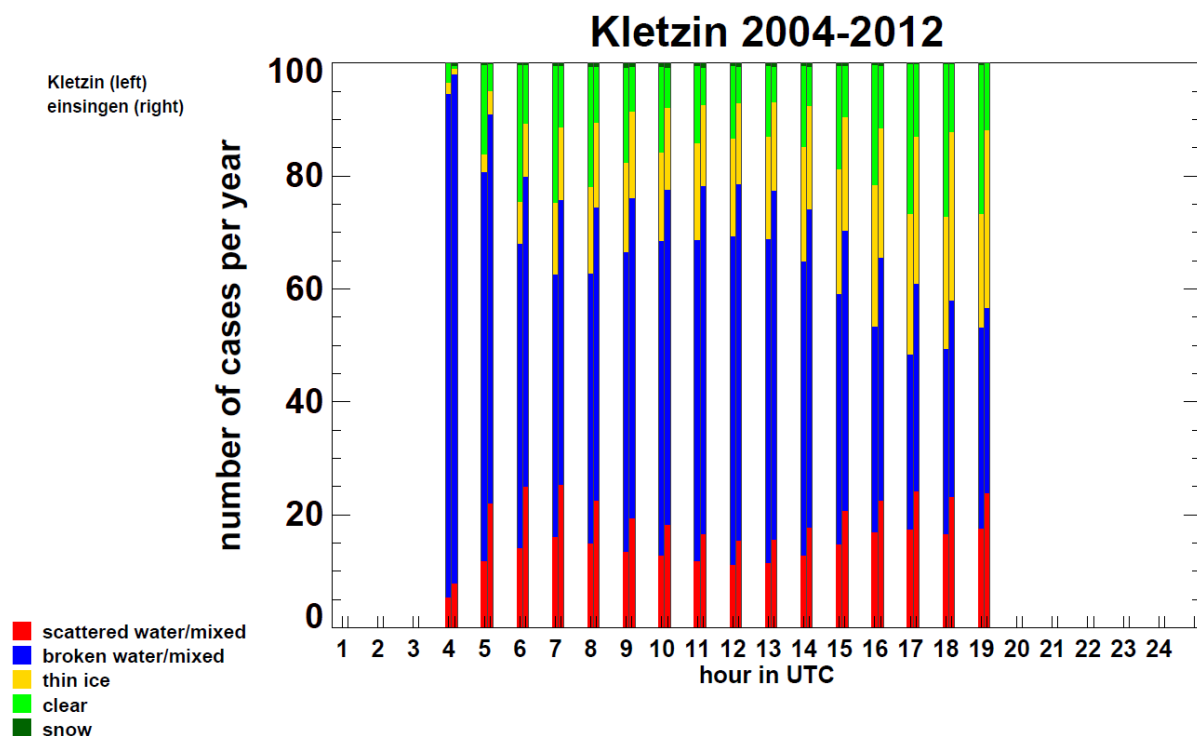


Fig. 3-19: Number distribution of scattered/broken/thin ice/clear and clear+snow conditions at Kletzin as the reference (green) compared to the Ulm Einsingen test site and over the time of the day.

The two stations show a slight difference in cloud occurrence at the pixel of the station itself. Kletzin has approx. 4% more cloudy cases than Einsingen. Low level water clouds are more frequent in Kletzin, while Ulm has more medium and high level water/mixed phase clouds. The number of thin cirrus cases is similar within 1% of occurrences. During the winter months November to February,

there are less broken cloud situations in the surroundings of Eisingen, but more thin cirrus and scattered cloud conditions. During March to October the number of scattered cloud cases is larger in Eisingen and also the broken cloud conditions are slightly more frequent. Overall, Eisingen is more cloudy during the summer months than DEMMIN. During the day, both stations show a noon minimum of scattered cloud situations, while the broken cloud conditions are more frequent during noon hours. This results also in a maximum of cloud cases during noon hours. The peak of cloud cover at 4 UTC may be not very reliable due to the low sun conditions resulting generally in an overestimation of cloudiness by the satellite. Nevertheless, Eisingen shows a significantly larger number of cloudy conditions in the morning hours, which is expected in the Ulm region due to the river Danube. Looking into individual months, January and February are characterized by a large number of cloudy cases over the whole day, March to September show more the characteristics as seen in Fig. 3-20 with a morning and a noon peak, while October to December show a dedicated early morning peak (Fig 3-20 for the winter half year) – actually in both stations, but slightly less in DEMMIN. Based on our results on the differences between DEMMIN stations and the knowledge from comparing other locations with much larger differences, we state that comparing Eisingen to Kletzin allows comparing the DEMMIN site as a whole versus the Ulm case for our purposes of the assessment of NWP accuracy.

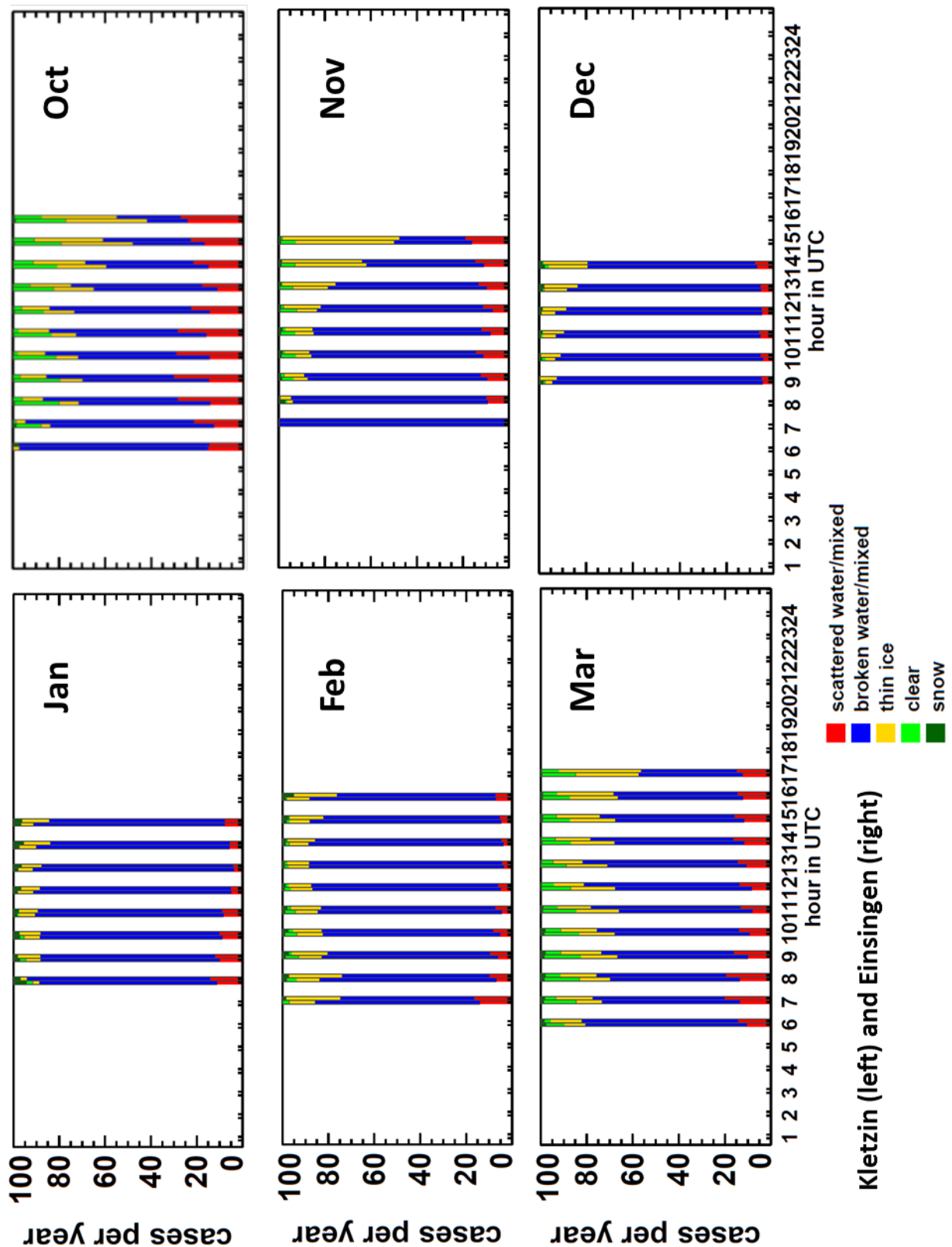


Fig. 3-20: Number distribution of scattered/broken/thin ice/clear and clear+snow conditions at Kletzin as the reference (green) compared to the Ulm Einsingen test site and over the time of the day.

3.2.5 Satellite-based variability characterization

Recently, a number of variability classes for the 1 min resolved variability inside an hour have been introduced (Jung, 2015; Schroedter-Homscheidt, 2016). Eight classes have been selected due to their varying direct normal irradiation (DNI) and the number of fluctuations. DNI is chosen as it is more

sensitive to variability induced by clouds, while GHI variability is always damped by the diffuse fraction and never reaches the zero value during daytime. Additionally, DNI is already normalized by the cosine of the sun zenith angle. Fig. 3-21 provides example hours (marked by red boxes) which have been attributed to one of the eight classes. Yellow lines indicate the 1 min DNI observations, while the black line represents a 10 min moving DNI average. Dashed lines indicate the clear sky DNI.

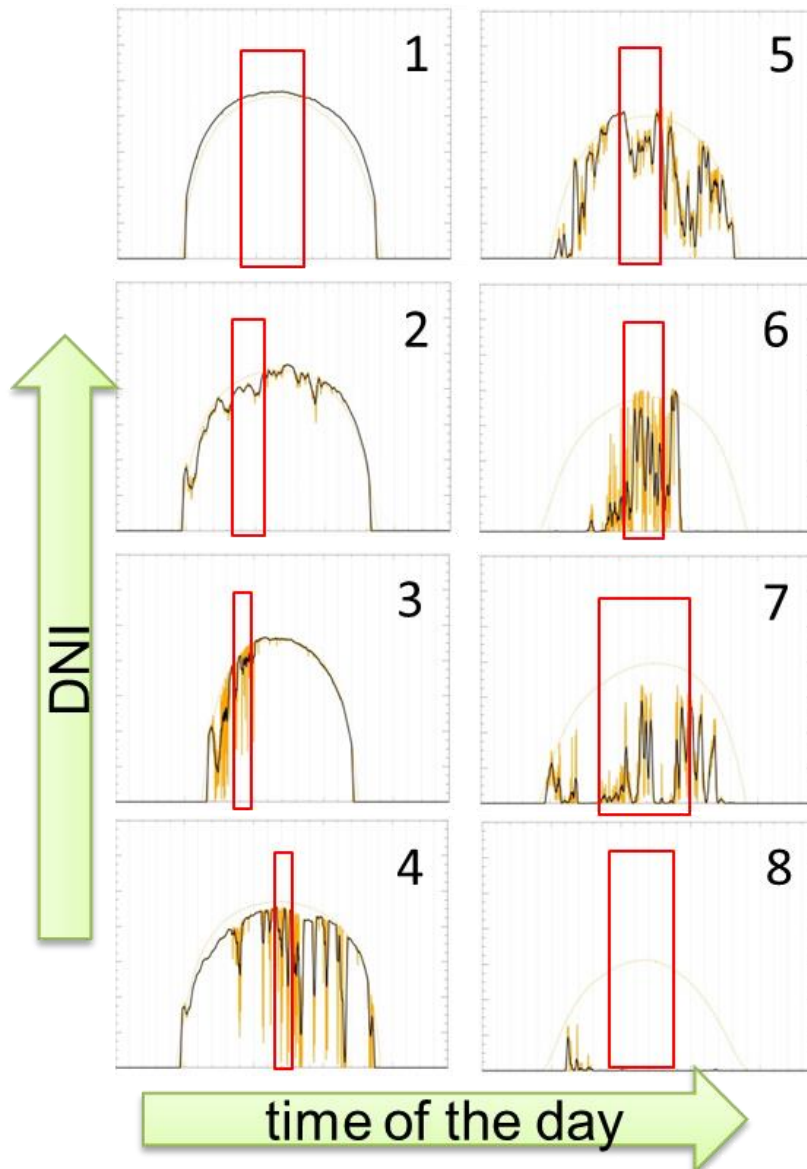


Fig. 3-21: Arbitrarily chosen examples of the variability cloud classes 1 to 8. Hours being classified in one of the classes are marked by a red box. For some classes, the red box extends the range of a single hour and illustrates several hours being included in the reference database. Minute values (yellow), 10 min moving averages (black) and McClear clear sky values (thin) are given.

The class definition is done with respect to direct normal irradiances, but nevertheless, the class characterization can also be done with respect to global horizontal irradiances (GHI) and the variability indices applied to the 1 minute resolved GHI observations. The number of direction changes in GHI, the number of overshootings above 5% (NOVER_5) of the clear sky value and the

number of overshootings (NOVER₁₀) being larger than 10% of the clear sky value. Table 3-1 provides the typical statistical characteristics of each variability class.

Tab 3-1: Variability class characterisation with respect to GHI – mean k_c , the number of direction changes in GHI within the hour, NOVER 5%, and NOVER 10%.

Class	short name	mean k_c	no. of DCH in GHI	NOVER 5%	NOVER 10%
1	VHD_LDCH	0.97	0-2	0	0
2	HD_LDCH	0.96	0-6, mean 1	0-41, mean 2	0-14, mean 1
3	HD_MDCH	0.96	0-15, mean 7	0-18, mean 4	0-9, mean 1
4	HD_HDCH	0.86	6-33, mean 15	0-34, mean 11	0-24, mean 5
5	MD_MDCH	0.88	0-12, mean 5	0-30, mean 4	0-26, mean 2
6	MD_HDCH	0.77	4-22, mean 13	0-34, mean 11	0-27, mean 8
7	LD_MDCH	0.64	0-18, mean 7	0-13, mean 3	0-10, mean 1
8	LD_LDCH	0.20	0-7, mean 1	0	0

Following the cloud statistics used above and as described in Wey and Schroedter-Homscheidt (2014), an automatic classification of the variability classes is applied (and described in more detail in Schroedter-Homscheidt, 2016). Here we apply the cloud variability classification for the DEMMIN sites and report the number distribution of all stations for 2004-2013. DEMMIN is dominated by classes 2, 5 and especially 8. The station Sommersdorf shows slight differences and more often class 8 and less often class 5. The same applies for the station Beggerow, which has more often class 1 and 8 and less cases with class 2 or 5. Also the station Verchen is more frequent in class 8 and less in class 5.

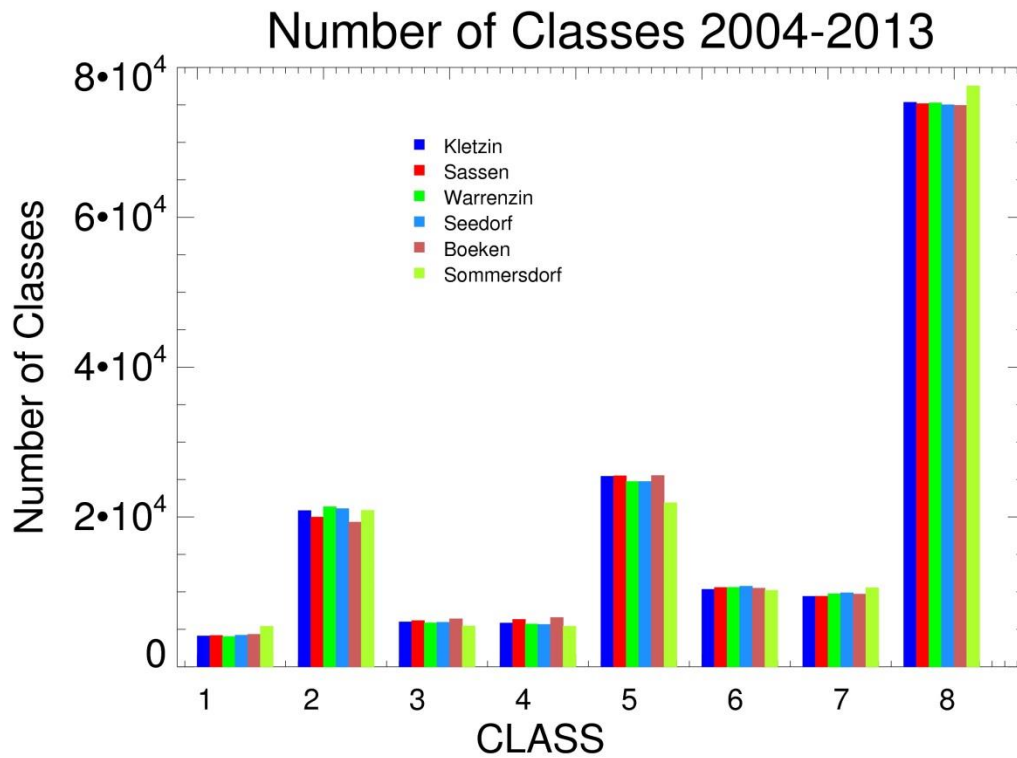


Fig. 3-22: Number distribution of satellite-based variability classes at Sassen, Warrenzin, Seedorf, Boeken, Sommersdorf with Kletzin as the reference (left).

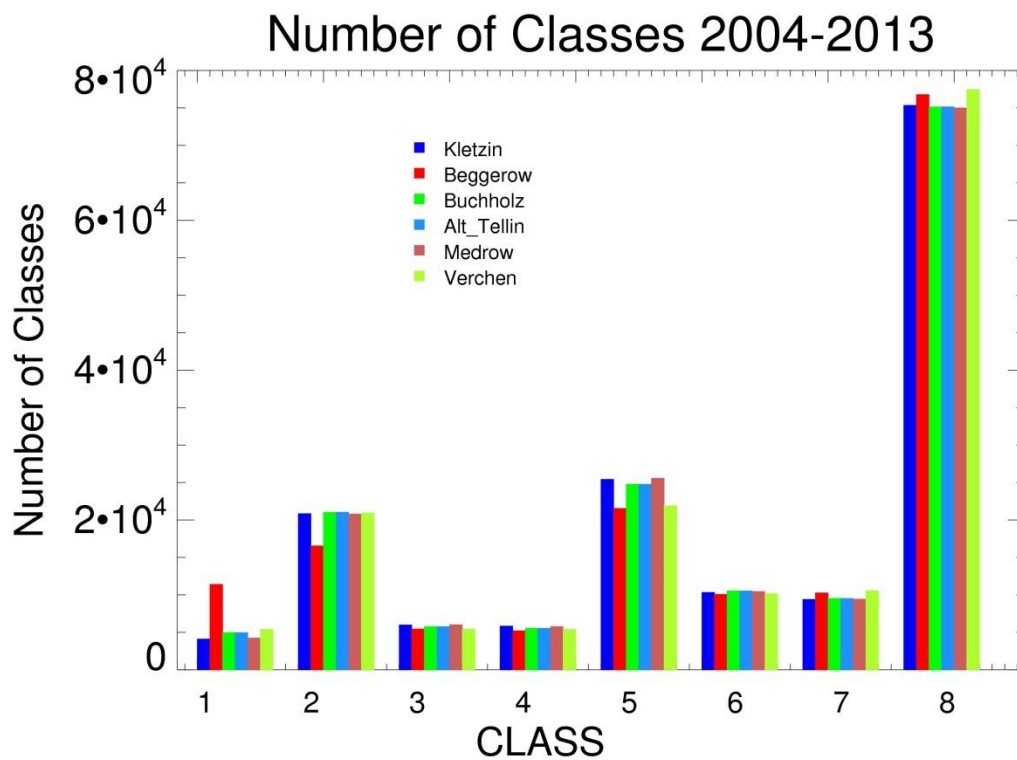


Fig. 3-23: Number distribution of satellite-based variability classes at Beggerow, Buchholz, Alt-Tellin, Medrow with Kletzin as the reference (left).

3.2.6 Ground observation variability

Based on the variability classes found by the satellite image classification, we assume a significant number of cases with variable irradiances. Fig. 3-24 shows the observations as taken in Buchholz, Kletzin, and Medrow as an example. All stations are very similar in all station characteristics given above, but differ in their individual measurements. Here the hourly averages are given. The variability in the original 15 min observations is higher.

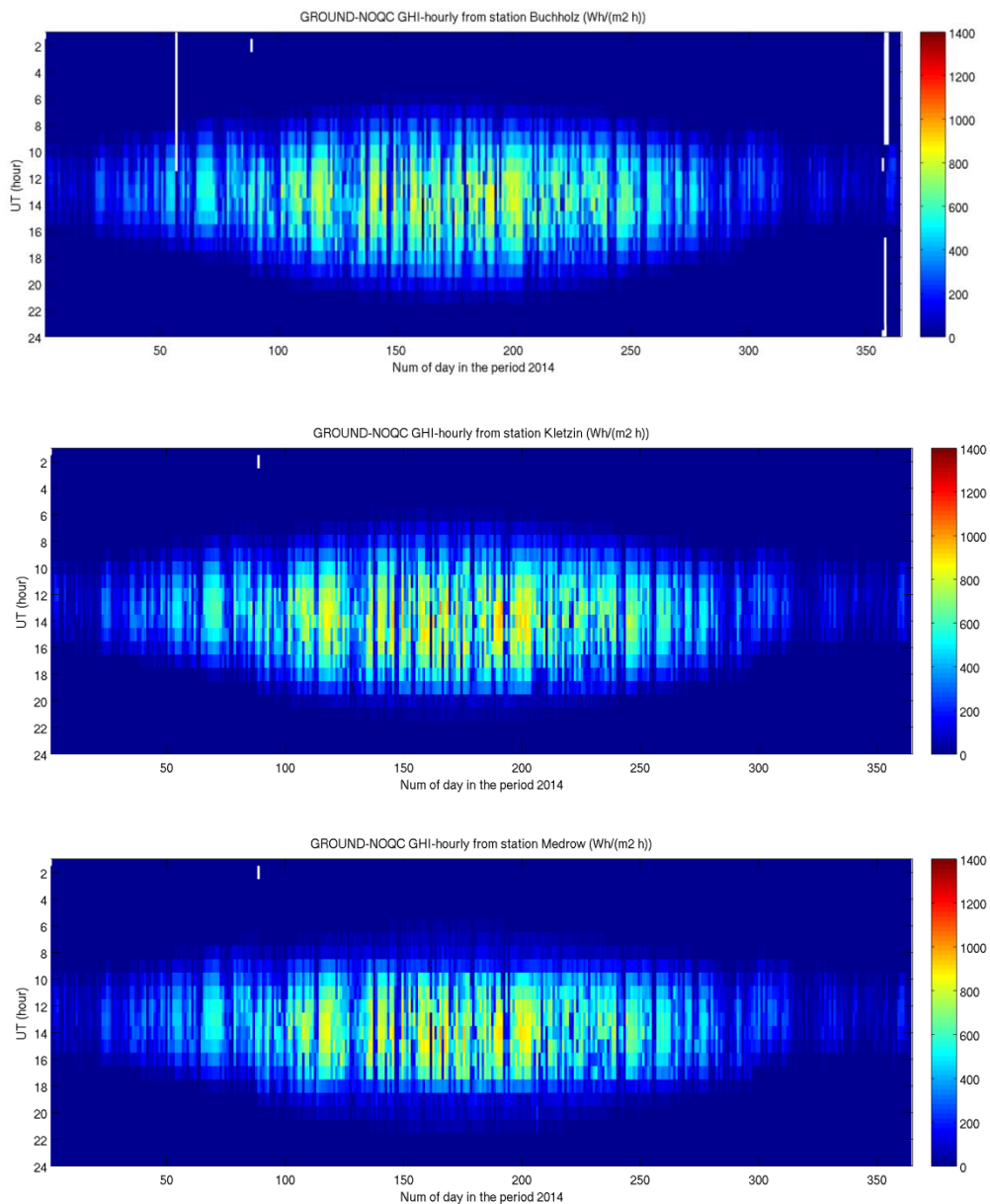


Fig. 3-24: GHI observations as taken in 2014 at Bucholz, Kletzin, and Medrow.

Fig 3-25 illustrates the empirical variograms. Relative root mean square deviation (rRMSE) of the hourly GHI time series at two stations is given over their distance between both stations. Each data point represents a pair of stations being compared. Altogether a typical variogram is derived. It gives insight about the typical variability to be expected as function of distance from the location of any ground measurement. These variograms are largely region dependent.

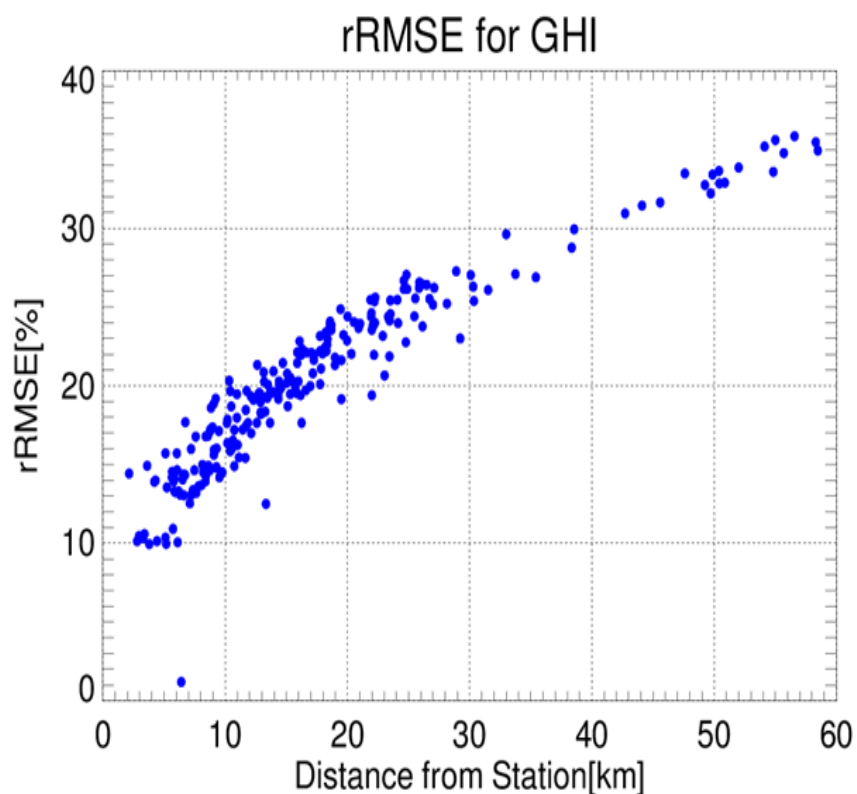
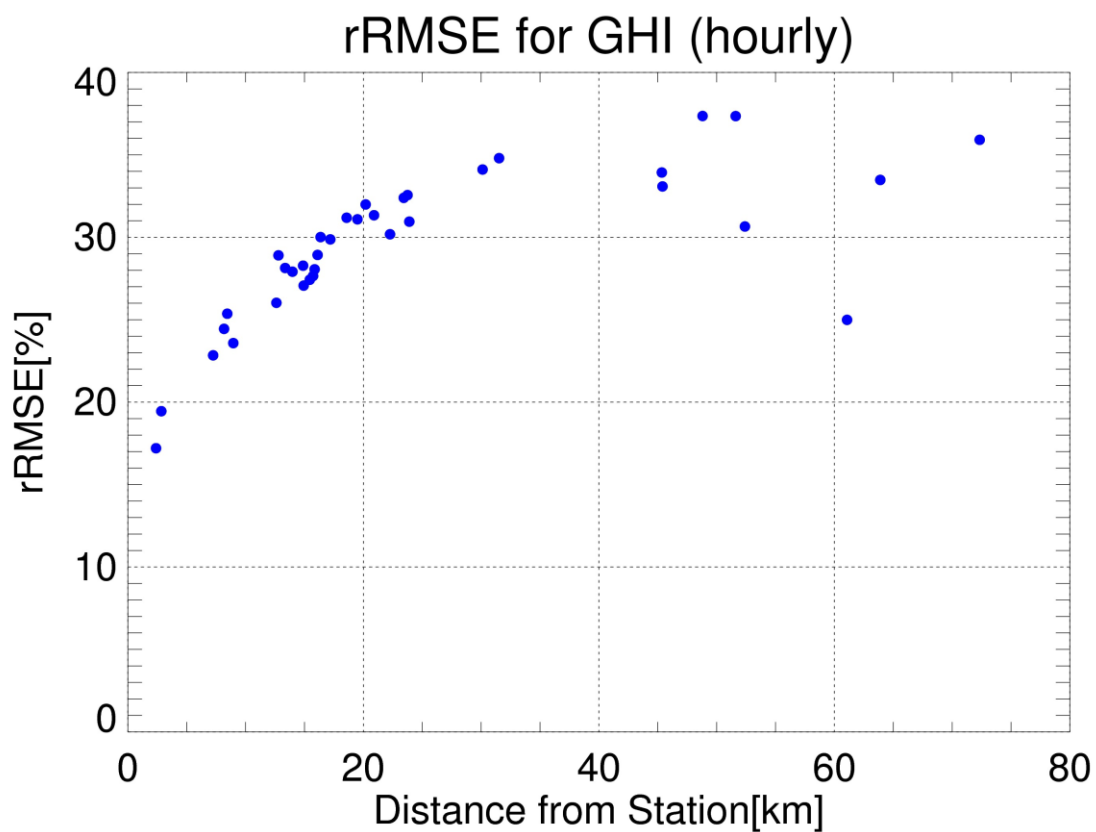


Fig. 3-25: Variogram for hourly resolved GHI observations in 2014 based on DEMMIN stations (upper) and Copernicus CAMS radiation service (formerly known as MACC-RAD) satellite GHI observations at the DEMMIN station locations (see Fig 3-7).

The variograms have been derived on the basis of GHI ground observations and Copernicus Atmosphere Monitoring Service (CAMS) radiation data. The CAMS radiation service has formerly been known as MACC-RAD and used already in OrPHEuS (HS Ulm work in WP3). Here we use the satellite-based observations at the station locations (see Fig 3-7) to compare their variability. As expected the satellite observations show smooth variability due to their pixel size. And therefore, the rRMSE observed in ground data is higher in distances below 40km than observed from the satellite (Fig 3-25).

4 Application area – Understanding failures in heat demand modeling on the whole infrastructure level in Skellefteå

4.1 Stakeholders and their needs

Stakeholders interested are the providers of district heat and operators of district heating networks. In order to maintain the availability of heat for the customers at any time, and to run this heating network profitably, the stakeholders need trustable predictions of the total heat demand in their network. For these predictions, meteorological information is needed as an essential input.

Skellefteå Kraft (SKR), the example stakeholder in this study, is a local energy provider in Skellefteå, and is the operator of the remote heat network at the Skellefteå demo site.

4.1.1 User system

Heat for the district heating network (Fig. 4-0) in Skellefteå is mainly produced in the Hedensbyn combined heat and power (CHP) plant. The CHP has a large hot water tank as storage capacity, making it possible to pre-produce heat in times when higher prices are paid for the also produced electric power. Besides the central Hedensbyn CHP, there are several oil boilers that can be used to cover peaks in heat demand with additional heat demand being not available from the Hedensbyn CHP. As the oil boilers only produce heat but no electricity, SKR has an interest to avoid the usage of oil boilers whenever it is possible.

4.1.2 User requirements

The users' goals are to avoid oil boiler usage whenever it is possible, and to shift heat production at CHP to times of high electricity prices. The meteorological information has to contain forecasts of all parameters that are relevant for heat demand prediction. For some meteorological parameters, the relevance for heat demand prediction still is not fully clear. Additionally, there is no existing study on the forecast accuracy requirements for this purpose. Therefore, in chapter 4.2.3 the relevant meteorological parameters for Skellefteå are identified, including the corresponding forecast accuracies needed.

Following SKR, typical errors being acceptable should not be above than 3-4 K differences in the forecast horizon on the next 2 days, while over the next 3-5 days the general structure of temperatures should be met in order to plan the heat storage state properly. The colder the situation will be the smaller temperature errors should be.

Additionally, the timing of any ramps of more than 3-4 K over time should be well met.

4.1.3 Demo site

This application is of main interest for the Skellefteå demo site.

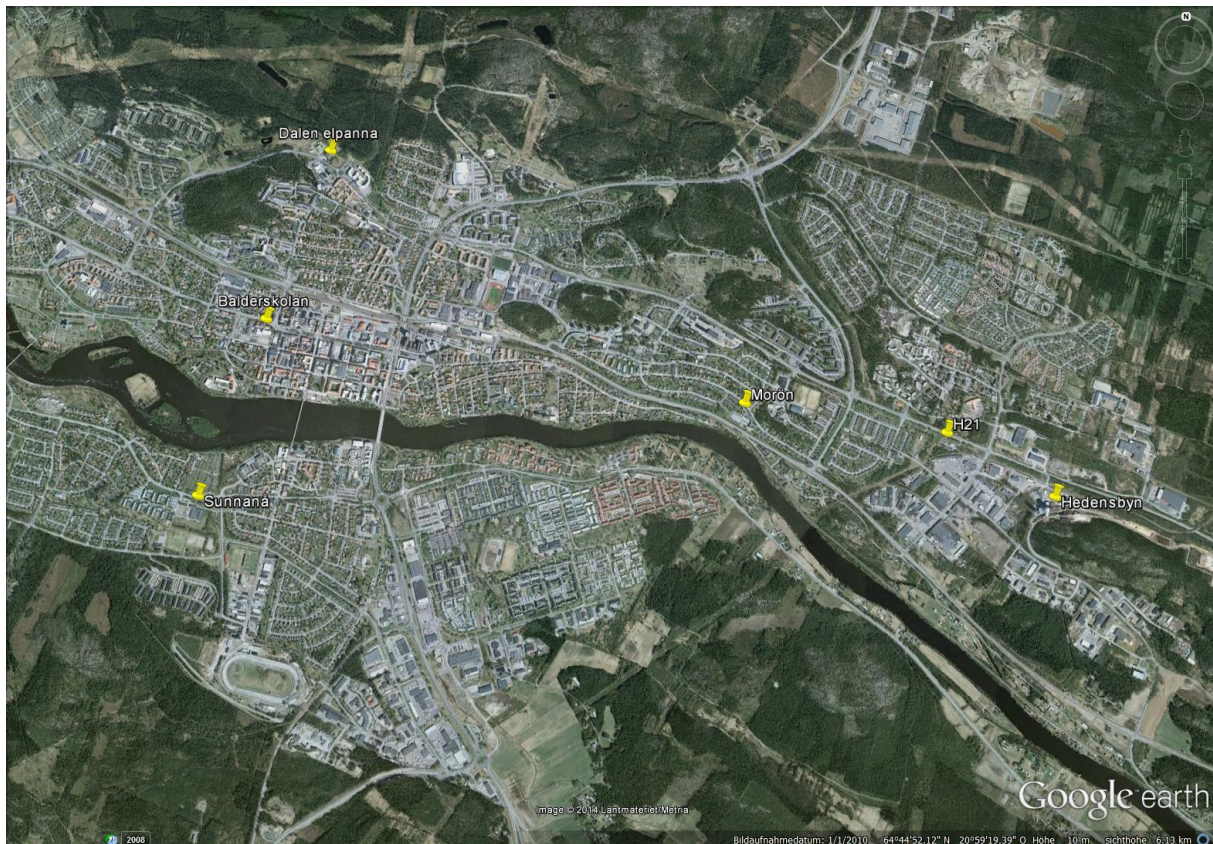


Fig. 4-0: Map of Skellefteå showing the different temperature measurement sites. Sunnanå and Balderskolan are schools, while the other sites are SKR production sites.

4.1.4 Relevant use cases and control problems

Use cases: all

Control setup 1 ('Cooperative green supplier')

4.1.4.1 Relevant use cases and control problems

The application area is of interest for the following use cases: 1 (Phase out of peak oil generation), 2 (Single- vs. multi-utility generation and customer supply), 5 (Dynamic end-user loads), 6 (Special extreme situations). Relevant control setup is Control setup 1 ('Cooperative green supplier')

4.2 Work performed

4.2.1 Study rationale

In chapter 4.1.1.2 of OrPHEuS D3.3.1 report, SKR's requirements for a sophisticated temperature forecast are specified. They contain a temperature error of not more than 3 to 4 K for a forecast horizon of 48 hours, as well as the correct timing of ramps of more than 3 to 4 K.

At the moment, SKR receives temperature predictions for the following day (so, up to 48 hours) from SMHI. This prediction is the best choice of the SMHI meteorologist on duty. The meteorologist on duty chooses between the output of several NWP models, and various post processing methods. The temperature forecast is one of the main data inputs for the heat demand prediction system. To deal

with the occurring forecast errors, the prediction is adjusted by SKR's own temperature measurements, which are currently taken at the Hedensbyn CHP. It has to be noted that the Hedensbyn CHP measurements of air temperature do not fulfill the WMO requirements for air temperature measurements. Therefore, it cannot be expected that any numerical weather prediction can successfully predict the measurements as provided at the CHP (at a location in the sun resulting in radiation errors and not on the standard height above surface). There are always biases to be expected. Even any perfect numerical weather prediction model will only provide a good forecast of the 2 m air temperature measured in a standard WMO configuration. In the following study we want to quantify this effect. This knowledge will allow to further use the Hedensbyn measurements in the daily control.

As SMHI Hirlam E05 (see section 6 model overview) model forecasts are not stored by SKR, DLR has obtained time series of historical forecasts directly from SMHI. Additionally, ECMWF based forecasts are available (see section 7 for a dataset description). By comparing temperature forecasts of both Hirlam and ECMWF models to ground observations both at the airport and at Hedensbyn this systematic effect can be quantified.

Please note that SMHI will change to the AROME model operationally in the future (see section 6.2.2), therefore any assessment of HIRLAM model output is of restricted future use. Only the results for ECMWF will be sustainable. This is one of the reasons to include ECMWF forecasts in our study.

Weather forecast fail due to various reasons. To identify these cases, we have to analyze a relevant time series of forecasted meteorological parameters, in-situ measurements of the same parameters at the demo site, and also data of the modeled and measured heat demand (section 4.2.2).

Besides utilizing any wrong forecast of a parameter, it may also happen, that another geophysical parameter is influencing but no forecast is obtained and used due to lack of knowledge on its relevance. We call this an incomplete input. In our case we investigate if there is another forecast parameter which has an influence on the heat demand, but is not part of the derived meteorological forecast. To identify these parameters, we have to combine the information of failures in heat demand modeling with in-situ meteorological measurements or with NWP reanalysis, respectively (section 4.2.4).

4.2.2 Evaluation of SMHI/ECMWF forecast accuracy for Skellefteå

To analyze the forecast accuracy of SMHI and ECMWF forecasts against a standard observation, we compare first the forecast with measurements taken at Skellefteå airport. There is no other station available in Skellefteå for this purpose, because the other SKR measurement sites in Skellefteå (including Hedensbyn CHP and at all sub-stations as operated by SKR) do not fulfil the WMO requirements for a proper measurement site (see chapters 4.2.3 and 5 of this report). To evaluate the accuracy of ECMWF and HIRLAM E05 model output over all seasons, we analyzed one full year of data (June 2013 to May 2014). For both models the evaluated forecast horizon is up to 48 hours. ECMWF is analyzed in an hourly interpolated temporal resolution, while HIRLAM E05 forecasts are available in 3 hours (up to 24h forecast horizon) and 6 hours (up to 48hours forecast horizon) temporal resolution.

Figures 4-1 (ECMWF) and 4-2 (HIRLAM E05) show colored scatter plots of measured and forecasted temperatures. Colors represent the forecast horizon hour. For visibility reasons there is a separate plot for every 6 hours forecast horizon interval. Measured temperatures are on the X axis, while forecasted temperatures are on the Y axis.

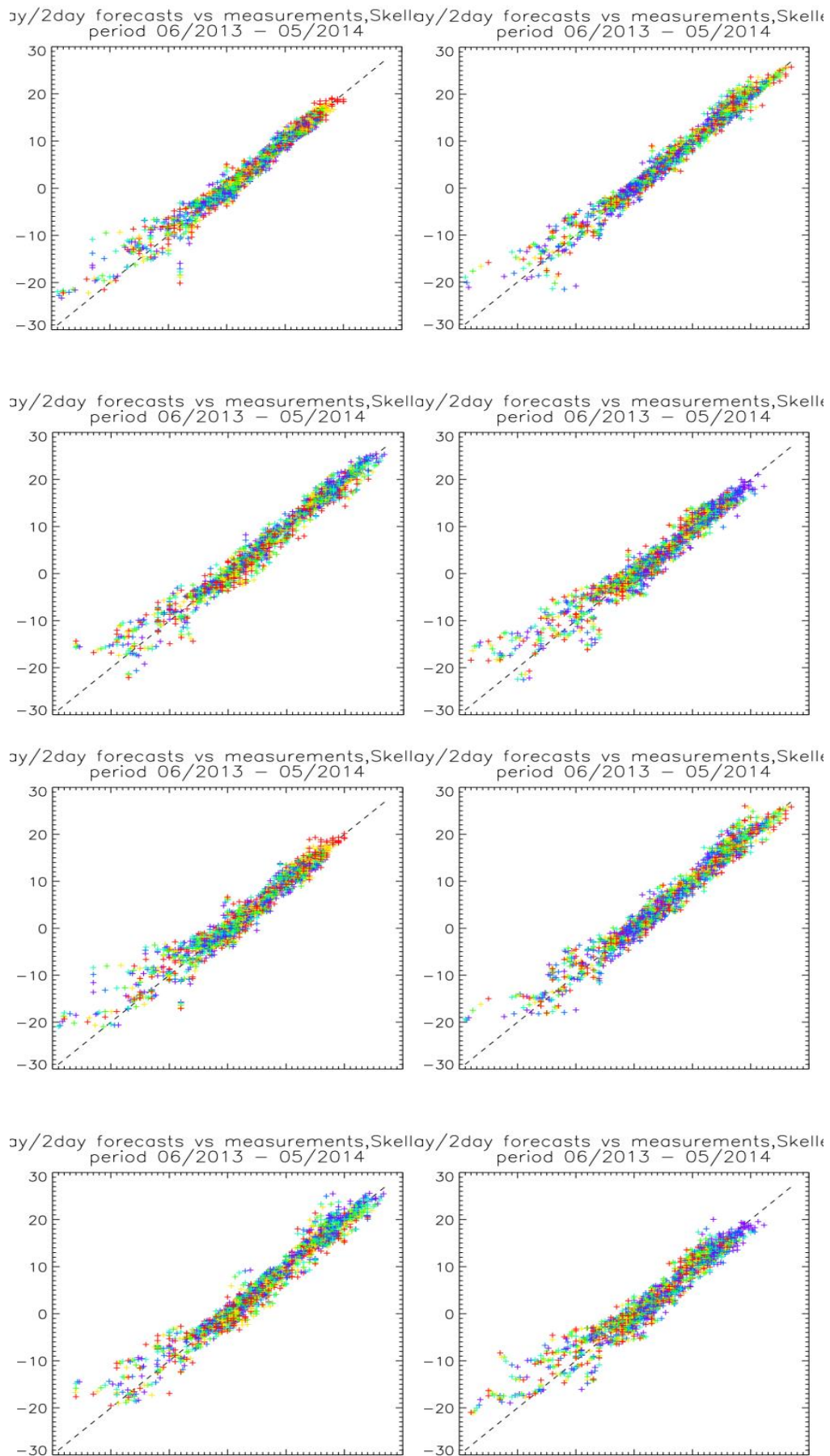


Fig. 4-1: ECMWF temperature forecast vs. measurements taken at Skellefteå airport, plotted separately for various forecast horizon intervals

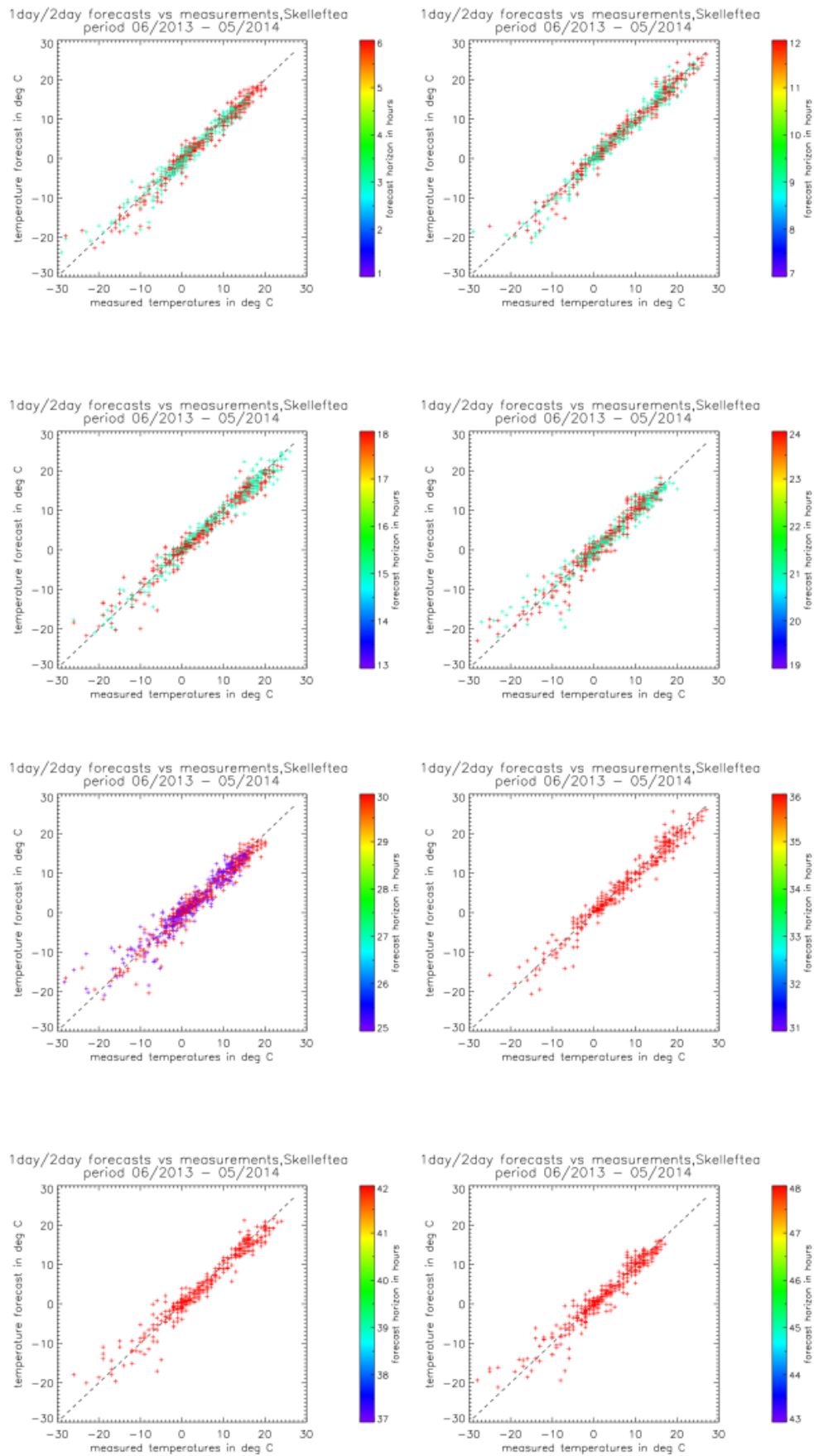
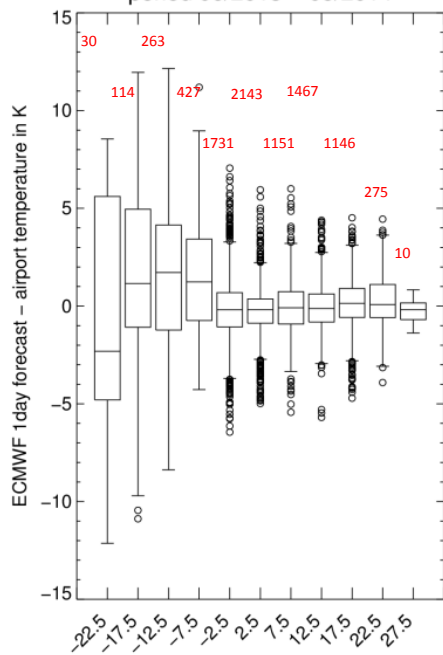


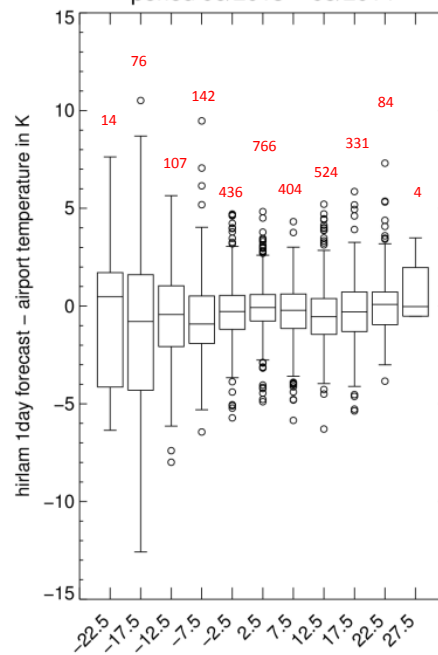
Fig. 4-2: HIRLAM temperature forecast vs. measurements taken at Skellefteå airport, plotted separately for various forecast horizon intervals.

1day ECMWF forecast vs Skelleftea airport measurement, period 06/2013 – 05/2014



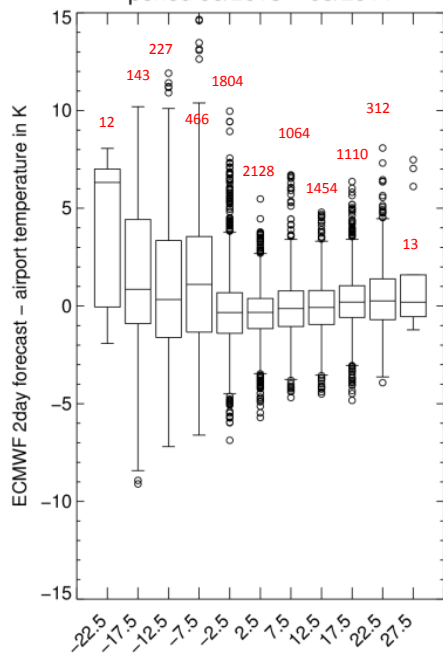
ECMWF 1day temperature forecast in deg C

1day hirlam forecast vs Skelleftea airport measurement, period 06/2013 – 05/2014



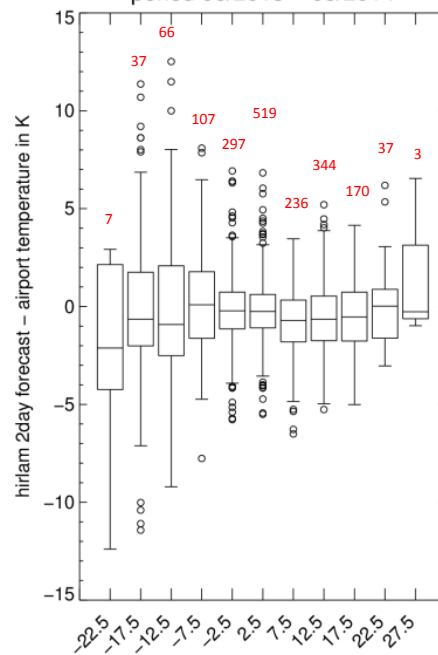
Hirlam 1day temperature in deg C

2day ECMWF forecast vs Skelleftea airport measurement, period 06/2013 – 05/2014



ECMWF 2day temperature in deg C

2day hirlam forecast vs Skelleftea airport measurement, period 06/2013 – 05/2014



Hirlam 2day temperature in deg C

Fig. 4-3: Differences between temperature forecast and measured temperature at Skellefteå airport as function of the forecasted temperature itself. Left column: ECMWF forecasts. Right column: HIRLAM forecasts. Upper row: 1 day (up to 24h) forecast horizon. Lower row: 2 days (from 25h up to 48h) forecast horizon. The number of data points contributing to each bin is printed in red inside the plots.

As the evaluated forecasts are always started at 00UTC, the forecast horizon can also be interpreted as a time of day value here. As Figures 4-1 and 4-2 show, forecast accuracy for both ECMWF and HIRLAM E05 forecasts is not a function of the time of the day. In general, the spread seems to be larger for lower temperatures. Also, differences of more than 10K between temperature forecasts and temperatures are very rare. Plots in Figure 4-3 allow a closer look on the dependency of forecast accuracy and forecasted temperature. Also in these plots the spread in forecast accuracy is larger for lower temperatures.

It has to be noted that the number of data points with very low temperatures is small compared to the number of data points for higher temperature, we have to be very careful with the interpretation of these results. Please divide case numbers (red in Fig 4-3) by 24 to know the number of calendar days being represented.

However, forecast accuracy tends to be worse with falling predicted temperatures for both NWP models and independent from the forecast horizon. This is just the opposite of SKR's announces user requirements, requesting a better forecast accuracy for cold temperatures than for warm temperatures.

ECMWF and HIRLAM E05 forecasts do well agree in their predictions, when predicted temperatures are high. For very low temperatures, the predictions differ more often (see Figure 4-4) and generally, the spread of the box-whiskers increases (Fig. 4-3). The difference in the temperature predictions between the two models for low temperatures is not systematic for all cases.

Figure 4-3 indicates that in those cases within June 2013 and May 2014 with low temperatures, the HIRLAM performs slightly better than ECMWF. This most probably reflects the better regional adaptation of the regional model. Nevertheless, due to the small number of low temperature cases this cannot be generalized. Further years should be investigated up to a 10 year period.

The question if differences in the 24hour and 48hour forecast for a certain day (this is also called "jumpiness") can be used as an indicator for the expected forecast accuracy can be answered with help of Figure 4-5. Both ECMWF and HIRLAM E05 jumpiness cannot be used as a warning system for large prediction errors.

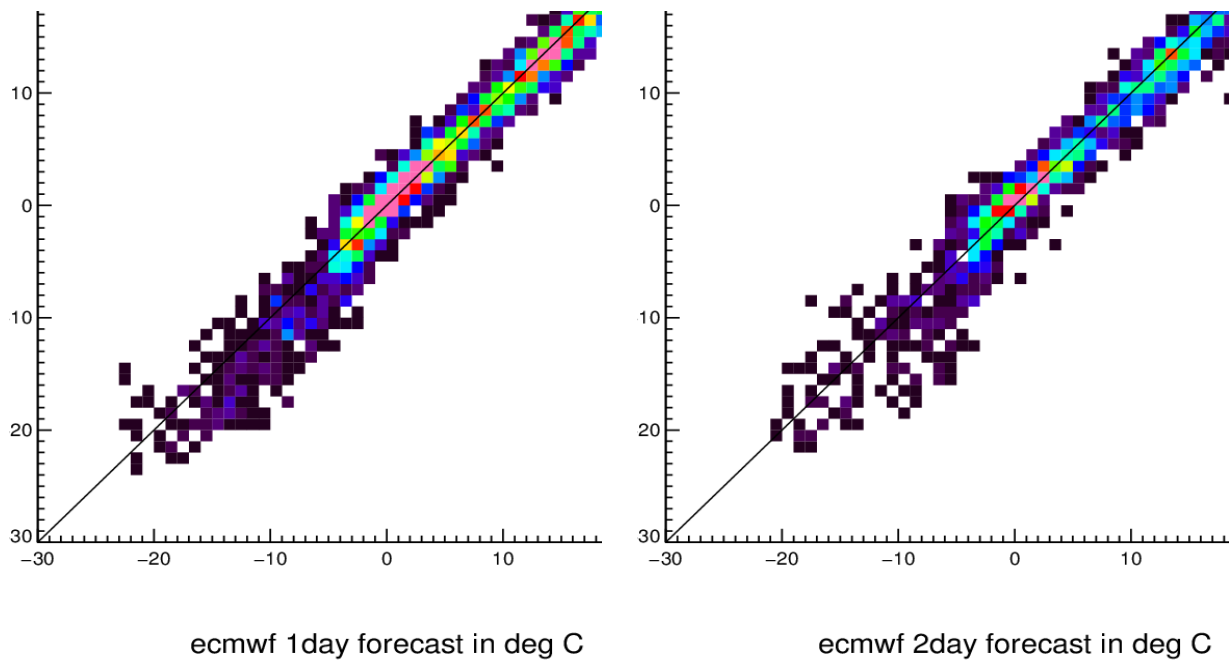


Fig. 4-4: Density scatter plot of ECMWF and HIRLAM E05 24 hour forecasts (left side) and 48h forecasts (right side). Each color represents a number of counts, explained in the color bar at the right side of the plots.

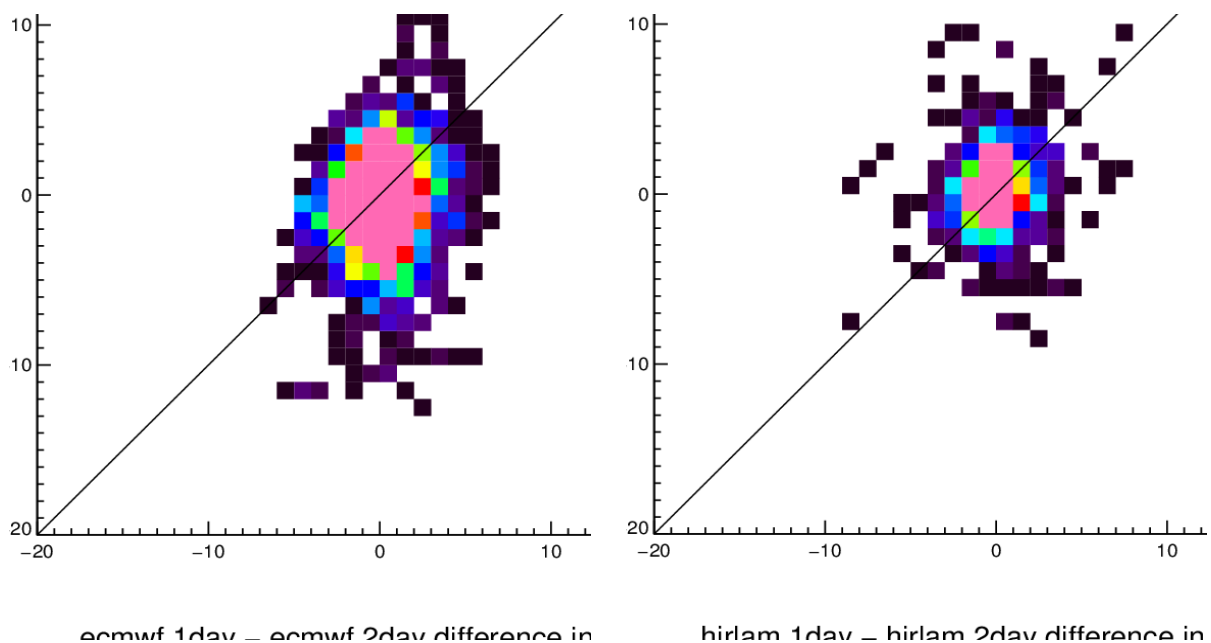


Fig. 4-5: Scatterplot of deviation of measurements from 1day forecasts vs differences between 1day and 2 day forecast ("jumpiness"). Left side: ECMWF forecasts. Right side: HIRLAM E05 forecasts

4.2.3 Assessment of SKR measurements and measurement sites (including Balderskolan)

In this subchapter we check for each measurement site separately, if the WMO criteria introduced in chapter 4.1.2.2 of D3.3.1 report are fulfilled. Therefore, we analyze photographs of the measurement devices of each measurement site, as well as the environment. Figure 4-6 gives a brief overview of all substations locations.

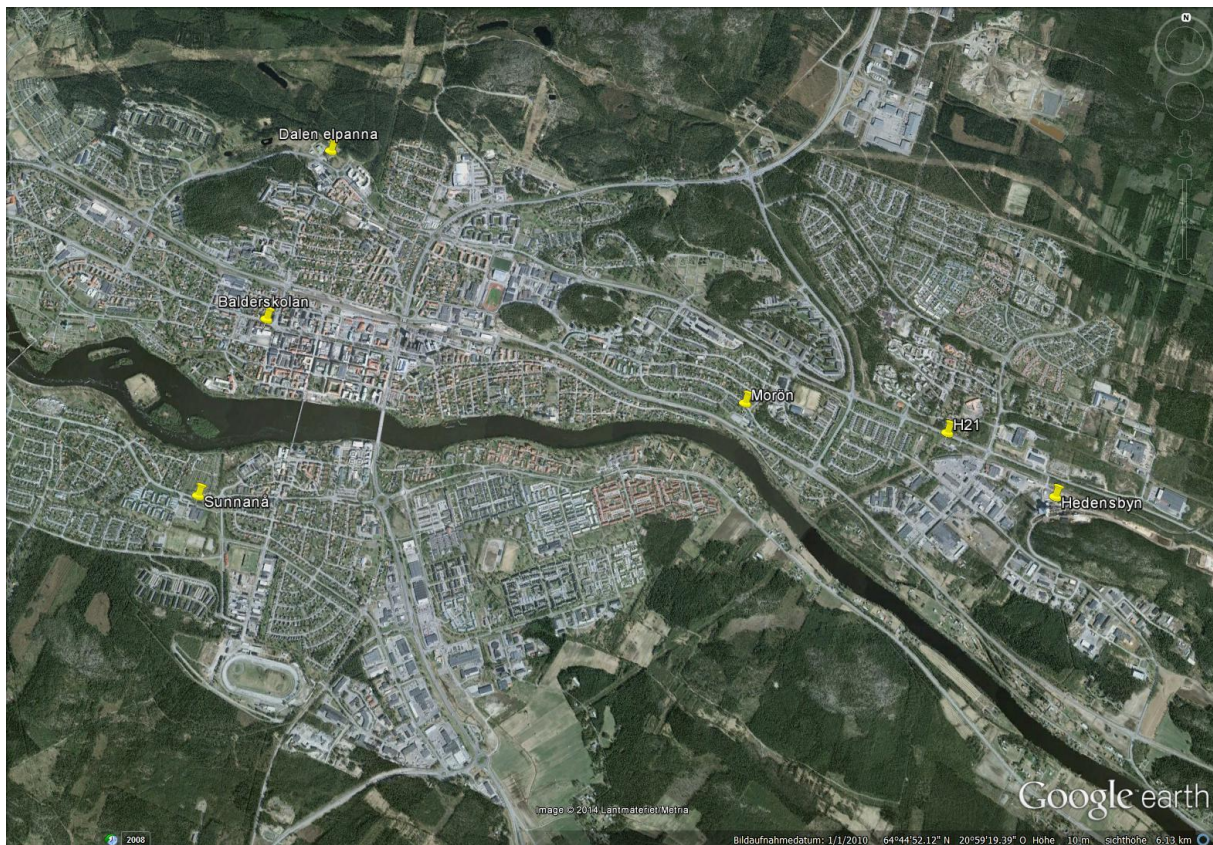


Fig. 4-6: Map of SKR measurement sites and Balderskolan. Image: Google earth. Coordinates: SKR

4.2.3.1 Assessment of SKR measurement site Dalen

The temperature measurement device at Dalen measurement site is placed directly at the building's wall. This wall is exposed to the northwest. Each sunny afternoon starting at around 3p.m., the wall is exposed to the sunlight. As the building wall is made of metal and painted in a dark brown color, temperature measurements at Dalen site are strongly affected by the sunlight and will not measure the ambient temperature. Although the measurement devices are protected from direct sunlight, the whole wall heats up under sun exposure and this heat is conducted to the measurement devices by the metal wall (See Figure 4-7). Thus Dalen measurement site surely does not fulfil the WMO requirements for temperature measurement sites.

4.2.3.2 Assessment of SKR measurement site Morön

Also at Morön measurement site, measurements are taken directly at a building's wall. Unlike the Dalen site, this wall is painted in a very bright grey, and at least parts of the wall are permanently shaded by the roof. The wall is exposed to the northeast. For this reason, it is possibly exposed to direct sunlight during the morning hours in summer. The measurement device itself is very likely shaded most of the time but it is very close to the roof, which is painted in a dark brown and is certainly strongly affected by heating from the sun (see Figure 4-8). For that reason and the direct installation at the wall, Morön site does not fulfil WMO's requirements.



Fig. 4-7: Photograph of temperature measurement devices at the Dalen substation. Photograph was taken by SKR.



Fig. 4-8: Photograph of temperature measurement devices at the Morön substation. Photograph was taken by SKR.

4.2.3.3 Assessment of SKR measurement site H21

H21 measurement site's devices are installed directly at the wall of a metal container (see Figure 4-9). The wall is exposed to the west, which results at direct sunlight exposure starting at around noon. The measurement device is not shaded at all. The container is painted in a dark grey. For these reasons, also H21 measurement site does not fulfil the WMO requirements.



Fig. 4-9: Photograph of temperature measurement devices at the H21 substation. Photograph was taken by SKR.

4.2.3.4 Assessment of SKR measurement site Sunnana

Like all previously assessed SKR substations, the measurement device at Sunnana substation is directly placed at a building wall, just a few centimeters above a door (see Figure 4-10). The wall is exposed to the north, with a shading roof above the measurement device. Although the measurement device appears not to be directly exposed to the sunlight, it does not fulfil WMO's requirements.

4.2.3.5 Assessment of Balderskolan measurement site

Balderskolan's measurements are not taken by SKR, but by the school itself. They contain temperatures, and also global radiation, wind speed, wind direction and relative humidity. Google StreetView images show a typical meteorological measurement configuration on the roof-top. Therefore, Balderskolan's meteorological data is expected to be much more reliable than the data from SKR's substations.



Fig. 4-10: Photograph of temperature measurement devices at the Sunnana substation. Photograph was taken by SKR.

4.2.4 Study on meteorological Parameters influencing heat demand in Skellefteå

This section focuses on the impact of the different meteorological parameters on the heat demand in Skellefteå. The goal is to identify the relevant parameters.

Previous studies examined the relation between meteorological parameters and the heat demand of single households (Nielsen and Madsen, 2000 and 2005) or district heating networks (Wojdyga, 2008). They agree that the ambient temperature is the most important meteorological parameter affecting heat demand. Also, global radiation and humidity are identified as important parameters, whereas wind speed seems to be less important.

To check the importance of the meteorological parameters temperature, global radiation, relative humidity, wind speed and wind direction, measurements from Balderskolan (all these parameters) and from the Hedensbyn CHP (temperature) are used.

Data for the heat vs. temperature scatter plot (Fig. 4-11) was provided by SKR. It gives a first impression that temperature is the most important meteorological parameter for heat demand predictions. But as heat demand differs for the same temperatures also as a function of the calendar month, we expect at least one additional meteorological parameter influencing the heat demand in the network. SKR mentioned that global irradiance might be this additional parameter.

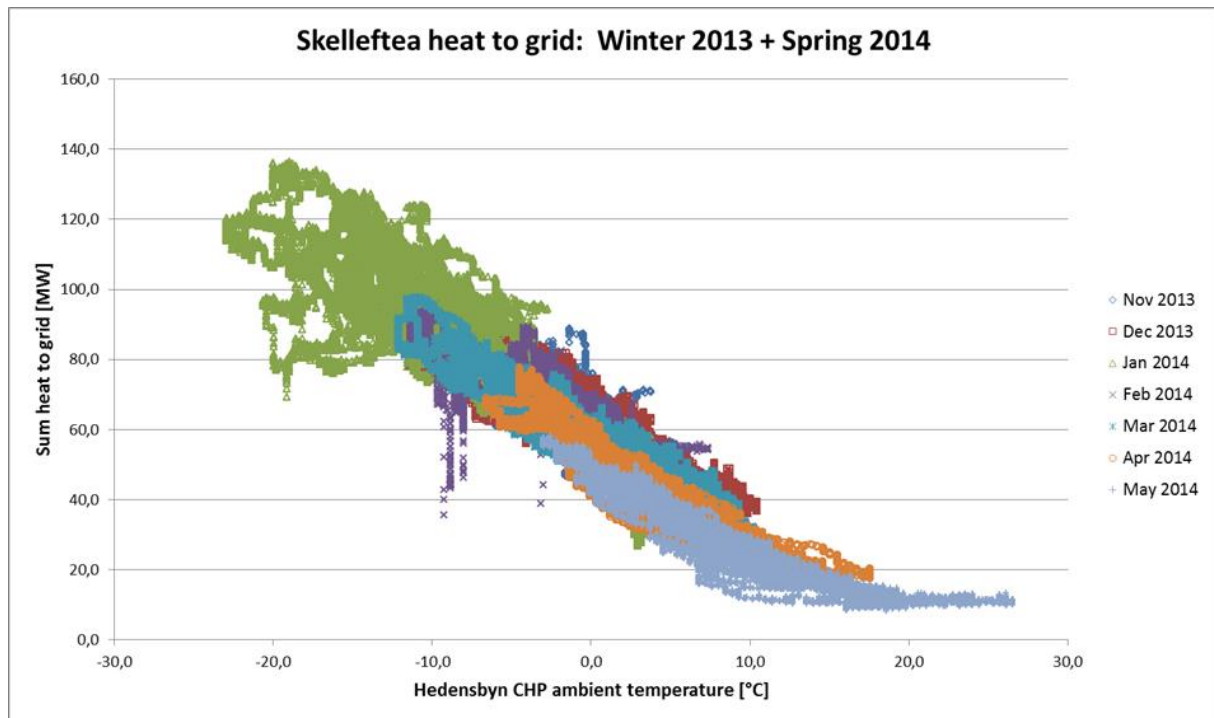


Fig. 4-11: Plot of heat sum fed into the heating network vs. the measured ambient temperature at Hedensbyn CHP, for the period from November 2013 to May 2014. Each month is plotted in a different color.

While the values in Figure 4-11 all were taken every second, Balderskolan data has a resolution of 30 minutes. Therefore, the following analysis uses 30min averages of ambient temperature and heat to grid data from Hedensbyn CHP. All hours of the day including night time are included.

Table 4-1 shows the correlation of Hedensbyn heat to grid to the analyzed meteorological parameters. A correlation of zero implies that there is no statistical relation between the two variables, while a correlation of one is the strongest possible relation. A minus sign indicates that while values of one variable are rising, the values of the other variable are falling. For example, heat to grid values rise when the temperature falls. Thus the Pearson correlation of these two variables is negative (-0.93, see Table 4-1). The strongest correlations have been found between heat to grid and ambient temperature (-0.93), followed by GHI (-0.38) and relative humidity (0.24, the only positive correlation). Wind speed and wind direction's correlation with heat to grid values are very close to zero, so that their influence on heat demand is negligibly small.

Table 4-1: Pearson correlations of recorded heat to grid vs meteorological parameters taken at Hedensbyn CHP and Balderskolan.

	Pearson correlation
Temperature at Hedensbyn CHP	-0.93
Balderskolan GHI	-0.38
Balderskolan relative humidity	0.24
Balderskolan wind speed	-0.08
Balderskolan wind direction	-0.05

Pearson correlation statistics has been motivated by previous work from (Nielsen and Madsen, 2000 and 2005). Nevertheless, our further investigation illustrates, that the dependence on GHI, relative humidity, wind speed, and wind direction is by no means linear. Therefore, this parameter is not suited to describe the data distribution.

Figures 4-12 to 4-16 show the relations of heat to grid (H2G) and the meteorological parameters GHI, relative humidity and wind in detail for the whole 1 year period. There is no clear overall dependency visible for GHI and relative humidity. Please note that GHI close to zero is certainly night time and very low GHI approx. $< 50 \text{ W/m}^2$ mostly originate from morning and afternoon hours in twilight conditions. For hours with $\text{GHI} > 50 \text{ W/m}^2$, the H2G has a very low sensitivity on GHI in the annual plot. For the wind direction a peak in high H2G values can be found for easterly and north-western winds and reflects the local orography and the frequency of weather situations occurring as a result of that.

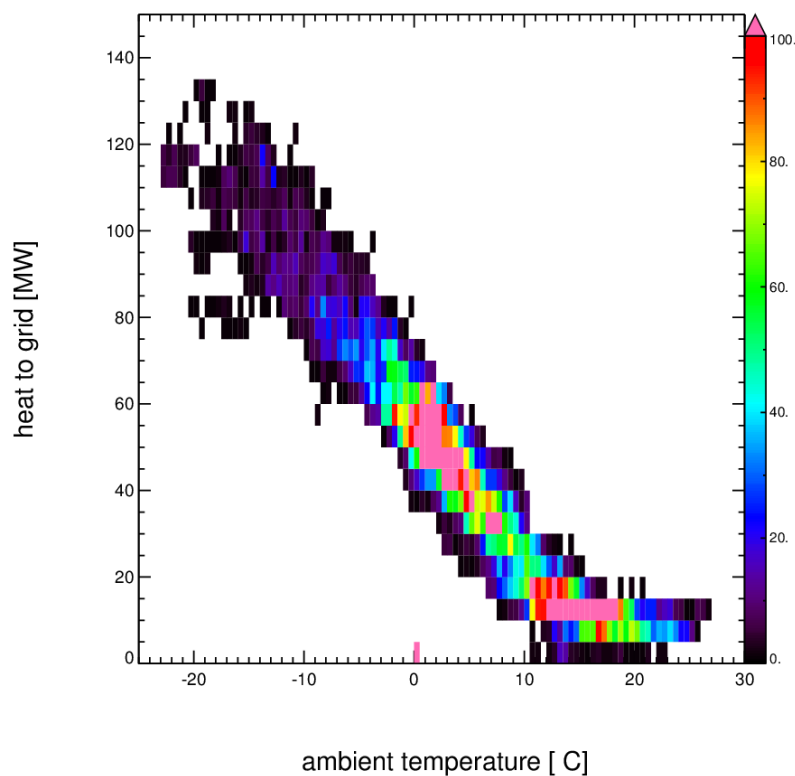


Fig. 4-12: Density scatter of the total SKR network heat to grid in MW vs Balderskolan's ambient temperature in °C. The Colour represents a number of counts, which is indicated at the right side of the figure.

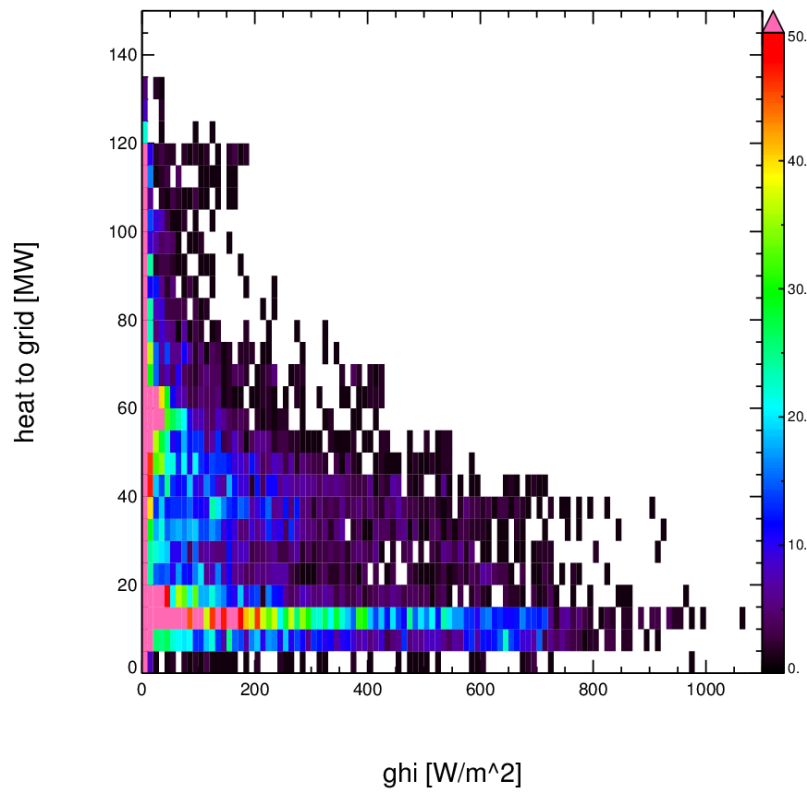


Fig. 4-13: Density scatter of the total SKR network heat to grid in MW vs Balderskolan's global horizontal irradiance (GHI) in W/m². The colour represents a number of counts, which is indicated at the right side of the figure.

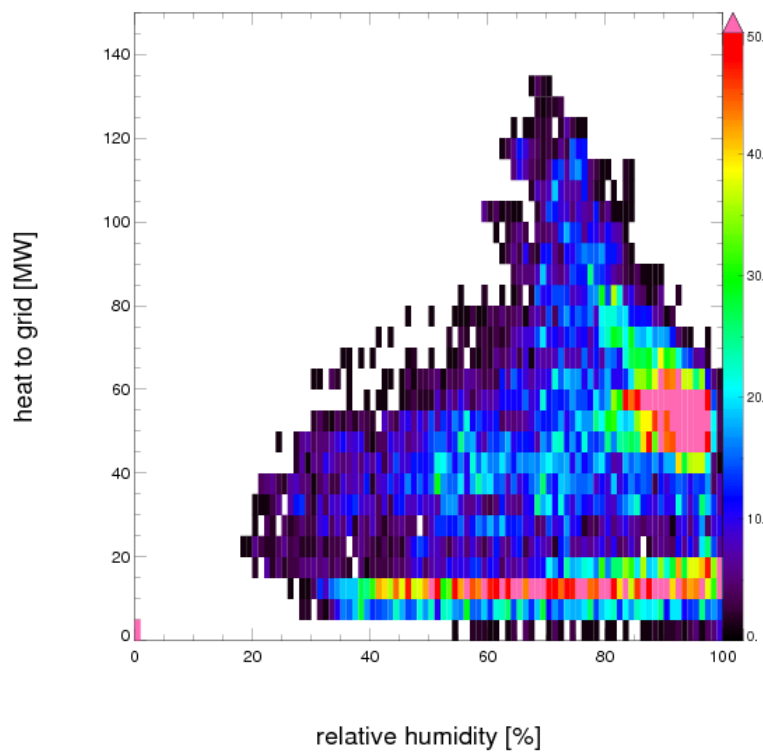


Fig. 4-14 : Density scatter of the total SKR network heat to grid in MW vs Balderskolan's relative humidity in %. The colour represents a number of counts, which is indicated at the right side of the figure.

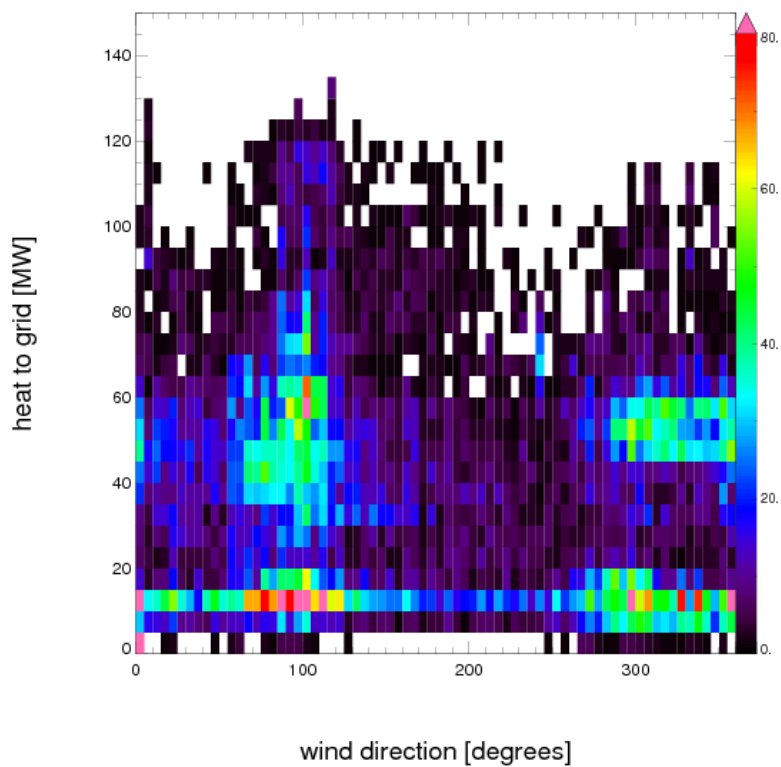


Fig. 4-15: Density scatter of the total SKR network heat to grid in MW vs Balderskolan's wind direction in degrees. The Colour represents a number of counts, which is indicated at the right side of the figure.

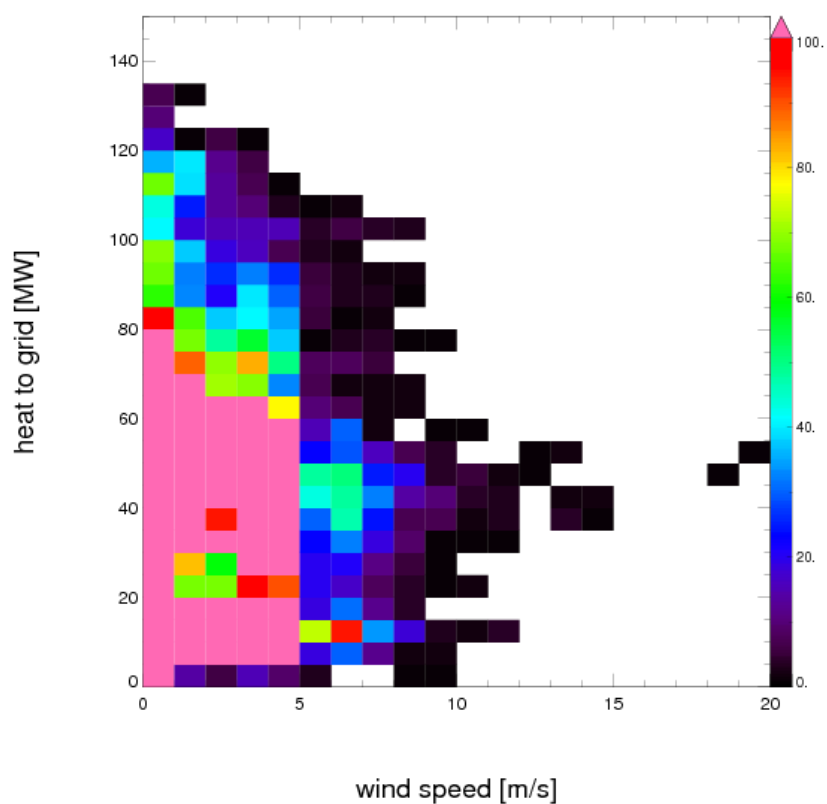


Fig. 4-16 : Density scatter of the total SKR network heat to grid in MW vs Balderskolan's wind speed in m/s. The Colour represents a number of counts, which is indicated at the right side of the figure.

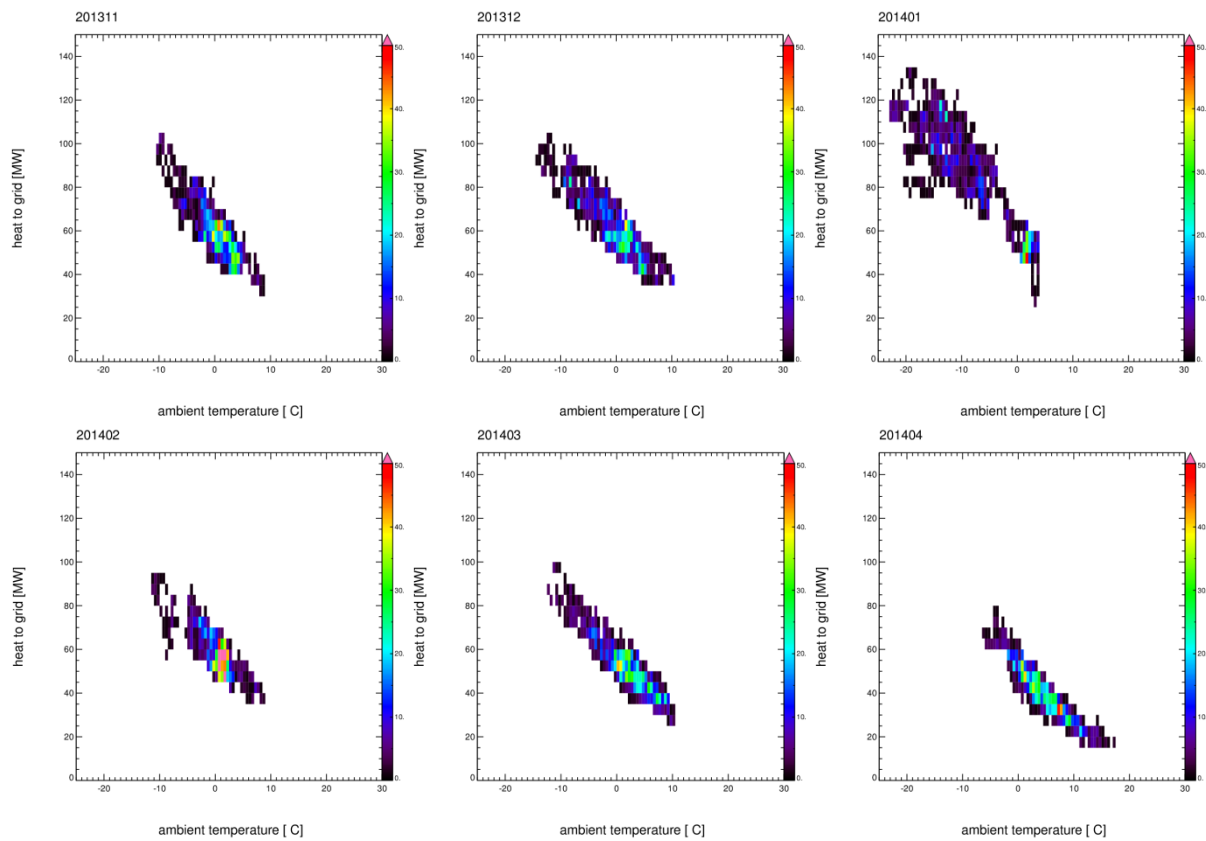


Fig. 4-17 Monthly Hedensbyn heat to grid vs ambient temperature density scatter plots from November 2013 to April 2014, with number of counts indicated as color.

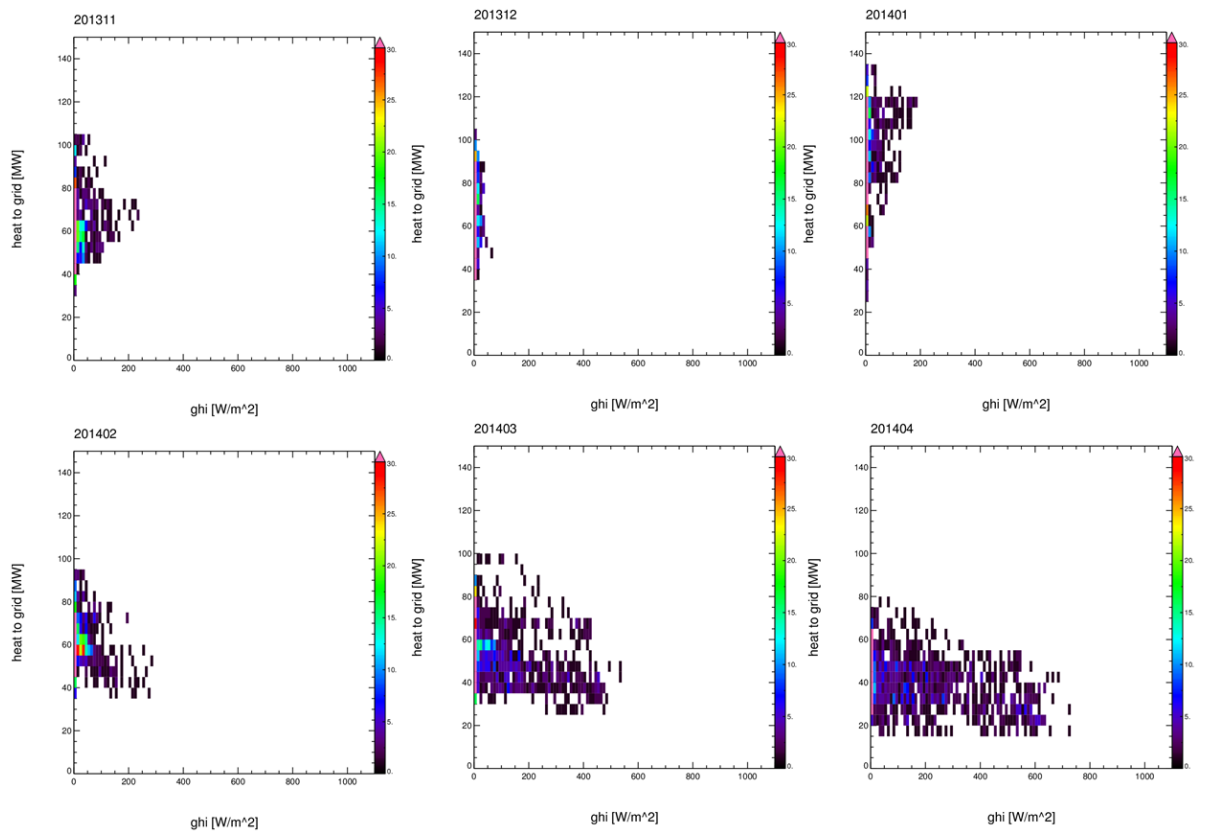


Fig. 4-18: Monthly Hedensbyn heat to grid vs GHI density scatter plots from November 2013 to April 2014, with number of counts indicated as color.

Following the literature, GHI and relative humidity are typically found as relevant parameters for heat demand in buildings. In order to compare with Fig. 4-11 we split the dependences to all parameters in the same months. Fig. 4-17 shows density scatter plots of heat to grid vs ambient temperature like in Fig. 4-12, but separately for the months from November 2013 to April 2014. Regarding this monthly plots, we find that there generally is a large area of overlap between two subsequent months. Heat to grid values in the same temperature interval seem not to shift from one month to another and also the width of the distribution (perpendicular to any imagined line fit) is quite similar (with exception of January). So, the first impression from Fig. 4-11 about the dependency of the H2G vs temperature dependence on the month and especially in the spring months cannot be confirmed. This was the hypothesis raised by SKR and the motivation of this study.

4.2.4.1 H2G vs ambient temperature

Remarkably is the large scatter in the very cold situations in January. In January, the dependence of H2G from ambient temperature is less clear than in other months. This holds especially for the below -10°C cases. This cannot be caused by the speculated influence of irradiances. Irradiance in January is very low (Fig 4-18) and therefore, it cannot be assumed that irradiance provides a significant additional energy source influencing the thermal balance and the thermal needs/demand.

Also, the linearity of the H2G vs temperature relation is less given for April (and May, see Fig. 4-11) where the density plots get a more 'banana like' form. We follow SKR's view that there is any meteorological independent process causing a minimum H2G supply needed independent on temperature in warm conditions (e.g. hot water demand still existing, but less heat demand).

At this point of the study we conclude, that a temperature based control is possible in November, December, February, and March; and also in April onwards if taken the 'banana-like' form into account. Only the very cold cases in January show a large deviation from any imagined fit line being used as control rule. We assume, that there is any other process influencing H2G besides air temperature and GHI in the very cold cases.

4.2.4.2 H2G vs GHI

In order to understand if GHI is still responsible for the width of the H2G – temperature relation, we investigate in more detail the monthly dependence on GHI to follow the ideas of SKR about any not yet included GHI influence in spring. We also analyze monthly Balderskolan global irradiation data as the only available reliable GHI observation inside Skellefteå. Monthly density scatter plots of heat to grid vs GHI in Fig. 4-18 show that in late winter and early spring months, rising GHI values in are accompanied by a drop in heat to grid values. This relation can also be found in September and October (not shown), but there it seems to be weaker. In summer (not shown) and December/January, this relation cannot be found.

It has to be noted, that high GHI values are most of the time accompanied by relatively high temperatures. But a direct comparison of temperature vs GHI shows a remarkable scatter, both parameters are linearly correlated in spring months, but not very strongly. Therefore, GHI may add additional information into a control procedure independent of temperature. Nevertheless, it has to be checked if this additional information content is of any relevance in the control procedure at all.

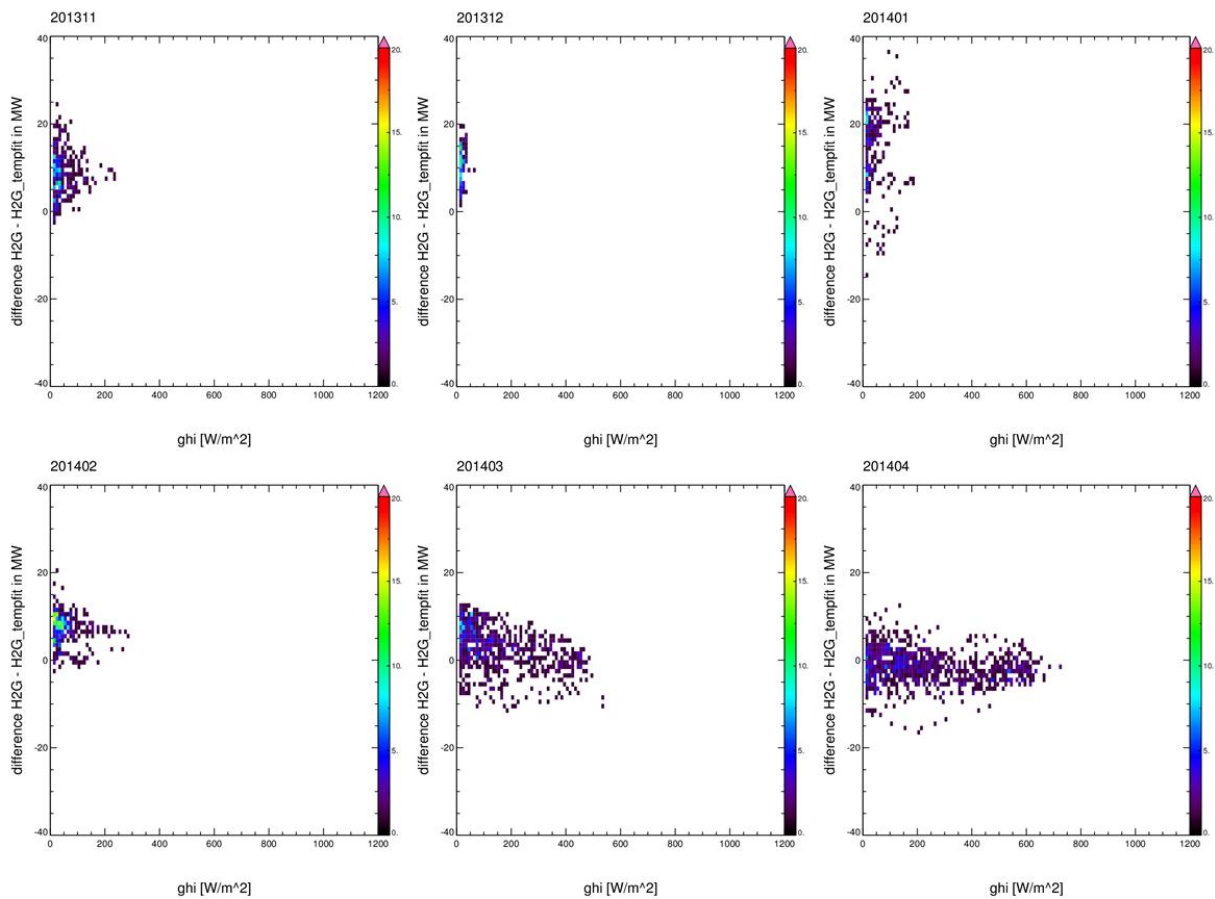


Fig. 4-19: Difference of measured H2G – H2G temperature fit vs Balderskolan GHI. Only day values with GHI values greater than $10\text{W}/\text{m}^2$ are taken into account here.

Based on Fig 4-17 a linear fit of H2G vs temperature has been derived as

$$\text{H2G_fit} = -2.8096328 \cdot \text{temperature} + 55.885820 \text{ in MW}$$

Plots of measured H2G deviation from the H2G -temperature fit are plotted vs measured GHI in Fig. 4-19. They illustrate the deviation from a purely temperature driven control of H2G. They support the thesis of GHI as additional information in February and March. This is also the case in autumn, but just in October (not shown here). In winter and summer GHI tends not to be a meaningful additional parameter in heat demand modeling. It has to be noted, that a shift in time between GHI and response in H2G could not be observed. This has been checked with similar scatter plots like in Fig. 4-19 but with a shifted time of 30 min, 1 and 2 hours (not shown here).

And we recall that we cannot explain the large H2G vs temperature scatter as seen in 4-17 in January by the GHI (as already discussed above).

4.2.4.3 H2G vs ambient relative humidity

As monthly density scatter plots of heat to grid vs relative humidity in Fig. 4-20 show totally different patterns in spring than in winter months. For March and April no relation between H2G and relative humidity can be found, and the same is seen for other summer months (not shown here). For November to February a linear related small part of the density plot can be found for high relative humidity and therefore probably cloudy or very humid (night time?) situations, but the cases with lower humidity with constant H2G values being independent of relative humidity occur often as well.

January differs significantly from the other months: The large H2G values are closely connected to relative humidity between 60 and 80 %, while larger relative humidity close to 100% shows low H2G values. It is assumed that the latter cases consist of either very humid (e.g. night time close to fog situations in the valley around the river) or cloudy situations where ambient temperature tends to be warmer. Clouds and large humidity typically prevent the ground from an extreme cooling like a 'feather bed'.

For the large H2G values > 60 MW we recall, that they are connected to cold temperatures below -5°C and the H2G values > 80 MW occur at temperatures below -10°C. For such small air temperatures, the relative humidity measurement is typically at the edge of the measurement range as the absolute humidity is getting extremely low. Therefore, the scatter is expected and most probably contains no useful systematic information, but reflects the noise of the relative humidity sensor in such conditions. When removing these values in Fig. 4-20, the difference in the January image compared to the other months disappears. Please note, that this measurement restriction in low temperature cases most likely affects only the relative humidity measurement, but not the temperature measurement itself. Therefore, the large H2G scatter vs. air temperature in January is still not explained.

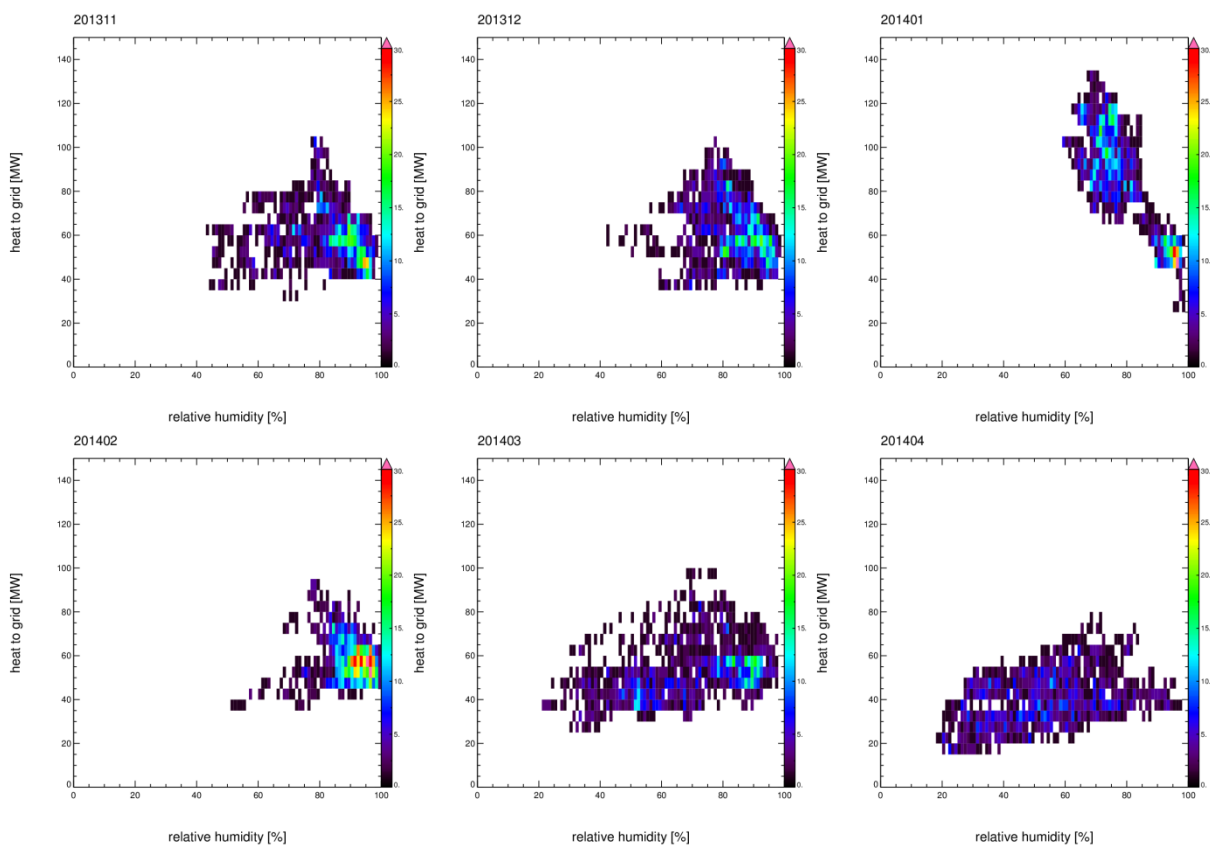


Fig. 4-20: Monthly Hedensbyn heat to grid vs relative humidity density scatter plots from November 2013 to April 2014, with number of counts indicated as color.

A comparison of measured H2G deviation from H2G temperature fit like in Fig. 4-19, but as a function of relative humidity instead of GHI, shows no clear correlation in winter and spring months. On the other hand, for the summer months a clear correlation is observed (see Fig 4-21). During

these months H2G is significantly reduced when relative humidity is high, while dry air is aligned with higher H2G values.

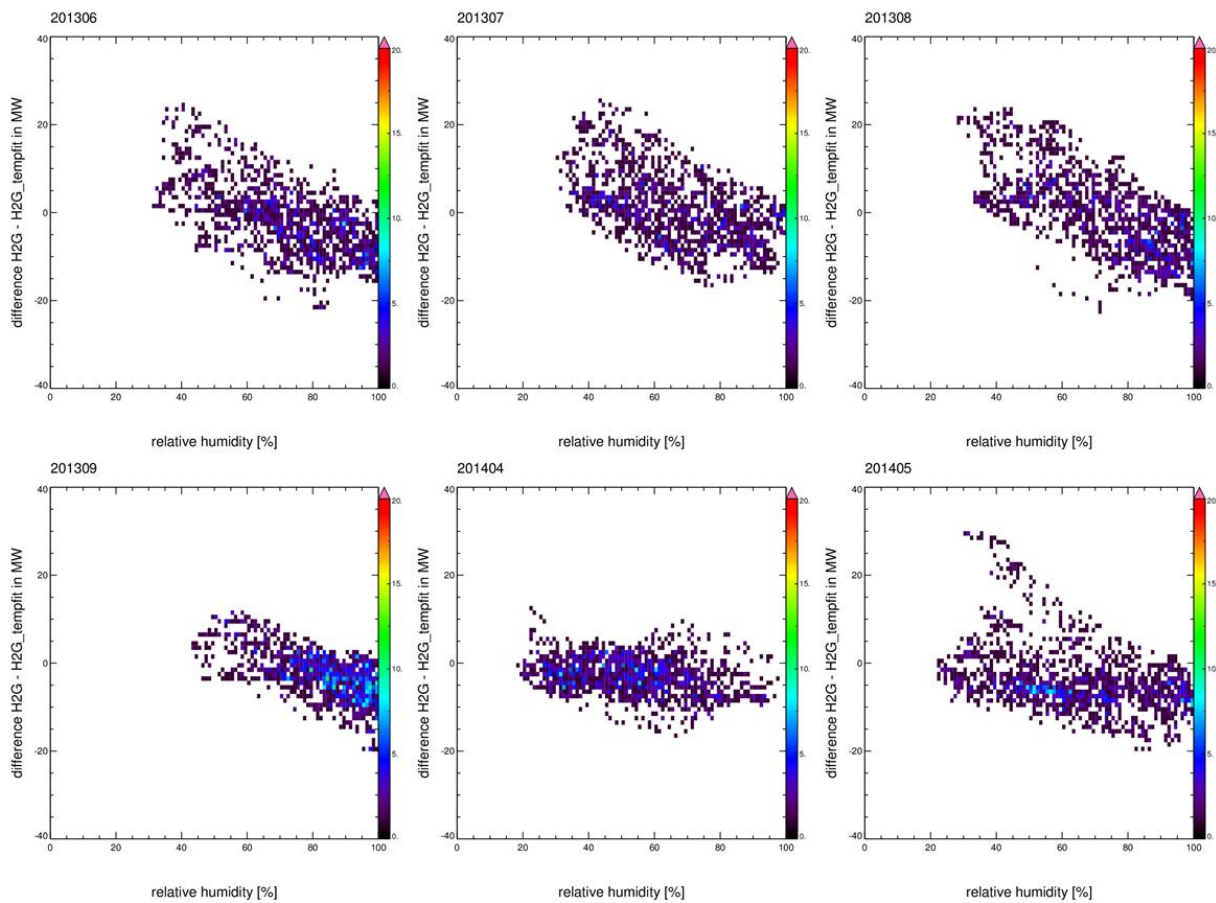


Fig. 4-21: Difference of measured H2G – H2G temperature fit (function: $H2G_{fit} = -2.8096328 * temperature + 55.885820$ in MW) vs Balderskolan relative humidity. Shown months are June to September 2013 and April to May 2014.

In order to identify the relevant meteorological parameters influencing heat demand, we analyzed their impact on H2G values. Results show that temperature clearly is the dominant parameter, while the importance of GHI and relative humidity depend on the season. GHI is mostly relevant in spring and autumn, while relative humidity should be taken into account during summer months.

4.2.5 Study on failures in temperature predictions in Skellefteå

While chapter 4.2.2 contains a general analysis of forecast accuracy in Skellefteå, specific cases with large prediction errors are focused here. The goal is to identify circumstances under which these large errors are likely to occur. Like in chapter 4.2.2, both ECMWF and HIRLAM model outputs are compared to temperature measurements taken at Skellefteå airport. All three large deviations over more than 1 or 2 hours duration between forecasted and observed temperature occur in high pressure systems. This cannot be interpreted that always in high pressure systems, the forecast fails. But if it failed largely during the period investigated, always high pressure system situations are present.

These three specific cases during the cold temperature season are presented here:

- a case with predicted temperatures more than 10K warmer than measurements (19th Jan.)
- a case with predicted temperatures more than 10K colder than measurements (20th Jan.)
- a case with a missed ramp event (28th Jan.)

The first specific case is the 19th January 2014. During the whole day, measured temperatures are significantly below predictions of both models and for both 24 hour and 48 hour forecasts. Left side of figure 4-22 shows model output and measurements. This specific day is aligned with a strong high pressure system over the northern part of Baltic Sea, covering also large parts of north west Russia (see Wetter3.de GFS reanalysis in figure 4-20 right side).

The high pressure system remains present during 20th January 2014 (2nd case discussed), extending its covered area to the East (Figure 4-23 right side). During the first hours of that day, measured temperatures remain significantly lower than all shown predictions. Then temperatures start to rise until noon, reaching a constant level of roughly -5°C. This ramp is well met also in the weather forecasts. Starting at around 16UTC, all forecasts drop significantly below that level. But the predicted temperature drop does not occur, and in the late evening the measured temperatures are about 10K above the predictions.

Just the opposite case is shown in Figure 4-24. On January 28th around noon, measured temperatures start to drop about 15K within 10 hours. This drop is not predicted by any of the models (Figure 4-24 left side). As GFS reanalysis in right side of Figure 4-21 shows that the weather situation Scandinavia is again strongly influenced by a large high pressure system, this time with a core over north west Russia.

For all the specific cases shown here, large high pressure systems dominate weather conditions in the Skellefteå area. They are aligned with winds from East to Southeast, and they are not fully covered by the HIRLAM E05 model domain, because of their enormous size and their extension to the East. Generally, model domains are selected with respect to the major upstream direction. For the Northern European countries the major upstream direction is typically to the West. But these cases show an atmospheric flow being dominated from the east and seem to be not fully covered in HIRLAM in the E05 model domain.

The ECMWF model domain is global. But also the ECMWF is not capable to model these high pressure systems sufficiently well. The ECMWF model is used to provide boundary conditions in the large scale HIRLAM model domain C11. Please note, that with the change to AROME, another global model will be used to provide boundary conditions. So, these findings may change.

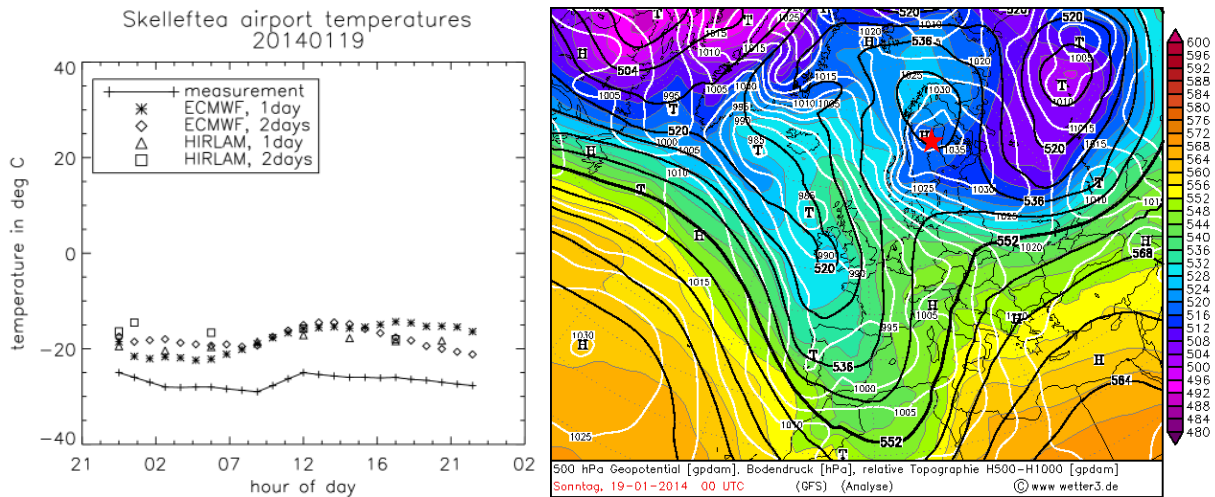


Fig. 4-22 left: Skellefteå airport temperature measurements vs ECMWF and Hirlam forecasts on 19th January 2014. Right: GFS reanalysis of Europe, the Mediterranean area and the Northern Atlantic Ocean for 00:00 UTC on 19th January 2014. White lines indicate isobars at ground level. Color information (relative topography between 1000hPa and 500hPa levels) and black lines (geopotential at 500hPa level) can be ignored for the purpose of this report. Source: Wetter3.de. We have marked the location of Skellefteå with a red star.

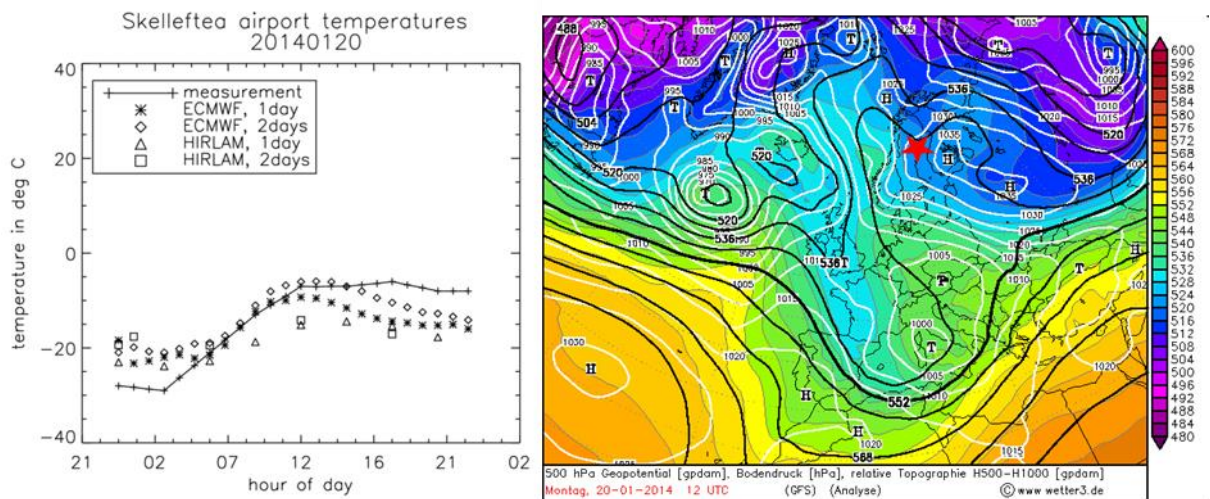


Fig. 4-23 left: Skellefteå airport temperature measurements vs ECMWF and Hirlam forecasts on 20th January 2014. Right: GFS reanalysis of Europe, the Mediterranean area and the Northern Atlantic Ocean for 12:00 UTC on 20th January 2014. White lines indicate isobars at ground level. Color information (relative topography between 1000hPa and 500hPa levels) and black lines (geopotential at 500hPa level) can be ignored for the purpose of this report. Source: Wetter3.de. We have marked the location of Skellefteå with a red star.

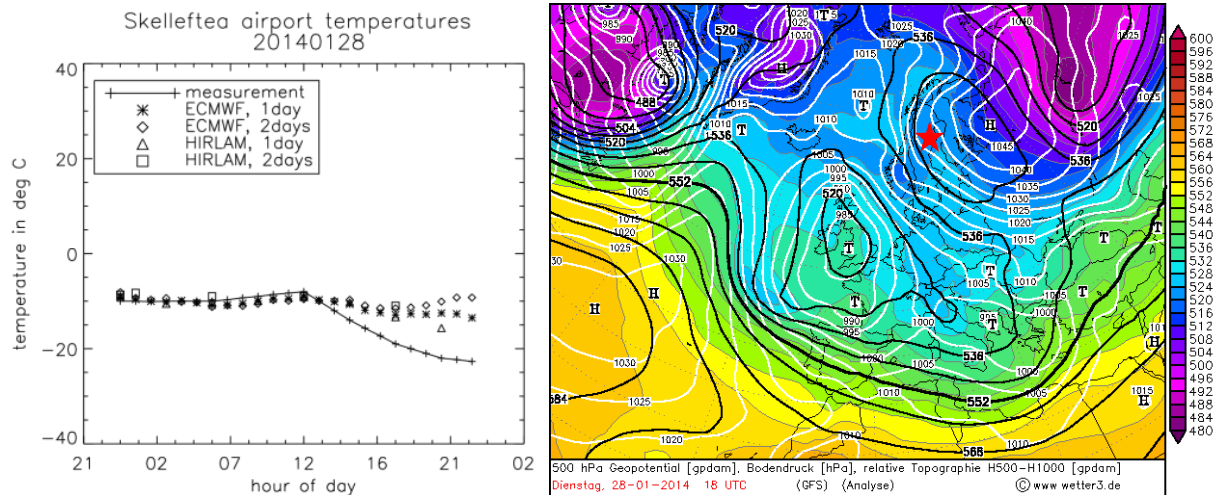


Fig. 4-24 left: Skellefteå airport temperature measurements vs ECMWF and Hirlam forecasts on 28th January 2014. Right: GFS reanalysis of Europe, the Mediterranean area and the Northern Atlantic Ocean for 18:00 UTC on 28th January 2014. White lines indicate isobars at ground level. Color information (relative topography between 1000hPa and 500hPa levels) and black lines (geopotential at 500hPa level) can be ignored for the purpose of this report. Source: Wetter3.de. We have marked the location of Skellefteå with a red star.

5 Application area – Understanding outliers in heat demand modeling on sub-grid level in Skellefteå

5.1 Stakeholders and their needs

Stakeholders interested in this application area are the providers of district heat and operators of district heating networks. As already mentioned in chapter 4, the stakeholders need trustable predictions of the total heat demand in their network, to maintain the availability of heat for the customers at any time, and to run this heating network profitably.

As a heating network can be extended over a large area with complex terrain, a single point temperature measurement maybe is an inconvenient method to adjust the temperature forecasts.

5.1.1 User system

As already described in chapter 4, the example user system is the district heating network in Skellefteå. As shown in Fig. 4-1, the heating network covers both borders of Skellefteå river. The river valley ranges from the West to East, so that the northern border of the river is slightly tilted towards the sun at noon, whereas the southern border is slightly facing away from the sun.

Besides the central Hedensbyn CHP, several oil boilers are used to maintain the heat supply in the entire network. Heat for the district heating network in Skellefteå is mainly produced in the Hedensbyn combined heat and power (CHP) plant. The CHP has a large hot water tank as storage capacity, making it possible to pre-produce heat in times when higher prices are paid for the also produced electric power. The oil boilers are used to cover extra demand if needed.

5.1.2 User requirements

In order to correctly adjust heat demand predictions, the user has to know if a single point temperature measurement is representative for the entire network, or if there are special deviations that have to be taken into account.

5.1.3 Demo site

This application is of main interest for the Skellefteå demo site.

5.1.4 Relevant use cases and control problems

Use cases: 1 (Phase out of peak oil generation), 2 (Single- vs. multi-utility generation and customer supply), 5 (Dynamic end-user loads), 6 (Special extreme situations)

Control setup 2 ('Carbon-free heating')

5.2 Work performed

As weather forecasts normally are output of Numerical Weather Prediction (NWP) models, the spatial resolution with a few square km is coarse compared to the area covered by the local heating network and its separate transmission pipes. The typical forecast is valid for a single grid box with a spatial extension of several km². Local variations within the network area normally are not predicted. This also is the case for the heating network of Skellefteå.

By now, Skellefteå Kraft is taking ambient temperature measurements at the central CHP at Hedensbyn and the other sites shown in Fig. 4-2. Other meteorological parameters are only measured at Balderskolan (humidity, global radiation, wind speed and wind direction) and at Skellefteå airport (global radiation, wind speed), which is located around 14km south of Skellefteå centre.

Systematic differences in temperature data between the sites can have two reasons: A different micro climate (e.g. differences we want to find) or differences due to measurement specifics that don't fulfil WMO's standards.

In order to check whether the WMO criteria for standardized (and therefore comparable) measurements are fulfilled, detailed information about the measurement location is required. To get an impression how this information is used, here are some questions that have to be answered to decide if WMO's criteria are fulfilled:

- Are the temperature measurement devices protected from direct sun radiation?
- Are the measurements taken at the correct height above the ground (e.g. 2m for temperature measurements, 10m for wind measurements)?
- Are the radiative measurements taken at a place, which is far enough away from any obstacles to avoid shadows?

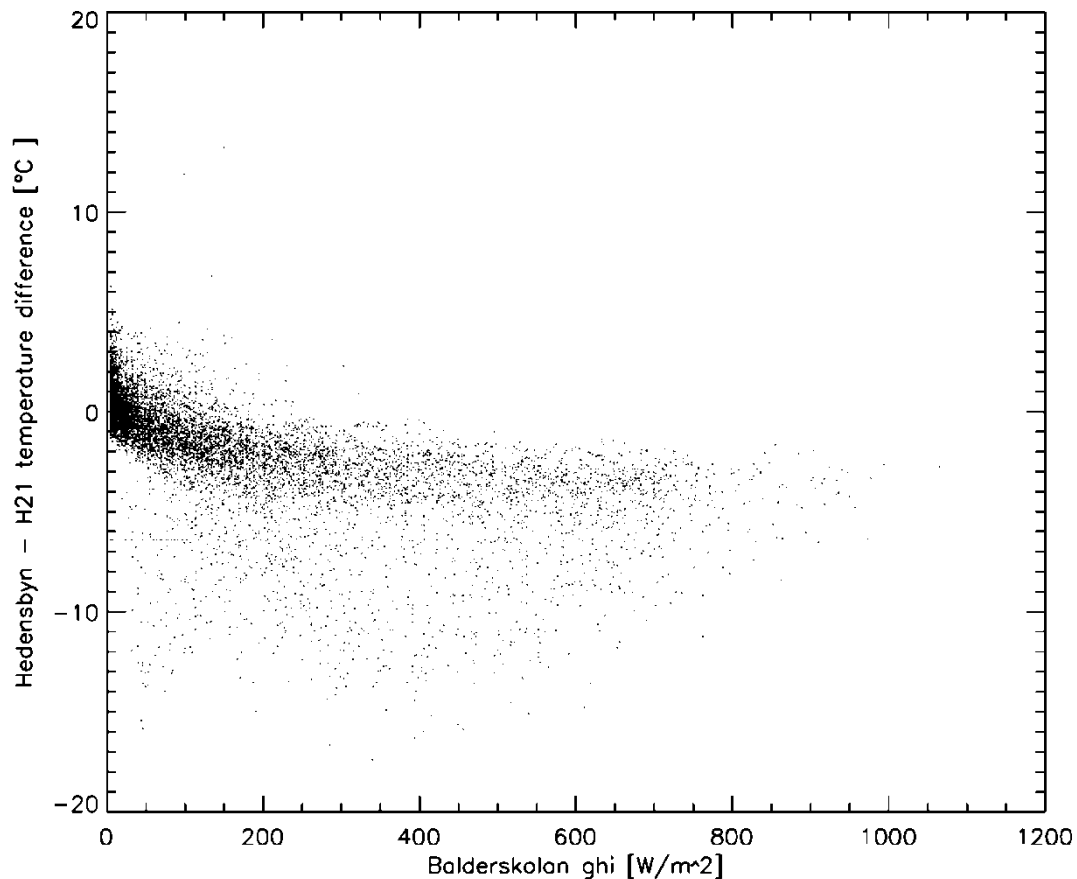


Fig. 5-1: Plot of the temperature difference between Hedensbyn and the H21 oil boiler vs. the global horizontal irradiance at Balderskolan. Each dot represents a 30 min average. Period: June 2013 to May 2014

Besides Skellefteå airport, none of the measurement sites fully fulfills WMO criteria. This has already been pointed out in chapter 4.2.3. To illustrate the importance of fulfilling WMO criteria, Fig. 5-1 shows an example of two stations which don't fulfil the criteria.

Hedensbyn CHP and the oil boiler "H21" are both located at the northern river border, the distance between both measurement sites is only 400m. The temperature difference between these sites shows a systematic behavior, depending on global irradiance values. During the night when global irradiance is close to zero, temperatures at Hedensbyn are higher than at the H21 boiler. During the day, H21 temperatures are significantly higher. In many cases the difference even exceeds 10°C. Plots comparing Hedensbyn with other sites than the H21 boiler show a quite similar behavior. At H21 boiler site, temperature sensors are installed directly at the building wall (refer to Fig. 4-9). This explains the warmer temperatures at H21 compared to Hedensbyn temperatures, while GHI is higher than 50W/m².

As a direct interpretation for data of stations that don't fulfil WMO criteria is not meaningful, we now try to find a proper post-processing or station selection process before we continue to work with these observations. Our first step is a systematic comparison of substation temperature data with temperatures from Skellefteå airport, which fulfil WMO criteria.

All six substations have a positive temperature bias between 0.36 and 1.64K compared to Skellefteå airport (see density scatter plots in Fig 5-2 to 5-7). RMSE is between 2K and 3K at H21 and Sunnana substations, while all other substations RMSE is below 2K. Pearson correlation between Skellefteå airport and the substations is 0.99 for all substation except H21, where it is only 0.97.

The smallest bias (0.36K) is observed for Balderskolan, besides the lowest RMSE values, MAE values and also line fit parameters very close to the unity line. As populated areas are well known to be warmer than its surroundings, a small positive bias can be expected. Thus it is valid to add a small correction of around 0.3K on forecasted temperatures values for Skellefteå. However, this added value is small compared to the 48 hour forecast error of 3 to 4 K that is rated as being still acceptable by SKR for their purposes.

Compared to the other substations, errors in temperature at Balderskolan and Hedensbyn remain small for high temperatures – this is an indication that their measurement devices are better protected against solar radiation than at the other substations. For very low temperatures, the spread of observed deviations of the substations from airport temperatures is generally higher, with a relatively strong positive bias for the lowest temperatures. This positive bias can be found at all substations, including Balderskolan and Hedensbyn. We tend to interpret this as well as a populated area effect. But as we know that temperature sensors for all substations except Balderskolan and Hedensby are placed directly at walls of buildings, it is impossible to exactly quantify this effect with only the substation measurements.

Having seen the same and for temperatures above -15°C being low systematic deviation of Balderskolan temperatures versus the airport measurements as in the comparison from Hedensbyn versus the airport, it seems to be justified to compare NWP forecasts versus Hedensbyn and Balderskolan. Comparing NWP forecasts to the other stations is not recommended as they have systematic differences, which are most likely due to their non-standard measurement conditions.

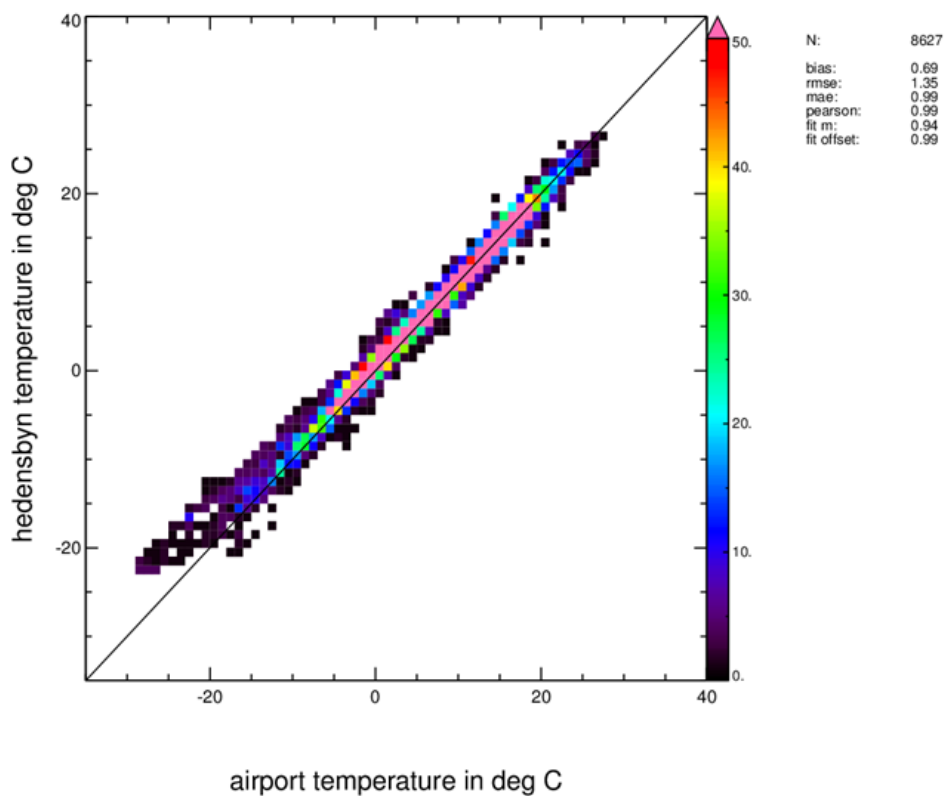


Fig. 5-2: Density scatter of Hedensbyn ambient temperature vs Skellefteå airport temperature. Statistical values given at upper right side are bias, root mean squared error (RMSE), mean absolute error (MAE), Pearson correlation, and slope (fit m) and offset (fit offset) of the fitting line (is not drawn here).

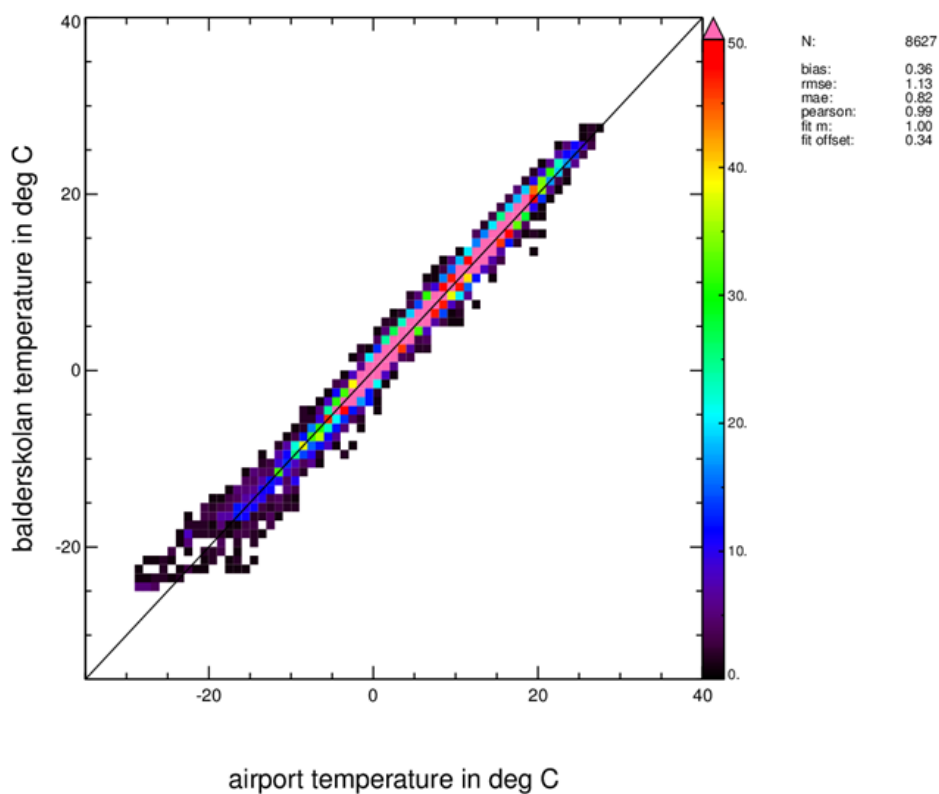


Fig. 5-3: Density scatter of Balderskolan ambient temperature vs Skellefteå airport temperature. Statistical values given at upper right side are bias, root mean squared error (RMSE), mean absolute error (MAE), Pearson correlation, and slope (fit m) and offset (fit offset) of the fitting line (is not drawn here).

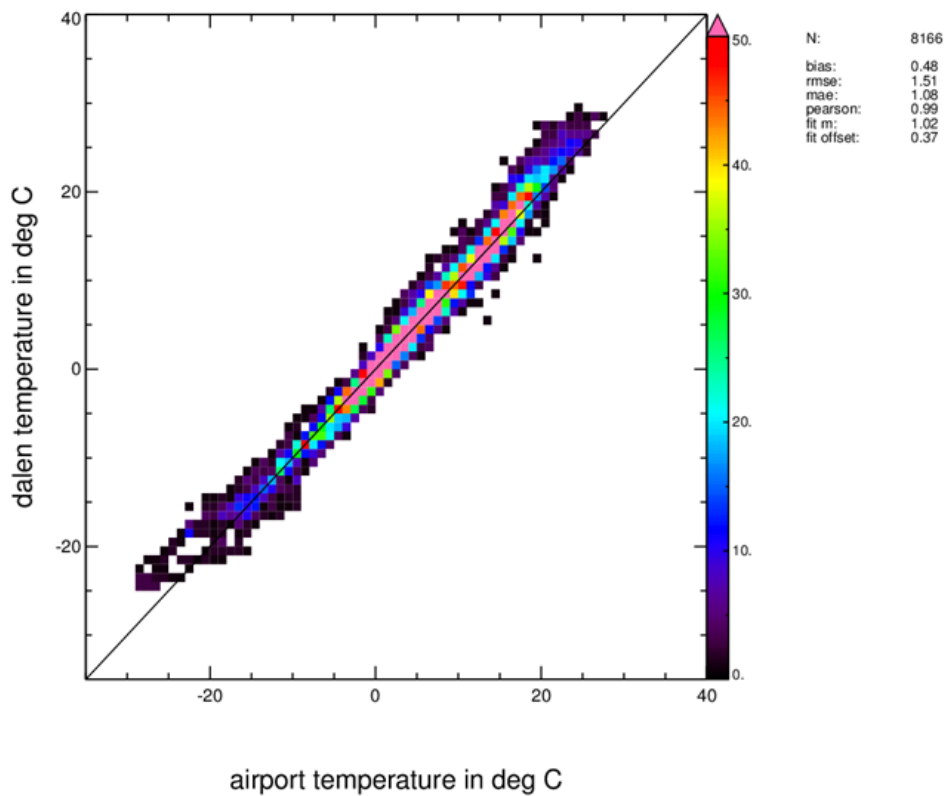


Fig. 5-4: Density scatter of Dalen ambient temperature vs Skellefteå airport temperature. Statistical values given at upper right side are bias, root mean squared error (RMSE), mean absolute error (MAE), Pearson correlation, and slope (fit m) and offset (fit offset) of the fitting line (is not drawn here).

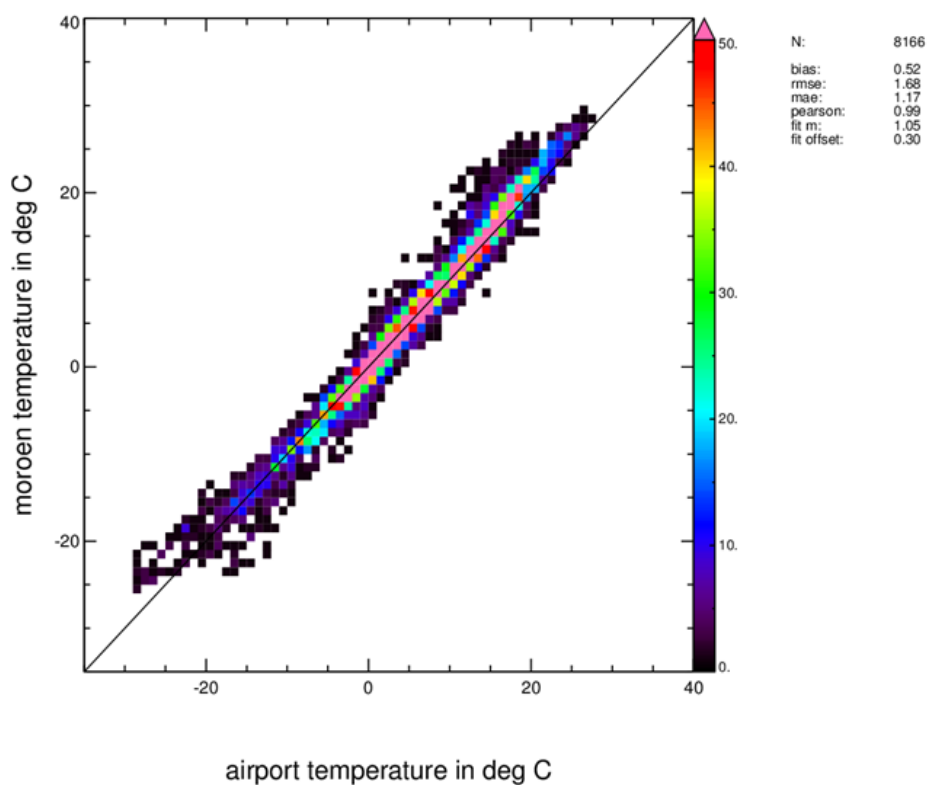


Fig. 5-5: Density scatter of Morön ambient temperature vs Skellefteå airport temperature. Statistical values given at upper right side are bias, root mean squared error (RMSE), mean absolute error (MAE), Pearson correlation, and slope (fit m) and offset (fit offset) of the fitting line (is not drawn here).

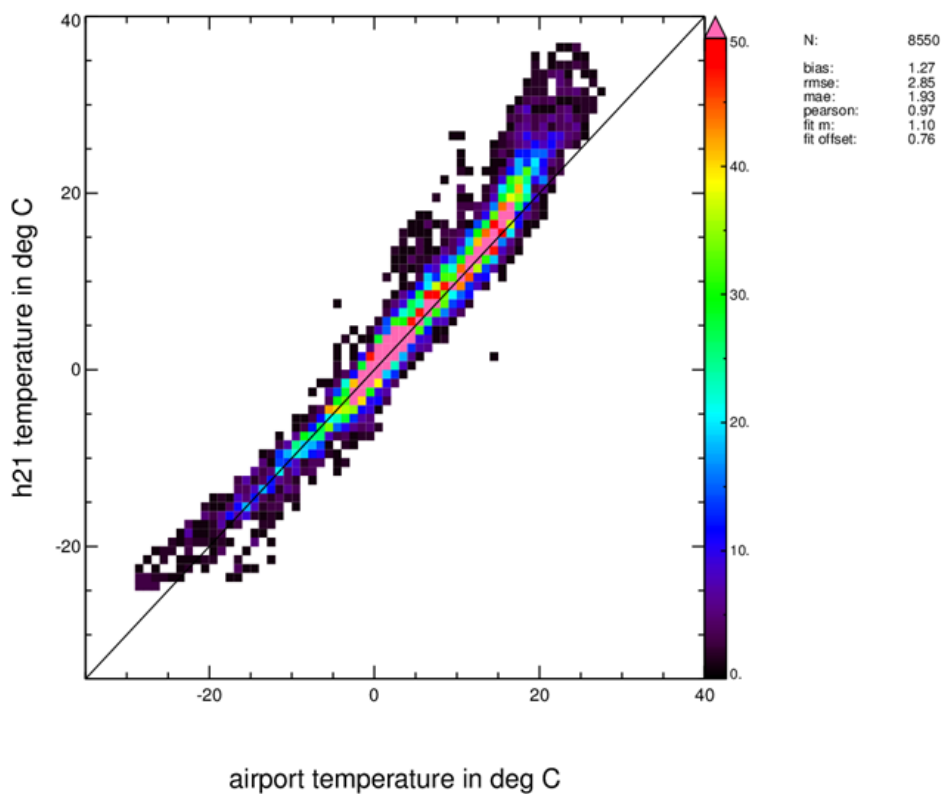


Fig. 5-6: Density scatter of H21 ambient temperature vs Skellefteå airport temperature. Statistical values given at upper right side are bias, root mean squared error (RMSE), mean absolute error (MAE), Pearson correlation, and slope (fit m) and offset (fit offset) of the fitting line (is not drawn here).

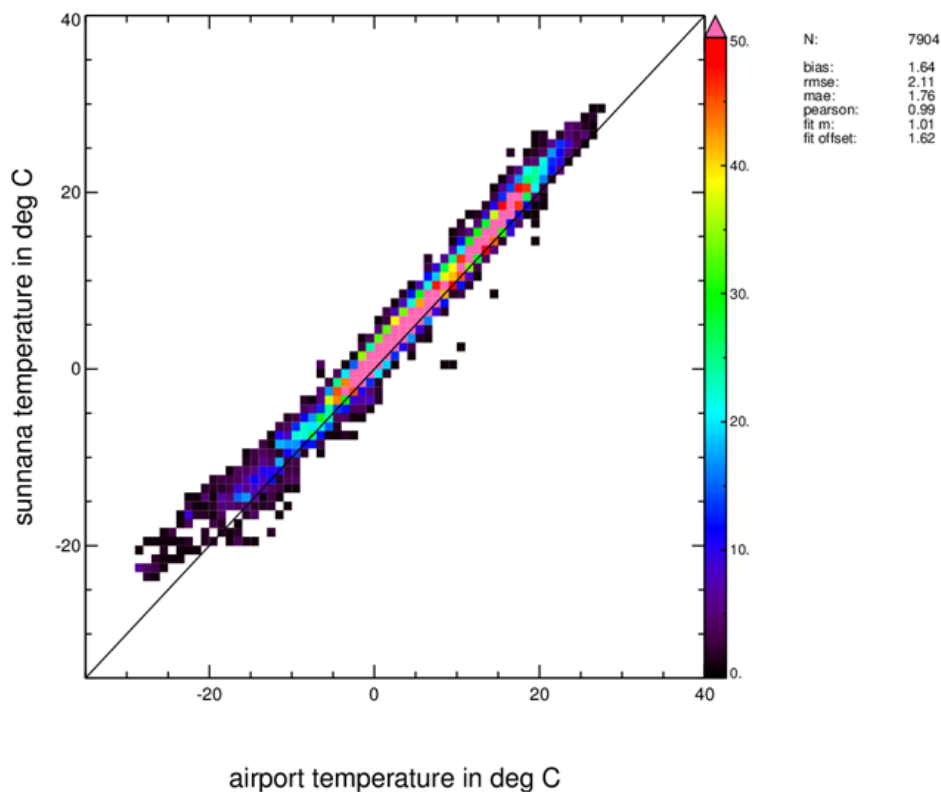


Fig. 5-7: Density scatter of Sunnana ambient temperature vs Skellefteå airport temperature. Statistical values given at upper right side are bias, root mean squared error (RMSE), mean absolute error (MAE), Pearson correlation, and slope (fit m) and offset (fit offset) of the fitting line (is not drawn here).

5.2.1 Set up additional measurement points

As announced in D3.3.1 chapter 5.2.2, SKR was “planning to set up more instruments in the near future”. Since then, we didn’t receive new information about new instruments. One possible explanation for this delay is that one person responsible for this field has left SKR recently.

If we assume that the non-standard measurement conditions are the reason for the systematic differences in Fig 5.4 to 5.7, a bias correction based on the structures seen in Fig. 5.4 to 5.7 could be applied. But this may also hide any micro-climate effects of these locations compared to Hedensbyn and Balderskolan locations, which cannot be separated from the non-standard measurement conditions. This may be solved by using a mobile, standard measurement station which is operated for at least a year at each station in Dalen, Sunnana, Morön, and H21. In case this measurement campaign shows similar results versus the airport observations, the remaining systematic differences could be used for a bias correction for Dalen, Sunnana, Morön, and H21. Also, an extension of the analyzed period for more years may further secure these findings.

5.2.2 Differences in heat demand between the two borders of the river

The Skellefteå district heating network is divided by the river into a northern border and a southern border area. As orography in both areas is slightly tilted towards the river, they show different exposures to the sun, especially at noon. To examine if the differently tilted borders do influence heat demand, a time series of total sums of heat demand on the two borders of the river will be needed. Unfortunately this kind of data is not measured separately for the two borders at the moment. Alternatively, a signal of the radiative effect due to different exposures to the sun can be searched within the temperature data of the different sites along the two borders of the river.

As already described in chapter 5.2.1, Sunnana substation has a high positive bias of 1.64K compared to airport temperature measurements, which is the largest bias of all substations. Nevertheless Sunnana temperature data will be used here, as it is the only substation located in the southern river border area. Its temperature data is compared to temperature and GHI data from Balderskolan, which is located just a few hundred meters away from Sunnana substation, but at the northern river area.

Fig. 5-8 shows the Balderskolan - Sunnana temperature difference vs Balderskolan GHI density scatter plot. A positive temperature difference means that Balderskolan temperatures are higher than temperatures at Sunnana substation. As Balderskolan is located at the northern river border which is slightly more exposed to the sun than the southern river border area, we expect a rising temperature difference when GHI values rise. As Fig. 5-8 shows, this expectation is not fulfilled. Sunnana temperatures are almost always higher than Balderskolan temperatures, and temperature difference values don’t change with rising GHI values. Certainly we do not see any radiation-dependent North-South gradient as we miss any increase/decrease with GHI. At least for large GHI values we would expect larger temperature differences.

Nevertheless, we do see a constant positive bias of Sunnana compared to Balderskolan in air temperatures. As it is not clear if the positive bias of Sunnana measurements as compared to the airport station is due to local micro climate effects or due to the non-standard measurement conditions, we finally cannot exclude the option of a North-South gradient in heat demand. But certainly the difference in air temperature between the airport and the Sunnana observations is

below approx. 5 K for individual values and on average 1.64 K (Fig 5-7). We assume that this is most likely the maximum deviation we expect from the non-standard measurement conditions.

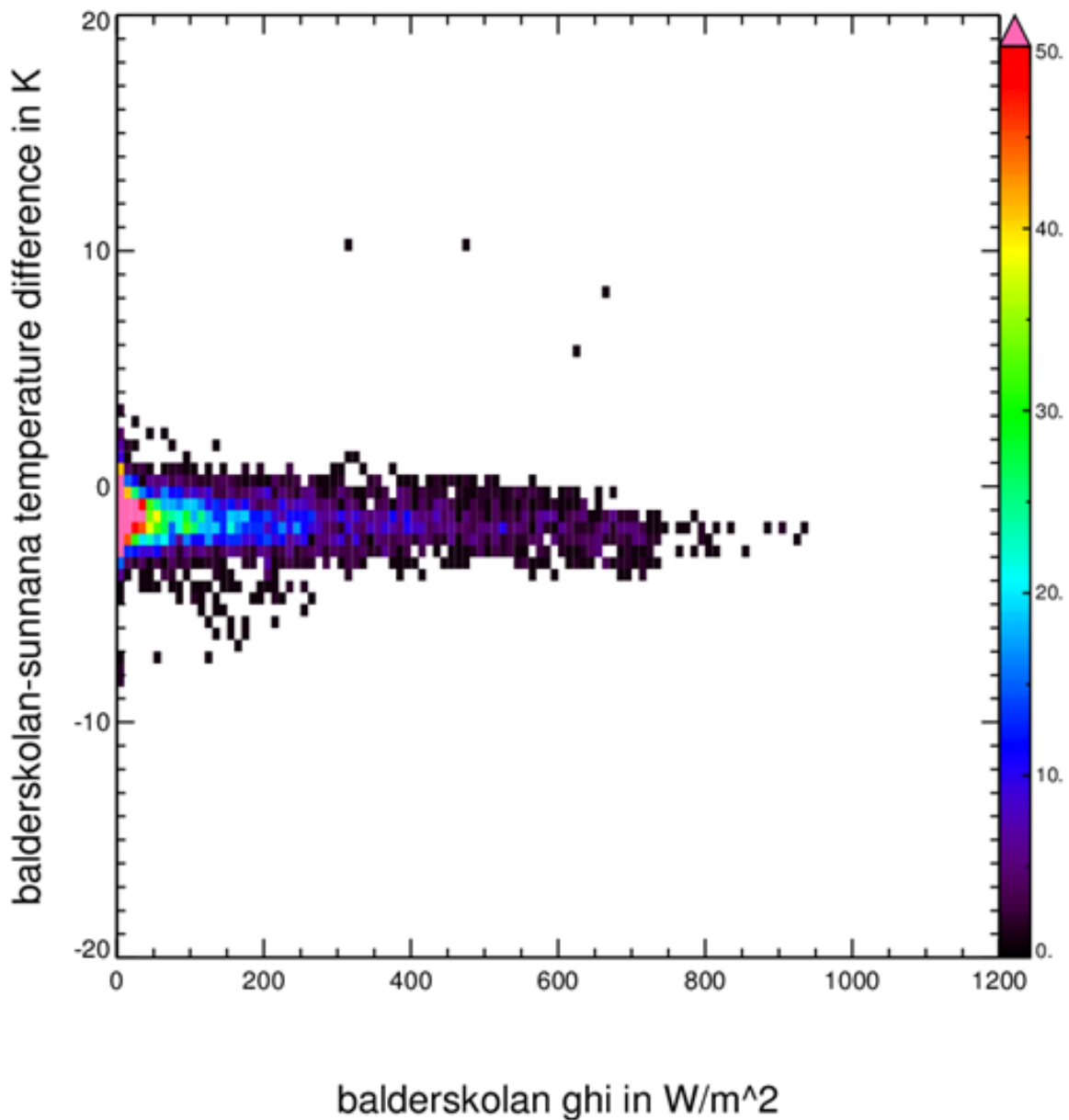


Fig. 5-8: Temperature difference between Balderskolan and Sunnana substations vs Balderskolan GHI.

Therefore, we exclude a very strong North-South gradient above 3 -5 K in air temperatures as otherwise it should have been visible in the Sunnana observations despite of the doubt about their measurement device location in non-standard conditions. Knowing that the required accuracy of air temperature is around 3 – 4 K according to SKR, we do not expect this North-South gradient to exist in any significant order.

Final comment:

We recall, that all findings in this chapter are based on non-perfect observations and should be read as a 'well-based, but not proven assumption'.

6 Application area – Dealing with non-perfect and real forecasts for technical system modeling

6.1 Stakeholders and their needs

OrPHEuS task 5.2 designs control algorithms for various use cases (see chapter 7.1.1) under different economic, social and technical conditions. The energy system setups are specified to reflect the demonstration site use cases and specific problems related to different control goals.

6.1.1 User system

OrPHEuS will focus on three main control setups as described in D5.2 ‘Algorithms for cooperative control strategies for hybrid energy networks’. They include a combination of

- Combined Heat and Power (CHP) + electrical boilers + windmills + storage (setup 1, ‘Cooperative green supplier’)
- CHP + oil and electric boilers + manageable heat demand (setup 2, ‘Carbon-free heating’)
- Photovoltaics + heat pumps + electricity storage + prosumers (setup 3, ‘Green community’)

6.1.2 User requirements

For setup 1, the following parameters are needed

- Air temperature, wind speed, humidity for heat demand
- Air temperature, irradiance for electricity demand (depending on usage of air conditioning or indoor lighting)
- wind speed for wind power generation
- solar irradiance for electricity price prediction (same as in chapter 7, electricity price prediction will be provided by TUW-EEG to partner NEC)
- 24 hours, hourly
- One average value per Skellefteå area

For setup 2, the following parameters are needed

- Air temperature, wind speed, humidity for heat demand
- solar irradiance for electricity price prediction (same as in chapter 7, electricity price prediction will be provided by TUW-EEG to partner NEC)
- 24 hours, more than hourly resolved
- Spatially resolved forecast for Skellefteå area to take local climate into account

For setup 3, the following parameters are needed

- Air temperature, wind speed, humidity for household’s heat demand
- Air temperature, irradiance for household’s electricity demand
- Global irradiance for solar power generation aggregated across the demo site (sum of all solar panels) and at all panels individually for detailed studies
- solar irradiance for electricity price prediction (same as in chapter 7, electricity price prediction will be provided by TUW-EEG to partner NEC)

- 24 hours from now, 15 minutes temporal resolution, updated as often as possible (hourly or better)
- One average value per Ulm area and one value per prosumer household

For a better overview the requirements of the setup are combined in Table 6.1.

Tab 6-1: User requirements for the three scenarios

	Air temperature	Wind speed	Humidity	Solar global irradiance
Setup 1				
Forecast duration	24 h	24 h	24 h	24 h
Temp. res.	1h	1h	1h	1h
Spatial res.	1 avg area Skell.			
Setup 2				
Forecast duration	24 h	24 h	24 h	24 h
Temp. res.	< 1 h	< 1 h	< 1 h	< 1 h
Spatial res.	Skell. Resolved < 3 km?			
Setup 3				
Forecast duration	24 h, hourly update			
Temp. res.	15 min	15 min	15 min	15 min
Spatial res.	1 avg. area Ulm + Household Ulm < 1 km	1 avg. area Ulm + Household Ulm < 1 km	1 avg. area Ulm + Household Ulm < 1 km	1 avg. area Ulm + Household Ulm < 1 km

6.1.3 Demo site

This application applies both for the Ulm (setup 3) and Skellefteå (setup 1 and 2) demo sites.

6.1.4 Relevant use cases and control problems

Use cases: all

Control setup 1 ('Cooperative green supplier'), 2 ('Carbon-free heating'), and 3 ('Green community').

6.2 Work performed

As already explained in Del. 3.3.1 there is only very restricted systematic knowledge on the use of real weather forecasts in technical control setups for smart grids and hybrid energy grids. Within the two stakeholders SKR and SWU, there is no ongoing practice.

Generally, this control studies aim at having forecasts which are (a) updated frequently e.g. in hourly or even better intervals, and (b) being valid from now on up to 24 hours. Both requirements can't be met by numerical weather prediction as it is operating nowadays – and the reasons for that are of principal nature. Therefore, it is not just a technical matter, but a very fundamental blockage. This reflects e.g. the characteristics of each numerical model, which needs a certain spin-up time – blocking the requirement of an immediately valid forecast. Also, meteorological services need some processing time for the observation collection, their quality control and the data assimilation to initialize the most recent model run, and, finally, to perform the model run. There are some experimental schemes under investigation to overcome this by a rapid-update-cycling model or an ongoing ensemble model with a subset definition based on observations in each forecast loop – but even in these settings an hourly update is the maximum being discussed today. And such schemes are far from being available operationally for our partners SKR and SWU.

For setup 1, one value per Skellefteå area is required. This is provided as grid box area average by all meteorological forecasts. For setup 2, spatially resolved forecasts are required – so, we have to investigate the spatial resolution being provided. The maximum e.g. at SMHI is 2.5 km, but it should be taken into account that for such high resolution models, the usage typically includes a spatial averaging to have reliable forecasts.

For setup 2, the temporal resolution required is 15 minutes. At least for Sweden this does not exist currently, while for Germany there is the EweLine project ongoing that started to provide such forecasts from Deutscher Wetterdienst (DWD) recently.

For setup 3, forecasts are required on household's scale – a scale being far from the 2.5 km spatial resolution in the highest resolved NWP forecast at SMHI and the 2.8 km provided by DWD/EweLine. And a scale being probably far from the physical understanding and modelling capabilities for meteorological processes on nowadays level of scientific knowledge. On the other hand, it needs to be investigated, if the error of assuming spatially constant meteorological conditions is the main driver in the accuracy of control strategies, or if the individual building state (age, type of building) and the inhabitant's behavior is the real issue and the missing spatial resolution of meteorological forecasts is not blocking at all.

For all three setups it is analyzed which deterministic forecast models are available. In the following the possible datasets of SMHI, DWD and ECMWF are presented and advices are given for their usability.

6.2.1 ECMWF's deterministic forecast

The operational ECMWF Integrated Forecast System (IFS) provides ECMWF's standard forecast including temperatures (T), wind speed (WS), and global irradiance (GHI) forecasts in a 3-hourly temporal resolution in near-real-time observations. From the archive, forecasts in 1-hourly resolution are available. OrPHEuS user may make use of the hourly resolved forecasts for research, but need to be aware that operationally this forecast resolution is not provided.

The parameter SSRD (solar surface radiation) is the irradiation sum of the previous hour. Several radiation schemes have been used during the different years (ECMWF, 2013): Since 2nd May 1989 (cycle 32) the radiation was modelled based on Fouquart and Bonnel (1980) as described in Morcrette (1991 and 2002). Since 5th June 2007 (cycle 32r2) a new radiation scheme RRTM-SW (McRad, Morcrette et al., 2008a and 2008b) is applied on the T399 grid (0.45°) and interpolated to a

domain-averaged radiation in the T799 grid box (ECMWF, 2009b). It is based on the McICA (Monte Carlo Independent Column Approximation) scheme. Finally, since 18th May 2011 (cycle Cy37r2) direct irradiance has been included in the output parameters. The operational IFS provides the following spatial resolution: 0.5° spatial grid before Feb 2006; an increased T799 (0.25°) spatial resolution since Feb 2006 (cycle 30r1), and finally a T1279 (0.15°) spatial resolution since 26 Jan 2010 (cycle 36r1). Aerosols in the IFS are based on a monthly mean climatology following Tegen et al. (1997).

According to the ECMWF homepage it is planned for the upcoming IFS cycle 41r2 (<https://software.ecmwf.int/wiki/display/FCST/Implementation+of+IFS+cycle+41r2>) to upgrade the horizontal resolution. The upgraded horizontal resolution will be about 9 km for the HRES and the data assimilation and about 18 km for the ENS up to day 15 and about 36 km for the extended range (monthly). The resolution of the ensemble of data assimilations (EDA) will be increased to 18 km.

An hourly temporal forecast resolution is needed following the requirements of the day-ahead and intraday electricity markets being relevant for the grid integration of solar power. In case of an operational scheme, the 3-hourly resolved forecasts from ECMWF need to be interpolated to hourly forecasts as described in the next paragraph.

For smaller time resolutions than 1 hour it is possible to perform the temporal interpolation from the original irradiation sum following Breitzkreuz (2008): Due to the strong non-linear behavior of irradiances during the day, the explicit interpolation of irradiances is not recommended. Instead of irradiances, the clear sky index – being defined as the ratio of the global irradiance divided by the clear sky global irradiance is used. Applying a clear sky model (Hoyer-Klick et al., 2010) the clear sky index is calculated for the irradiation sum provided every hour in the IFS forecast. The clear sky index is then interpolated linearly for each minute and averaged to hourly values. Finally, by using the clear sky model again, the global irradiance is calculated in hourly averaged resolution. As clear sky model inputs the Copernicus Atmosphere MCclear Service may be used (<http://atmosphere.copernicus.eu>).

6.2.1.1 ECMWF's reanalysis

A reanalysis is a numerical weather model run using observation datasets to reanalyze the state of the atmosphere at a given time in the past. The goal is to generate historical time series of meteorological parameters, even at locations where no observations have been made. Besides the IFS forecast system, ECMWF also provides the ERA (ECMWF Re Analysis) re-analyses (ECMWF 1996, 2004, 2009a).

Re-analyses can be used to gain information of special and temporal variability of meteorological parameters in the past. After registration, ERA re-analyses are available free of charge: <http://apps.ecmwf.int/datasets/>.

Tab 6-2: Availability, Modeled components, and resolution and available parameters of the different ERA reanalyses at ECMWF.

Dataset	Available	Time period	Atmosphere	Ocean waves	Land-surface
ERA-Interim	Yes	1979-present	Yes	Yes	Yes
ERA-20CM	Yes	1900-2009	Yes	Yes	Yes
ERA-20C	Expected soon	1900-2010	Yes	Yes	Yes
ERA-40	Yes	1957-2002	Yes	Yes	Yes
ERA-15	Yes	1979-1993	Yes	No	Yes
Dataset	Temporal resolution		Spatial resolution		Relevant output parameters due to chapter 7.1.1.2.3
ERA-Interim	6h		~80km		2m temperature, 10m winds, Surface net solar radiation
ERA-20CM	Monthly averages, 10members		~80km		2m temperature, 10m winds, Surface net solar radiation
ERA-40	6hourly surface fields		~79km		2m temperature, 10m winds, Surface net solar radiation
ERA-15	24h, every day at 12UTC		~79km		2m temperature, 10m winds

6.2.1.2 Available data for OrPHEuS

ECMWF test data for 2013 and 2014 have been downloaded by DLR for research but cannot be given to the partners due to licence agreements. The DLR is testing the advantages and disadvantages of these coarser data (compared to COSMO and HIRLAM) and will be giving advice.

For the OrPHEuS partners the datasets can be ordered in the following way:

Depending on the use that is intended for the data (commercial or research use) there are various avenues to obtain ECMWF's historical forecasts. For researchers within the Member and Co-operating states (valid for all OrPHEuS partners), <http://www.ecmwf.int/en/about/who-we-are/member-states> offers access to ECMWF's archive, free of charge, via the computing representative of the national weather service:

<http://www.ecmwf.int/en/computing/access-computing-facilities/computing-representatives>

This access is given at the discretion of the national weather service.

Alternatively, there is the possibility to obtain access to the historical forecasts archive, by paying a handling charge of 5,000 GBP/Year. Users within an ECMWF Member or Co-operating State, might still have to seek authorization from their national weather service (we will give them the right contact for that). This access is given via a web API (python based) and includes the following:

<http://apps.ecmwf.int/archive-catalogue/>

Several historic datasets like the ERA-Interim are freely available without contacting the local weather services, only a short online registration is required (<https://www.ecmwf.int/registration/>). The data can then be directly downloaded following an interface for the selection of subsets, time periods and parameters:

<http://apps.ecmwf.int/datasets/>

A general overview over the ECMWF forecast data can be found at http://www.ecmwf.int/sites/default/files/User_Guide_V1.2_20151123.pdf.

6.2.2 SMHI deterministic forecast

The Swedish Meteorological and Hydrological Institute (SMHI) is a member of the HIRLAM (High Resolution Limited Area Model) research cooperation. Other members are the national meteorological institutes of Denmark, Estonia, Finland, Iceland, Ireland, the Netherlands, Norway, Spain, and Lithuania. The HIRLAM cooperation currently has several NWP models in operations:

- The synoptic scale (5 -15 km horizontal resolution) HIRLAM model (Undén et al, 2002), The E05 model domain is shown in Fig. 6-1 (red frame).
- The meso-scale (2.5km) model HARMONIE (Driesenaar, 2009a), The model domain is shown in Fig. 6-1 (yellow frame).

General information on ensemble forecasts are being provided in the ECMWF related section 7.2.1.

Tab 6-3: Short overview of models run at SMHI both in the operational and the research department

Model	Update frequency	Relevant output parameters due to chapter 6.1.1.2	Spatial resolution	Temporal resolution	Available period
HIRLAM 7.3 (E05)	Every 6 hours	2m Temperature, 10m winds, 2m relative humidity, global irradiance	5.5 km	3h res. Spin up < 3 hours	20120615 – May 2016
HARMONIE-Aromacy38h1.1 (MetCoOp)	Every 3 hours assimilation, long forecasts up to 48 hours only 6-hourly	2m Temperature, 10m winds, only cloud cover archived – no irradiances in the archive, irradiances and 2m relative humidity only in the operational online processing mode	2.5 km	1 hour (MetCoOp operational), 3 hours (MetCoOp archive), spin up < 1 hour	Last 4 days (MetCoOp operational), since 24 th April 2014 (MetCoOp archive)

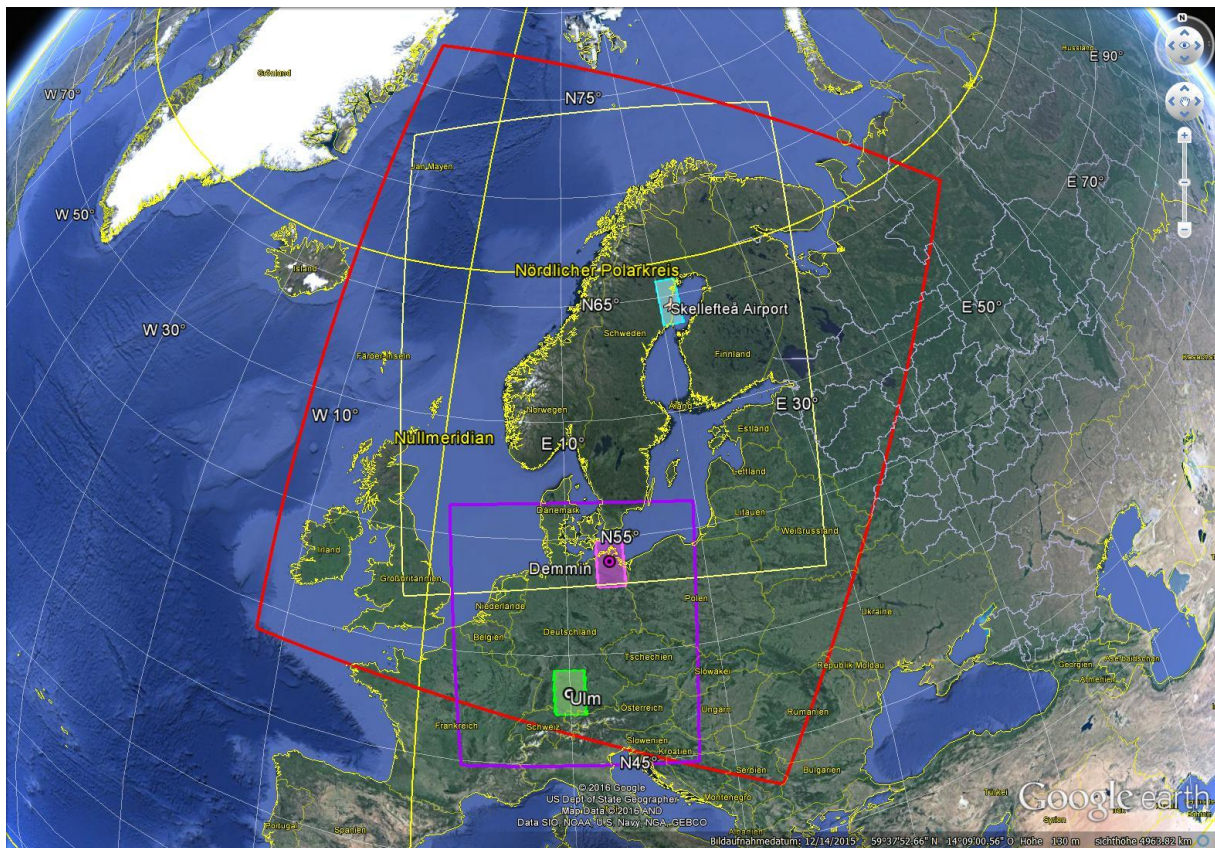


Fig. 6-1: Model domains of HIRLAM E05 (red), HARMONIE/AROME (yellow), and COSMO-DE (purple). Additionally marked are the regions of interest: Skellefteå (cyan), Demmin (magenta), and Ulm (green).

Data status:

As the AROME data are only available since 24th April 2014, it was decided to perform the comparisons with observation data at Skellefteå with HIRLAM E05 data. According to personal correspondence the HIRLAM E05 model will be out of service presumably at May 2016. A comparison between HIRLAM, AROME, ECMWF and Unified Model (Køltzow et al. 2012) has shown that there are some problems in AROME for the forecast of the temperature at 2m. For this parameter HIRLAM is clearly best of the four compared models. As HIRLAM is in this comparison also better than AROME on total cloud cover it is reasonable to work with the HIRLAM data.

The forecast data of the HIRLAM E05 and the AROME/HARMONIE models is available over the customer service and are delivered under Creative Commons by licence. This means, the data are free - only a delivery fee has to be paid – and the DLR is allowed to share the data with the OrPHEuS partners.

The data order at the SMHI customer service is performed via email order (dataveranser@smhi.se). Due to recent changes in data policy (Creative Common) and service performances the data order was time-consuming and only with help of intern contacts successful. Note that only complete scenes are provided by the customer service, as the cutting of smaller areas is very complex due to the rotated grid (section 7.3.1).

Following our contact person at SMHI R&D department, a HARMONIE forecast needs about 2 hours processing time, whereas a HIRLAM C11 run takes about 3 hours processing time.

6.2.2.1 Available data for OrPHEuS

The DLR has HIRLAM E05 archive data for the 00 UTC run for the period from 1st January 2013-31st December 2014 (2 complete years) for the following parameters at a time resolution of 3h for the first 24h and 6h for the following forecast steps::

- Temperature at 2m [K]
- Dewpoint temperature at 2 m [K]
- Net shortwave radiation [J/m^2]
- u-component of wind at 10m + 3 height levels[m/s]
- v-component of wind at 10m + 3 height levels[m/s]

The data received from SMHI is given in the data format GRIB, containing the complete HIRLAM E05 scene (see. Fig. 6.1) with a size of ~ 52 GB. For better handling of the data the area around Skellefteå airport and power station Hedensbyn was extracted and saved into netcdf-files (size ~ 10 MB). Thereby also the rotation of wind vectors from rotated grid to regular grid was performed.

In the same way it is possible to extract the data around Ulm and Demmin, as both areas are within the limits of the HIRLAM E05 scene.

6.2.3 DWD deterministic forecast

The numerical weather prediction model COSMO-DE is a convection-permitting model with a horizontal resolution of 2.8 km covering the area of Germany (Baldauf et al., 2011). Fig. 6-2 shows an orography map of the region combined with circles of latitude and longitude. COSMO-DE run –like the HIRLAM model- in a rotated grid. Fig. 6.1 shows the overlap of the different model domains.

The very high horizontal resolution of COSMO-DE allows to resolve (at least partially) deep convection, i.e. cumulonimbus clouds giving rise to shower and thunder storms. In forecast models with coarser horizontal resolution like ECMWF deep convection cannot be resolved explicitly but has to be parameterized. The higher resolution of COSMO-DE additionally allows for a better representation of topography like the highlands and mountains in the Alps and related flow features, e.g. mountain and valley winds or Foehn flows.

The smaller the atmospheric phenomena resolved by the NWP model the less is the life span and predictability of the systems. Large scale high and low pressure systems on one hand have a live span of several days; therefore the global forecast models can provide useful forecasts of such systems for three to five days ahead. On the other hand the life span of a thunderstorm is in the order of one hour, therefore useful forecasts will be possible only for a few hours ahead. With a rapid update cycle (RUC) of 3 hours, COSMO-DE provides thus only 27-h forecasts based on the analyses at 00, 06,09, ..., 18 and 21 UTC. A 45-h forecast is done based on the analysis at 03 UTC to support day-ahead forecasts for renewable energy (wind power and photovoltaic power).

The COSMO-DE provides forecasts for a multitude of meteorological parameters in hourly resolution, which is extended to 15 minutes for some parameters (see Tab. 6-4)

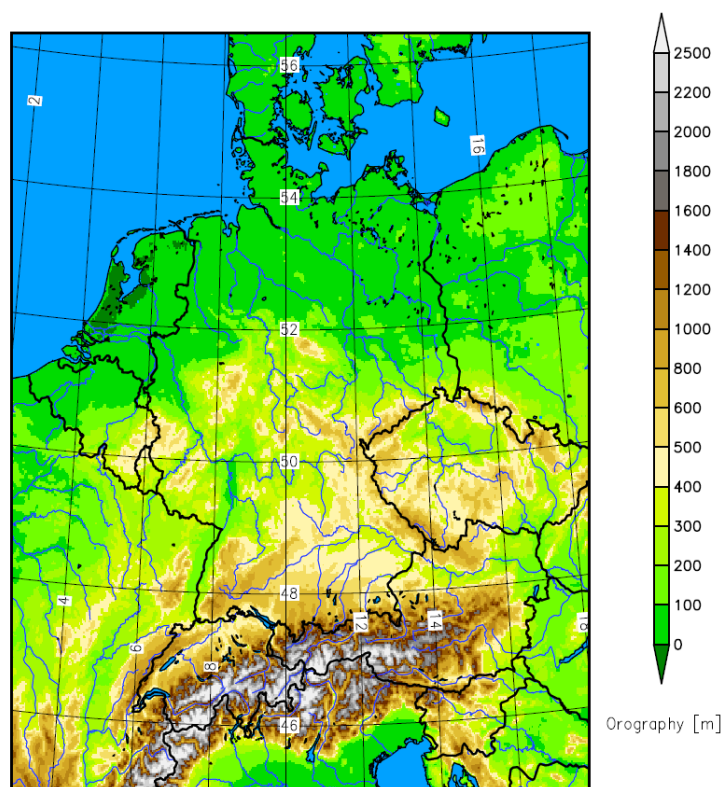


Fig. 6-2: COSMO-DE model area (color bar = orography, height above sea level in m)

Tab 6-4: Variables of interest for OrPHEuS in the COSMO-DE output

Variable name	Description	Temporal resolution	Time definition	Comments
HHL	half height of levels, geometrical height above sea level	constant value	N/A	
RLAT/RLON	geographical latitude/longitude	constant value	N/A	
U/V on model levels	zonal and meridional wind on model levels	hourly	instantaneous values at time interval end	vectors on rotated COSMO-DE grid
U_10M/ V_10M	Zonal and meridional wind in 10 m height	hourly and 15 min	instantaneous values at time interval end	vectors on rotated COSMO-DE grid
T_2M	2m temperature	hourly and 15 min	instantaneous value at time interval end	
RELHUM_2M	2m relative humidity	hourly	instantaneous value at time interval end	
ASWDIR_S	Direct shortwave irradiance at the	hourly and 15 min	Average of the time interval	Average in T_1 to T_2 is calculated as

	surface		from T=0 to T _i , end of interval is given time stamp.	$\{T_2 * ASWDIR_S_mean(T_2) - T_1 * ASWDIR_S_mean(T_1)\} / (T_2 - T_1)$ (see sect. 5.1.2.5 in Theis et al., 2014)
ASWDIFD_S	Diffuse downward shortwave irradiance at the surface	hourly and 15 min	Average of the time interval from T=0 to T _i , end of interval is given time stamp.	Average in T ₁ to T ₂ is calculated as $\{T_2 * ASWDIR_S_mean(T_2) - T_1 * ASWDIR_S_mean(T_1)\} / (T_2 - T_1)$ (see sect. 5.1.2.5 in Theis et al., 2014)
U/V on press levels	Wind speed on pressure levels	1000, 975, 950 and 850 hPa in 15 min, 1000, 975, 950, 50, 700, 600, 500, 400, 300, 250, and 200 hPa in hourly resolution		Generated via vertical interpolation from model levels, no hydrostatic equation!!!
T2_m ensemble products				Ensemble products as mean, spread, max, min, quantiles are provided
VMAX_10m ensemble products				Ensemble products as mean, spread, max, min, quantiles are provided

It has to be noted that the model is non-hydrostatic, which implies that the standard conversion between pressure levels and vertical coordinate in meters does not apply. The geometrical height of model levels above sea level is given as a separate variable HHL (height of half level).

An update cycle of 3 hours (00 UTC, 03 UTC, 06 UTC,...) is applied for the COSMO-DE and the forecasting horizon is 27 hours. This setup is appropriate for the intra-day forecasts, whereas selected runs will be extended to cover the day-ahead.

It is planned to extend the 03 UTC run from 27 to 45 hours in order to cover the day ahead. This is not yet available, but no restriction to this application area requiring 24 hour forecast horizons.

Within the EWeLiNE project the deterministic COSMO-DE is optimized towards improved wind power and PV forecasts. With regard to the probabilistic forecasts, the focus is on the generation and calibration of ensembles and to integrate the probabilistic information into decision making processes by developing user-specified products.

For research purposes historical data for defined periods can be delivered.

6.2.3.1 Available data for OrPHEuS

The HSU has received from the DWD deterministic and ensemble data with the permission of distribution within the OrPHEuS partners. These data are for better usability analyzed and reprocessed by the DLR.

The deterministic data are available for the time period from 1st July 2013 to 31st December 2014. The run starts at 00 UTC and has a forecast horizon of 23 h in 1 h time resolution. For each timestep one netcdf file is given for the whole COSMO-DE scene. Subset generation for OrPHEuS users can be performed on request.

Available parameters are:

- Downward direct short wave radiation flux at surface
- Downward diffusive short wave radiation flux at surface (mean over forecast time)
- 2 metre temperature
- 10 metre U wind component
- 10 metre V wind component

6.2.4 Overview over the available models

Tab 6-5: Overview over the models and assignment on usability for requirements described in Tab. 6-1: fulfilled (green), acceptable (yellow), and insufficient (red)

	Parameters	Spatial Resolution	Temporal Resolution	Forecast duration	Access	Runs	Ensemble	Format
ECMWF ERA Interim		0.125°	3 h	12 h	Free	00 06 12 18	N	GRIB + netcdf
MACC Reanalysis		0.125°	3 h	24 h	Free	00 06 12 18	N	GRIB + netcdf
ECMWF operational		0.125°	3 h in NRT/ 1h in archived forecasts	72 h	From ECMWF €	00 06 12 18	N	GRIB
SMHI HIRLAM E05		5.5 km	1 h / 6 h	48 h	From SMHI / DLR	00 06 12 18	N	GRIB
SMHI AROME	irradiances, humidity (only in operational online)	2.5 km	3 h			00 12	N	
DWD COSMO-DE		0.025° = 2.8 km	1 h	23 h	From HSU / DLR		N	netcdf

6.3 Consultations NEC / TUW: getting temperature data for scenario basis

20. April 2015: Request for Advice; getting weather factors for Skellefteå

Discussions between Tae-Gil Noh, NEC, Daniel Schwabeneder, TUW and Franziska Schnell, DLR, via email + telecon.

Advice from DLR was asked about weather data for scenario basis at WP 2,4,5. Especially “winter” factors were demanded as three cases: a) Fairly cold winter, b) Typical winter, c) mild winter.

6.3.1 Dataset advices

NEC had limited access to meteorological data from Meteonorm via AIT, but were not successful in determining the three wintercases cases. Meteonorm is a commercial collection of meteorological data. They use nearby measurement stations as well as satellite data to get their data. The data seems then to be interpolated for the wished station. It seems that it is not possible that the single measurement values could be showed with Meteonorm but only averaged values could be obtained.

After the study of the Meteonorm data a more transparent approach for the winter data was advised: the use of the long term archive of ERA interim data. ERA-Interim is a global atmospheric reanalysis from 1979 to present. It is produced with a 2006 version of the IFS (Cy31r2) and continues to be updated in real time (source: ECMWF-homepage). The data is freely available at the ECMWF and single parameters can be loaded.

The following procedure to determine the three cases was advised:

Load the parameter “2 metre temperature” for all available years (1979-2014) for the winter months (October – March) in 3 h resolution for the Skellefteå area:

- Choose all needed months (Oct-Mar)
- Select all times
- Select step 0 + 3 (so you get one value for each 3h time step)
- Select parameter “2 metre temperature”
- Click „Retrieve NetCDF“ (you can also get the data in GRIB format, but netcdf is so much nicer to handle)
- Define the Area, e.g. Custom 65.25°N, 20.50°E, 64.25°N 21.50°E
- Define Grid (= resolution): 0.125 x 0.125

This procedure should result in a file containing temperature data in a spatial resolution of ~12 km (= 9x9 Pixel) and a temporal resolution of 3 h.

6.3.2 Identification of winter cases

Harsh / mild winter can be defined by searching for the lowest / highest seasonal average temperature.

First all temperatures of one day including the night time measurements need to be averaged by:

$$\text{Daily average } T_D = \frac{1}{8} (T_{00} + T_{03} + T_{06} + T_{09} + T_{12} + T_{15} + T_{18} + T_{21})$$

In the same way an average for each month and each winter (T_w) can be calculated.

In meteorological research usually only the months December, January, and February are used as winter months. But for this study it was advised to analyse also the adjacent months (from October

to March) to identify the coldest months in Skellefteå. This study led to an extension of the winter months by including the November data as month with strong heating demand.

The winter average has then to be carefully built: E.g. winter 2008 = Nov 2008 + Dez 2008 + Jan 2009 + Feb 2009.

The 35 T_w can now easily be analysed for the case analysis:

- „harsh“: the year with the lowest winter average (Minimum of T_w)
- „mild“: the year with the highest winter average (Maximum of T_w)
- „typical“: use the year with T_w near the mean of the 35 T_w

This analysis resulted in the identification of the three cases of scenario 1:

- „harsh“: temperature dataset of winter 2010/2011 is used
- „mild“: temperature dataset of winter 2000/2001 is used
- „typical“: temperature dataset of winter 1991/1992 is used

6.3.3 Advice for further possibilities

For a more sophisticated identification of extreme weather events a thorough statistical analysis would need to be done. But this would go way beyond the scope of scenario 1.

Another way to identify the winter of a year as „harsh“/ „mild“ is to use the information given by the peak-boiler usage or the overall heat consumption.

6.3.4 Interpolation of data to 15-min time resolution

For scenario 1 the temperature data is needed in 15-min time resolution. Therefore the 3 h data of ERA needs to be interpolated. Instead of the easiest method of linear interpolation, which is probably not appropriate due to the daily cycle of the temperature, the DLR advised to use a spline interpolation. Another approach of Goettsche et al., 2001, was also proposed but was beyond the scope of the research.

7 Application area – Meteorological forecasts for business case development and economic system modeling

7.1 Description of use of meteorological information

7.1.1 Stakeholders and their needs

Within deliverable D2.1 ‘Report on technical, economic and social patterns of energy service provision’ partner TUW-EEG has described the stakeholders in a new hybrid energy system structure. This covers technical, economic and social aspects.

OrPHEuS is investigating several use cases as defined in deliverable D2.3 ‘Use cases’. They cover the following aspects:

1. **Phase out of peak oil generation** which is a result of municipality/utilities’ environmental policy and independent on the future oil prices.

2. **Single- vs. multi-utility generation and customer supply** – here the generators' economic targets as cost reduction or maximized profits are dominating.
3. **Optimal asset management** and extension planning of distribution grid following the grid regulator's and distribution grid operator's policy (e.g. optimal CAPEX-OPEX-management). This can e.g. result in delaying grid expansion, while at the same time a certain level of security of supply and a certain asset value of the grid is ensured.
4. **Maximize remote self-generation** with active prosumer participation enabling "democracy" in the energy supply chain
5. **Dynamic end-user loads** and comfort levels with an analysis of structural and dynamic parts of load profiles and energy efficiency methods together with their effects on DSOs and retailers. Customer segmentation of the retailer according to comfort levels is an option.
6. **Special extreme situations** on the seasonal scale as e.g. extreme dry/wet summer/winter

All these use cases will be treated by TUV-EEG as economical optimization problems taking innovative action options on the electricity markets into account.

7.1.1.1 User system

Depending on electricity market conditions and gate closure times different strategies of meteorological information usage can be applied:

- Use the Intra-day and Day-Ahead markets in parallel based on the same meteorological forecasts.
- Use more recent meteorological forecasts in the Intra-Day than in the Day-Ahead market with its longer period between gate closure and prediction period.
- Future markets will have shorter lead times between gate closure time and start of the schedule or even allow a continuous trading. This will allow using nowcasting methods in future as e.g. rapid update cycles in numerical weather prediction or satellite-based irradiance nowcasting.

For the Day-Ahead market the EEX power spot market operates a fixed 12 am CET auction time for hourly time periods or multi-hour blocks (as described above in the Intra-Day section) of the following day. The German national TSOs require 14:30 CET as gate closure time for tomorrow's schedule following the ETSO Scheduling System (ESS) guidelines.

In Sweden, the Nordic Electricity Exchange (NordPool) is the regional power spot market – covering the Nordic and Baltic countries and connecting to Germany. The Day-Ahead 'Elsport' market operates with as 12:00 CET gate closure time for the following days and with hourly blocks.

Today, the EPEX power spot market for Germany, France, Austria and Switzerland, already operates an intraday market with continuous trading in a 24/7 scheme and with different time slots. Time slots being used are hourly, blocks as e.g. peakload (8-20 CET), off-peak (0-8 and 20 – 24 CET), business (8-16 CET), afternoon (14-18 CET) or rush-hour(16-20 CET), and 15 minute blocks in Germany and Switzerland. Practically, there is a second requirement from the transmission system operator that each schedule announcement has to be provide at least 15 minutes before the ¼ hour – together with typical internal decision flows this results in about 45 minutes delay between a new forecast is

available and the start of any revised schedule. So, even a continuous trading is not an immediate trading, but has a typical delay of up to 1 hour. At the Nordic Elbas Intra-Day market, there is also a continuous market with 24/7 trading until 1 hour before the delivery of the schedule starts. Nevertheless, this is much faster as the system e.g. in Spain (Fig. 7-1), where several hours are between gate closure and schedule start also in the Intra-Day market. Therefore, the floor is open in both Germany and Sweden for any short-term update cycling weather prediction schemes currently being developed at the meteorological centres.

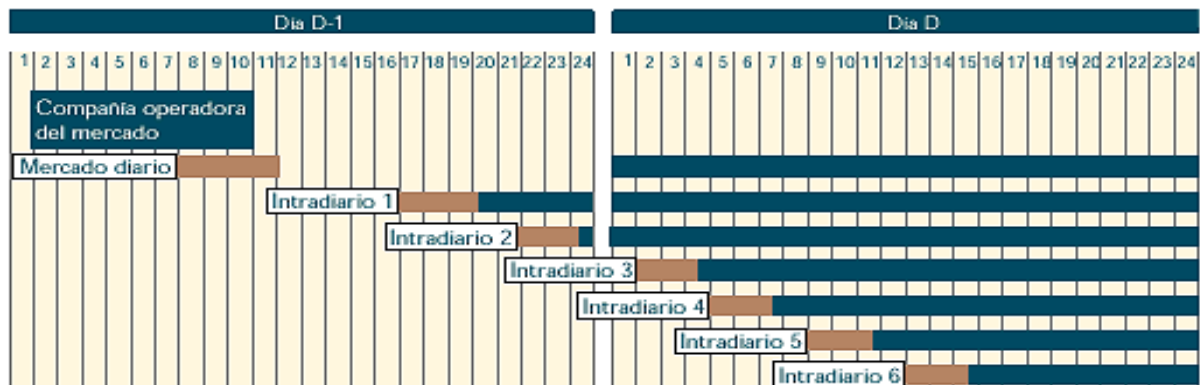


Fig. 7-1: Intra-Day example from Spain as a case with non-continuous trading and several hours lag (marked in brown) between gate closure and schedule (marked in blue)

It has to be noted, that the amount of power traded in the Intra-Day at EPEX-Spot is currently much lower than in the Day-Ahead. This is a sign that the Intra-Day is currently a less used option, resulting also in difficulties for market participants to find appropriate trading partners. It is expected that this will change in future with larger shares of renewables and probably rising costs for reserve power, but for the moment it should be kept in mind when developing business strategies for hybrid systems.

Finally, there is a market for reserve power being operated by the TSOs, resulting in 'penalty' prices for short and long positions (under- and overestimations) in power production for each producer. These prices reflect the actual costs of reserve power being necessary after the Day-Ahead and Intra-Day market activities of each producer and spot market participant. They are only known with several months delay (e.g. 3 months in Germany) and depend on the overall behavior of all market participants.

7.1.1.2 User requirements

7.1.1.2.1 Temporal requirements

Temporal duration:

At least 1 year of data in order to allow stable numerical conditions, 3 months Oct-Dec + 1 year months is even better to allow spin-up times in modeling.

Temporal resolution:

15 minute interval for system modelling

60 minute interval for modeling including trading processes

Forecast horizon:

48 hours for day-ahead markets

Shorter periods for intra-day markets, but gate closure times have to be respected.

Update frequency:

Once daily, 00 or 06 UTC forecast runs are appropriate for nowadays electricity markets.

Continuous trading might require further updates, but this is not urgently needed nowadays.

Interval definition:

In meteorological data, an hourly 15:00 UTC value consists of an averaging or summation of 14:00:01 to 15:00:00 UTC values. In the market model the 15:00 UTC value consist of the 15:00:00 to 15:14:59 UTC values. This shift will be taken into account in the TUW-EEG modeling.

Time definition:

UTC is used for all time stamps.

7.1.1.2.2 Spatial information:

Spatial resolution:

One forecast time series per test area in Ulm

Wind speed and direction at location of wind energy installation in Skellefteå.

Temperature in 2m height at location of small hydro power plant in Skellefteå.

Spatially resolved forecasts inside the test areas could be used to assess the optimum spatial resolution in a typical utility's area size.

7.1.1.2.3 Parameters needed

Wind speed and direction in 10 m height for Skellefteå

Wind speed and direction in 50m height for Skellefteå

Temperature in 2 m for Skellefteå

Global irradiation for Skellefteå and Ulm

Cloud cover is not used separately, only via the global irradiation.

The same is valid for aerosols and other atmospheric extinction – they are required but as input to the global irradiation calculation and not as separate input to the economic modeling at TUW-EEG.

7.1.1.2.4 Quality information

First priority is the correct representation of all forecasted values in a year, while for the economic modeling an individual forecast can be accepted even if it is wrong in its individual hourly values.

Only all conditions over the whole modeling period should be representative in order to avoid systematic errors.

The quality measure is the root mean square error (RMSE). RMSE as function of time of year (monthly) or time of day (hourly) is appreciated.

Confidence intervals are appreciated. Expected value and a P90 interval are useful.

Tab 7-1: Overview over the requirements for case development

	Temperature 2m	Wind speed + direction 10m	Wind speed + direction 50m	Global Irradiation (GHI)
Period	15 months (Oct – Dec)	15 months	15 months	15 months
Forecast duration	48 h, update daily (00 or 06 UTC)	48 h, update daily (00 or 06 UTC)	48 h, update daily (00 or 06 UTC)	48 h, update daily (00 or 06 UTC)
Temp. res.	15min (system) + 1h (trading processes)			
Location	Skell., at small hydro power plant	Skell., at wind energy installation	Skell., at wind energy installation	Skell. + Ulm
Spatial res.		-	-	Ulm: 1 time series per test area + smaller for optimum spatial assessment
Quality measure	RMSE	RMSE	RMSE	RMSE

7.1.1.3 Demo site

This application is of interest for both the Skellefteå and the Ulm demo site.

7.1.1.4 Relevant use cases and control problems

Use cases: all

Control setups: 1 ('Cooperative green supplier'), 2 ('Carbon-free heating'), and 3 ('Green community')

TUW-EEG will quantify the economic advantages of using meteorological forecasts in their use cases. In a first step the meteorological forecast will be treated as the ideal and perfectly correct forecast ('perfect foresight'). This allows the quantification of the maximum value of the use of meteorological information in hybrid energy systems.

In reality, each forecast has an error. In a second step, a typical RMSE-based error will be applied and a disturbed 'perfect foresight' will be created. So, the meteorological forecast values will be changed randomly with the typical RMSE as constraint. Several typical RMSE values for different data sources will be applied. This allows the quantification of the economic value of a meteorological forecast depending on its RMSE characteristics.

The use of meteorological information in continuous trading schemes will be only assessed with a low priority as this is a concept only for future markets with increased trade volume in intra-day markets.

7.1.2 State of the art

There is only very restricted systematic knowledge on the use of real weather forecasts in business model development for smart grids and hybrid energy grids.

Within the two stakeholders SKR and SWU, there is no ongoing practice.

7.2 Work performed

In this section we review the operationally and experimentally available meteorological forecasts from meteorological centers with respect to the user requirements as stated in chapter 7.1.1.2.

Thereby only the ensemble forecasts of ECMWF, DWD and SMHI are described. For an overview over deterministic weather models see chapter 6.2.

7.2.1 Ensemble data

An ensemble forecast is the combination of several runs of deterministic forecast models with variations in the initial and boundary conditions and model physics. For example, the COSMO-DE-EPS ensemble forecast of the DWD uses four different models to gain 20 forecast runs of the same scene (for details see chapter 7.3.4). Due to the model combination it is possible to eliminate outliers.

Probabilistic products can be derived from ensemble forecasts. Typical products that are used to provide a comprehensive description of the forecast statistic are the ensemble mean and variability, exceedance probability based on a defined threshold.

The general advantage of ensemble forecasts is shown in Figure 7.2: a schematic diagram of 36-h ensemble forecasts used to estimate the probability of precipitation over the UK. “A single forecast (red frame, centre) is generated by integrating the model forward in time from the analysis of initial atmospheric state (left). Small perturbations to the analysis, within known analysis uncertainty, provide an ensemble of forecast solutions, which sample the forecast uncertainty (multiple frames). These solutions are combined, including some spatial neighbourhood sampling, to provide a smooth estimate of probability of precipitation” (Bauer et al., 2015).

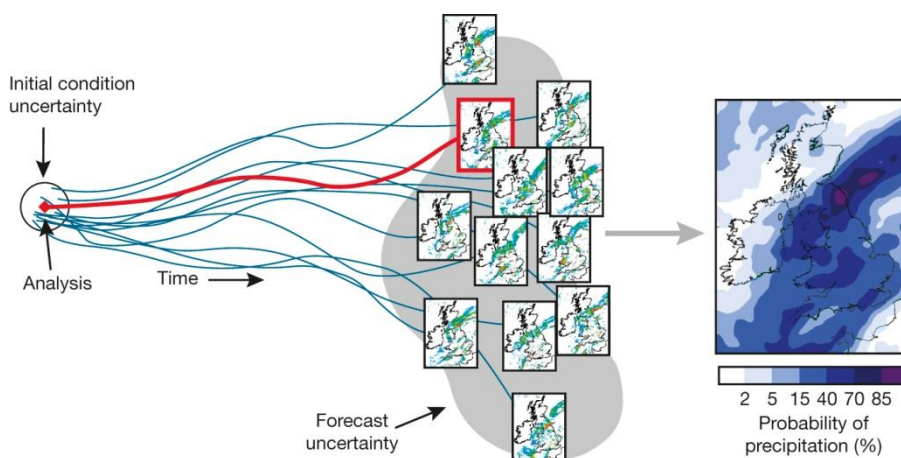


Fig. 7-2: Schematic diagram of 36-h ensemble forecasts used to estimate the probability of precipitation over the UK

Fig. 7-3 gives an example for the variation of forecast members for one forecast step. The shown region is South-Germany/Alpes around Ulm (46.3-50.3°N, 7.0-13.0°E). While the coarse structure of the parameter GHI is the same for all 20 ensemble members (here used: DWD ensemble COSMO-DE-EPS), small deviations in the forecasts can be detected. For example: the members 16-20 show a lower maximum value, the bow of the Alps is less intense yellow than for the other members. Also the fine structure at $\sim 47.6-49^{\circ}\text{N}$, 8°E is slightly varying from member to member.

Please note the rather small differences between the different members. This is discussed in section 7.2.1.2. It is a common feature found for solar irradiance ensemble forecasts both in COSMO-DE and ECMWF and needs to be treated before using ensemble forecasts.

This variation is usually used to calculate a mean value from all members (Fig. 7-4, left) and to estimate an uncertainty from the corresponding standard deviation. For the given example it is clearly visible that the variability and therefore the uncertainty of the forecast is the strongest (yellow in Fig. 7-4, right) in the Alps. This is probably due to the complexity of modeling within the mountainous terrain.

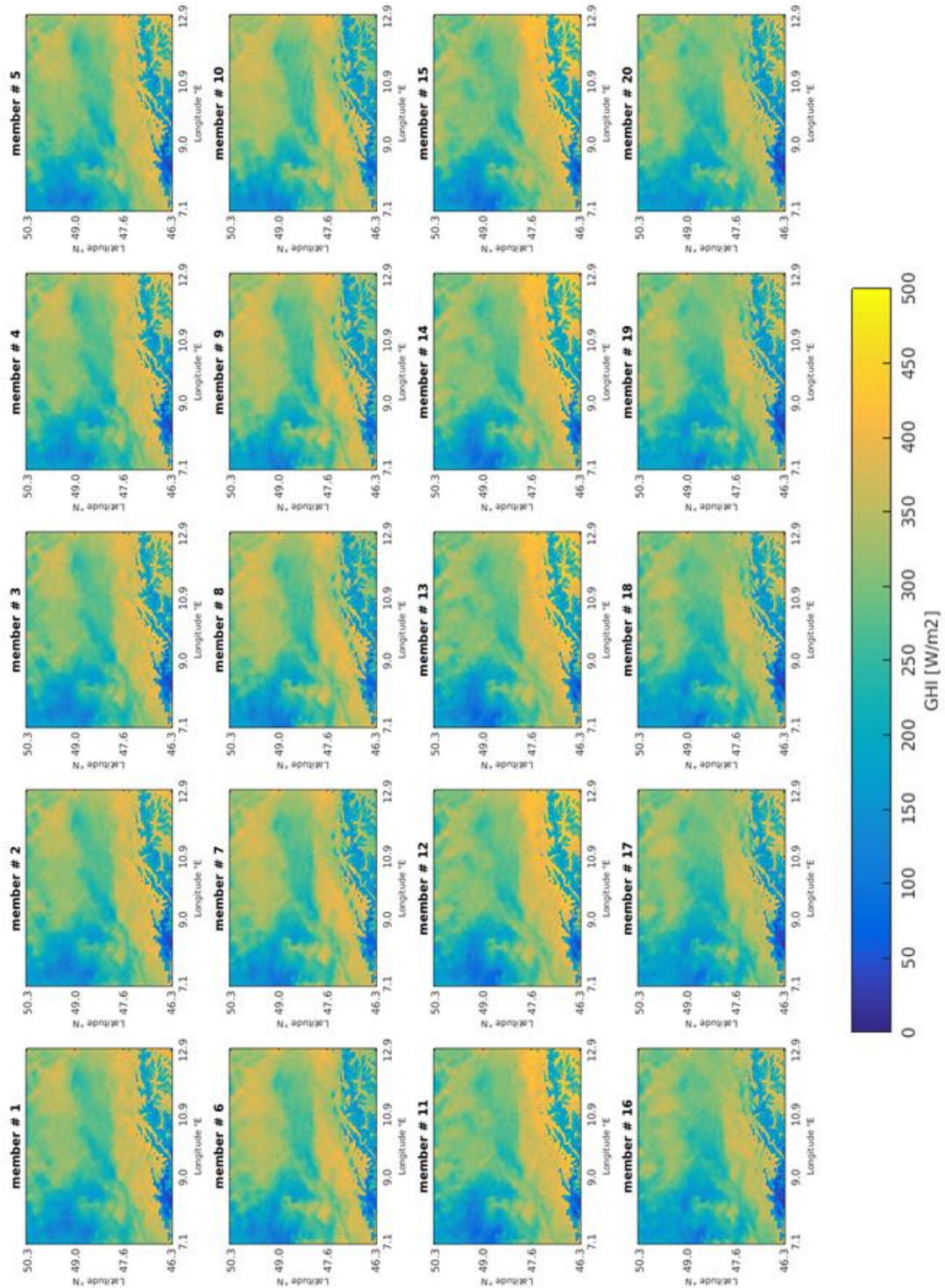


Fig. 7-3: Example of COSMO-DE-EPS: GHI for all members in the area around Ulm (46.3-50.3°N, 7.0-13.0°E) for the 3rd May 2013, forecast step 11 (= 14 UTC).

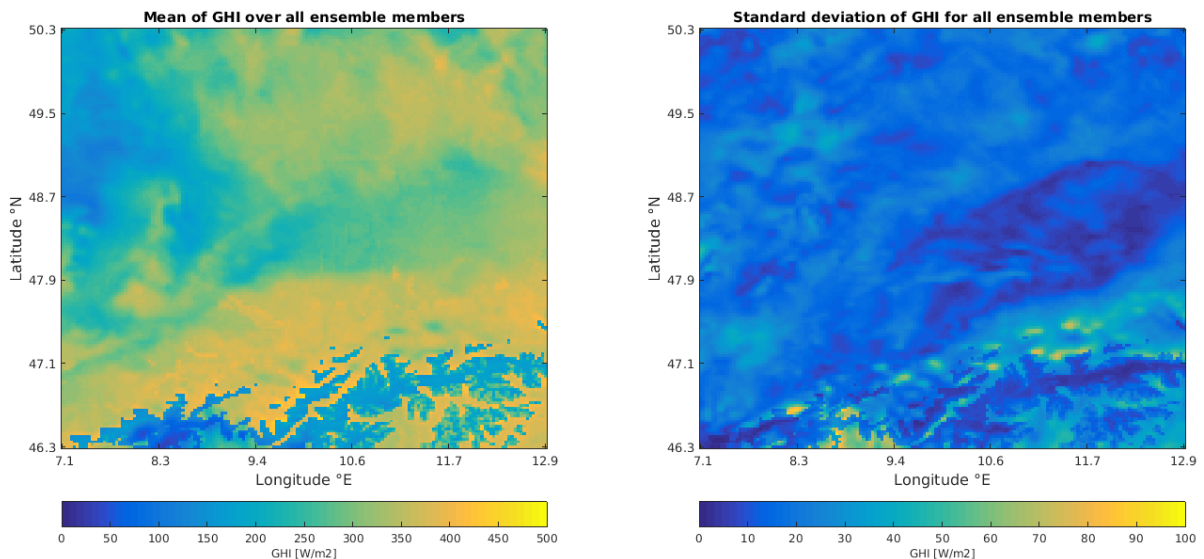


Fig. 7-4: Example of COSMO-DE-EPS: mean and standard deviation of GHI in the area around Ulm (- °N, - °E) for the 3rd May 2013, forecast step 11 (= 14 UTC).

7.2.1.1 Rank Histogram

A tool to estimate the reliability of an ensemble forecast at a given measurement site is the so called Rank histogram (also called Talagrand diagram, described e.g. in Candille et Talagrand, 2005).

The Rank histogram is used to analyze if an observation usually falls with respect to the ensemble forecast data. In an ensemble with perfect spread, each member represents an equally likely scenario, so the observation is equally likely to fall between any two members. The analysis is performed for a large dataset (e.g. one year of forecast and observation data). The form of the histogram gives information about the spread of ensemble: if the rank histogram is flat as seen in Fig. 7-5, the ensemble spread is suitable to represent the forecast uncertainty. An asymmetric shape points to a bias of the ensemble while a “U-shape” means that the ensemble spreads too small, many observations are falling outside the extremes of the ensemble.

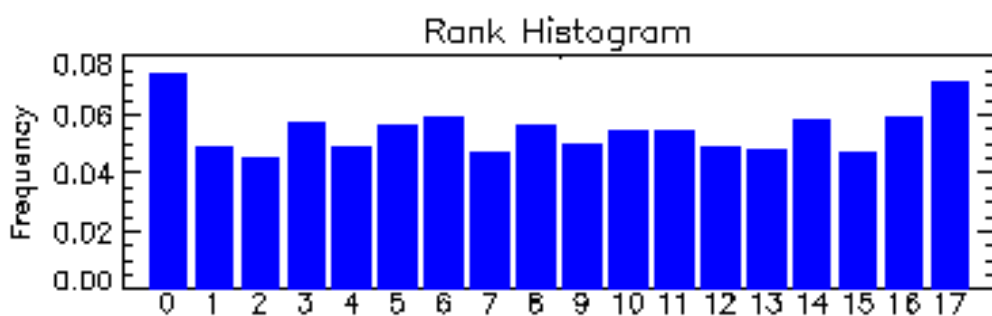


Fig. 7-5: Example for a Rank Histogram. (source www.cawcr.gov.au/projects/verification/verif_web_page.html)

Note: A flat rank histogram does not necessarily indicate a good forecast, it only measures whether the observed probability distribution is well represented by the ensemble.

7.2.1.2 Calibration

It happens that the ensemble forecasts and the observations at a given measurement site do not match very well. This can happen because of biases due to single member anomalies, ensemble members being too similar to each other or too smooth results.

Especially, global irradiances in COSMO-DE (as well as in ECMWF being discussed below) have been found to be modelled too smooth. The differences between the different members is too small, the ensemble is called under-dispersive. Such results have been shown at EWELine meetings and are under review for publication at the moment.

Fig. 7-6 illustrates the under-dispersiveness: all members of an ensemble forecast (grey lines) have very similar values, the observation (red line) is outside the spread of the ensemble. While the ensemble does describe the diurnal gradient of the radiation well, the absolute values are clearly wrong.

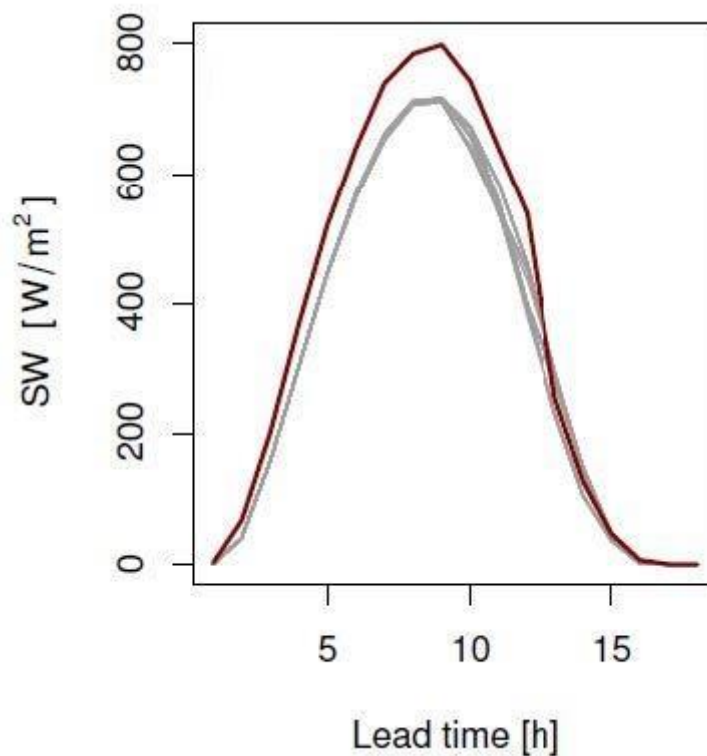


Fig. 7-6: Comparison of observation (red line) with ensemble forecast (grey lines). (Source: Bouallègue, 2015)

To correct ensemble data, it is possible to perform calibrations. There exist several methods like the Quantile Regression (QR) or the Penalized quantile regression in probability space (PQRPS). In Fig. 7-7 the QR method is performed for an ensemble forecast which overestimates the radiation for most of the day. By using the QR method, the spread of the ensemble is strongly enlarged. The corresponding Rank histograms (Fig. 7-8) affirm the improvement: while the U-shape of the uncalibrated data (left) identifies a too small spread, the Rank histogram of the calibrated data (right) shows a flat distribution.

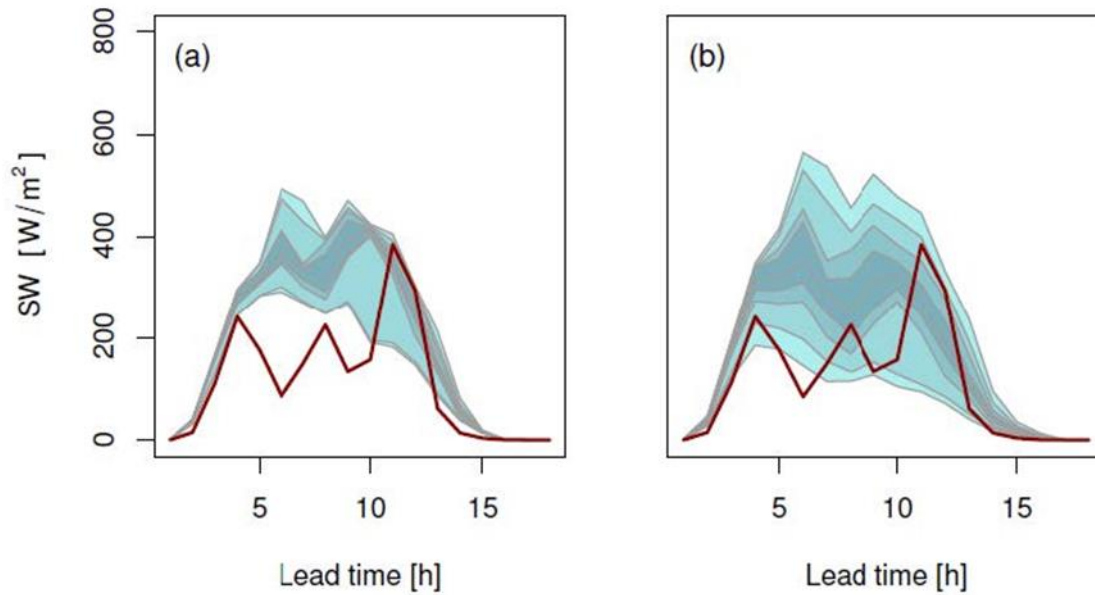


Fig. 7-7: Comparison of observation (red line) with ensemble forecast before (a) and after (b) calibration using quantile regression. Blue shades are the percentiles of the ensemble (Source: Bouallègue, 2015)

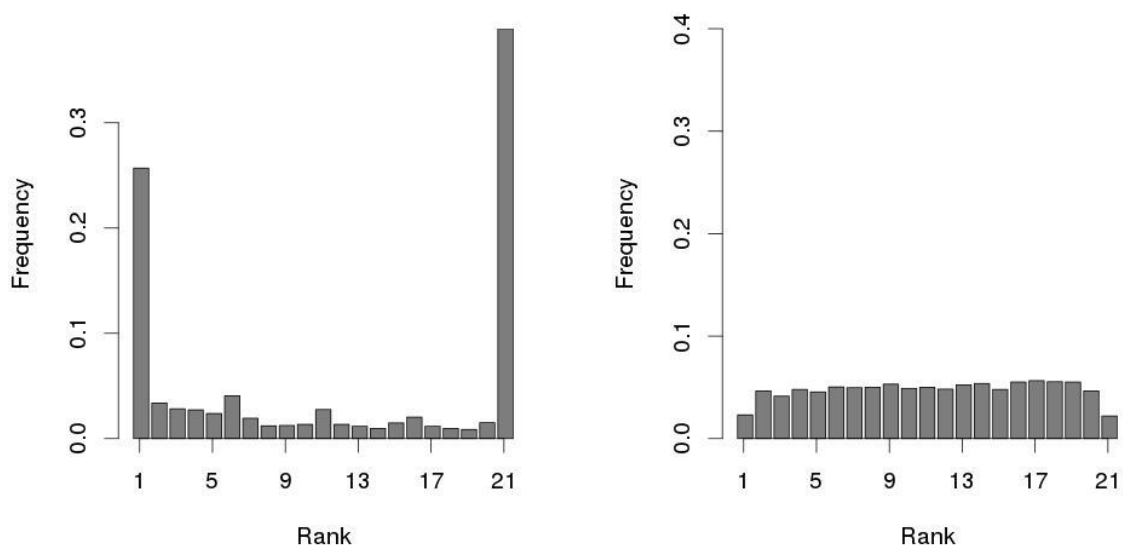


Fig. 7-8: Rank histograms to the data of Fig. 7-7 (Source: Bouallègue, 2015)

7.2.2 ECMWF Ensemble data

7.2.2.1 ECMWF's operational products

Besides the standard deterministic forecast (as described in section 6.2.1), a probabilistic ensemble model is also part of ECMWF's integrated forecast system. The ECMWF forecast ensemble (ENS) has been established in 1992 (Palmer et al., 1992), and since then has been continuously improved. Nowadays, it contains the standard deterministic forecast as control run, and a set of 50 perturbed members. The member selection process is a three steps scheme, containing perturbations of the

initial analysis, perturbations of the assimilation data set and perturbations of the physical parametrization schemes (ECMWF, 2013b).

The forecast containing the control run and each of the 50 perturbed members, is delivered every 12 hours with a spatial and temporal resolution depending on the forecast horizon (ECMWF, 2014). Following the forecast horizon of 48h as it is indicated in the user requirements in chapter 7.1.1.2, a spatial resolution of 0.25° x 0.25° in latitude and longitude is available for the whole globe. The corresponding temporal resolution is 1 hours. The starting times of the forecast are 00 UTC and 12 UTC every day. Among many other meteorological parameters, the forecast contains 2m temperatures, 10m and 100m wind speed and direction, and global irradiance. Pre-calculated ensemble means, ensemble standard variations and probabilities are also provided, but the parameters listed in chapter 7.1.1.2 are either not provided or only provided on model levels. Therefore, possibly needed statistics of these parameters have to be calculated by the users themselves. An overview about the complete set of parameters can be found here:

<http://www.ecmwf.int/en/forecasts/datasets/set-iii#III-i>

7.2.2.2 Available data for OrPHEuS

As done for the deterministic data (see chapter 6.2.1.3) the DLR has downloaded the datasets for the years 2013 and 2014 for the regions Ulm, Demmin and Skellefteå.

Due to the licence agreement of the ECMWF the DLR it is not allowed to redistribute the data to the partners: The ensemble data can be retrieved in the same way as the deterministic data.

7.2.3 SMHI ensemble forecast

Several HIRLAM and ALADIN institutes (including SMHI) are developing in cooperation the ensemble forecast GLAMEPS (Grand Limited Area Model Ensemble Prediction System). It has 54 members in total and covers an area from -11.5 to 37.6 °N and -52.4 to 12.1°E.

Tab 7-2: Short overview of GLAMEPS ensemble forecasts

Model	Update frequency	Relevant output parameters due to chapter 6.1.1.2	Spatial resolution	Temporal resolution	Available period
GLAMEPSv1	Every 12 hours (6 and 18 UTC)	2m Temperature, 10m winds, 2m relative humidity, global irradiance, 54 members	12 km	3 hours , up to 54h horizon	Since October 2011

7.2.3.1 Available data for OrPHEuS

The GLAMEPS dataset is still in development and data can only be used for scientific purposes after a lengthy registration process. At the moment it is not possible or advisable to use the GLAMEPS ensemble operationally.

7.2.4 DWD ensemble forecast

The deterministic weather prediction model of the COSMO-DE was already described in section 6.2.3.

The 20 member ensemble prediction system (EPS) based on COSMO-DE has been developed at DWD and is running operationally since 2012 (Theis et al., 2014). The COSMO-DE-EPS is provided on the same 2.8 km grid as the deterministic forecast.

COSMO-DE-EPS is created by perturbations of initial and boundary conditions and model physics. Four different global weather prediction models (global model GME of Deutscher Wetterdienst, Integrated Forecasting System IFS as operated at the ECMWF, the Global Forecast System GFS of US's NCEP centre, and the Global Spectral Model GSM of the Japan Meteorological Agency) are used for a variation in initial and boundary conditions in the COSMO-DE model – providing a variation in the COSMO-DE model output as part of the COSMO-DE-EPS which provides variability already in the very first hours of the ensemble forecasts. Furthermore, model physics are disturbed with at focus on different soil moisture schemes, the shallow convection, cloud microphysics, boundary layer and turbulence parameterizations. An illustration of the ensemble member generation can be seen in Fig. 7-9.

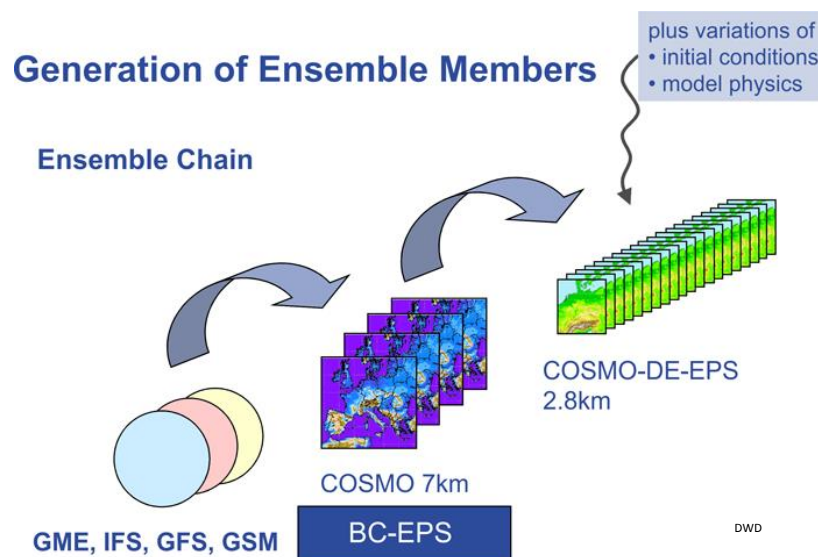


Fig. 7-9: COSMO-DE-EPS generation scheme

Probabilistic products can be derived from EPS. Typical products that are used to provide a comprehensive description of the forecast statistic are the ensemble mean and variability, exceedance probability based on a defined threshold, quantiles and extreme scenarios. They are provided for all grid boxes as standard products.

Both, the COSMO-DE and the COSMO-DE-EPS provide forecasts for a multitude of meteorological parameters in hourly resolution, which is extended to 15 minutes for some parameters.

To illustrate the ensemble forecast for COSMO-DE-EPS Fig. 7-10-15 show the so called spaghetti plots, box plots and rank histograms for temperature at 2m and global irradiance, compared to ground measurements in Ulm.

In the spaghetti plots (Fig. 7-10 + 7-11) each member of the ensemble is plotted individually over the forecast horizon. For a better estimation of reliability, the hourly average of the ground measurement at HS Ulm is added (black line).

The chosen day (16th May 2013) shows an average agreement between measurement and ensemble data for the analyzed year 2013: the order of magnitude is correct, also the diurnal behavior is tolerably matching. But the spread of the ensemble is often not large enough to embed the observations. This is most notably at the first time steps of the forecast where a separation between the ensemble plots can't be easily seen.

The box plots (Fig. 7-12 + 7-13) illustrate the ensemble data with help of statistical values. On each box, the central mark is the median, the edges of the box are the 25th and 75th percentiles, the whiskers extend to the most extreme data points not considered outliers, and outliers are plotted individually. Here the small deviation of the ensembles in the first time steps can even be better observed. For the temperature, the difference between box maximum and minimum of the first five time steps are negligible. The forecast of the global irradiance spreads stronger: the 25th and 75th percentiles are farther apart. Note that there is no solar irradiance at nighttime, so the value and the spread of the ensembles tend to zero at night, while the temperature spread generally increases with forecast time.

The rank histograms (Fig. 7-14 + 7-15) are calculated from the datasets of COSMO-DE-EPS and the observation data from HS Ulm for the whole year of 2013. Shown is the ranking for temperature at 2m and global irradiance respectively at time step 10 which corresponds to 12 UTC. For the two parameters the shape of the histogram is similar: a U-shape which confirms the assumption from the Spaghetti plots, that the spread of the ensemble is too small and that most of the observations are outside the ensemble region. So while the COSMO-DE-EPS data has already the advantage to deterministic data to deliver a uncertainty for each forecast step, the partners are advised to use a calibration (as described in 2.2.1.2) individually for each observation site for a better uncertainty estimation.

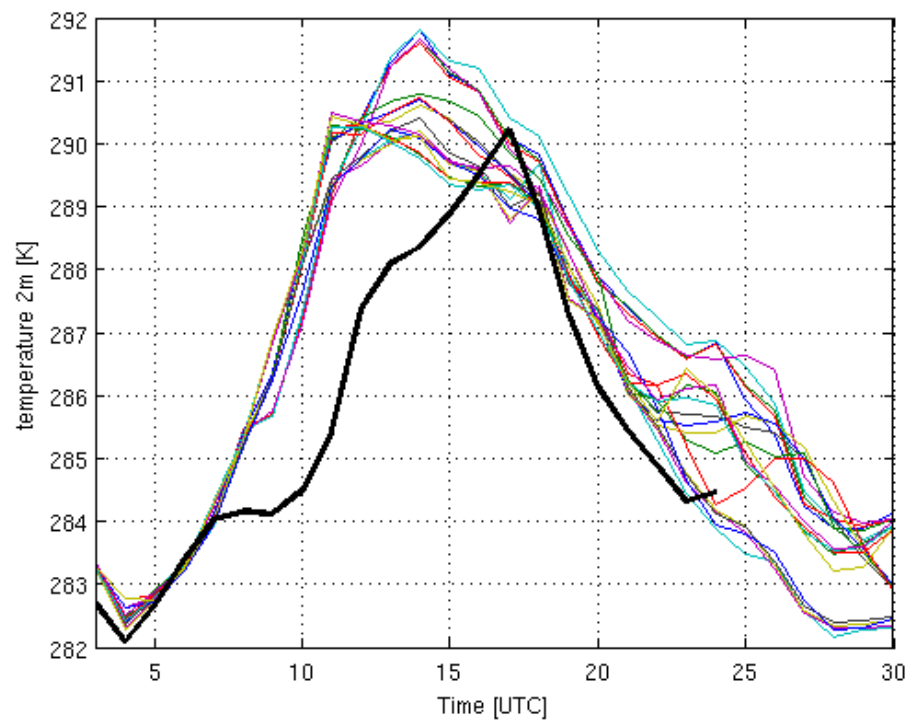


Fig. 7-10: Temperature forecast of all 20 ensemble members of COSMO-DE-EPS for Ulm area at 01.0116.05.2013 (run start 03 UTC + 21 27 h); black line: hourly average of ground measurement at HS Ulm.

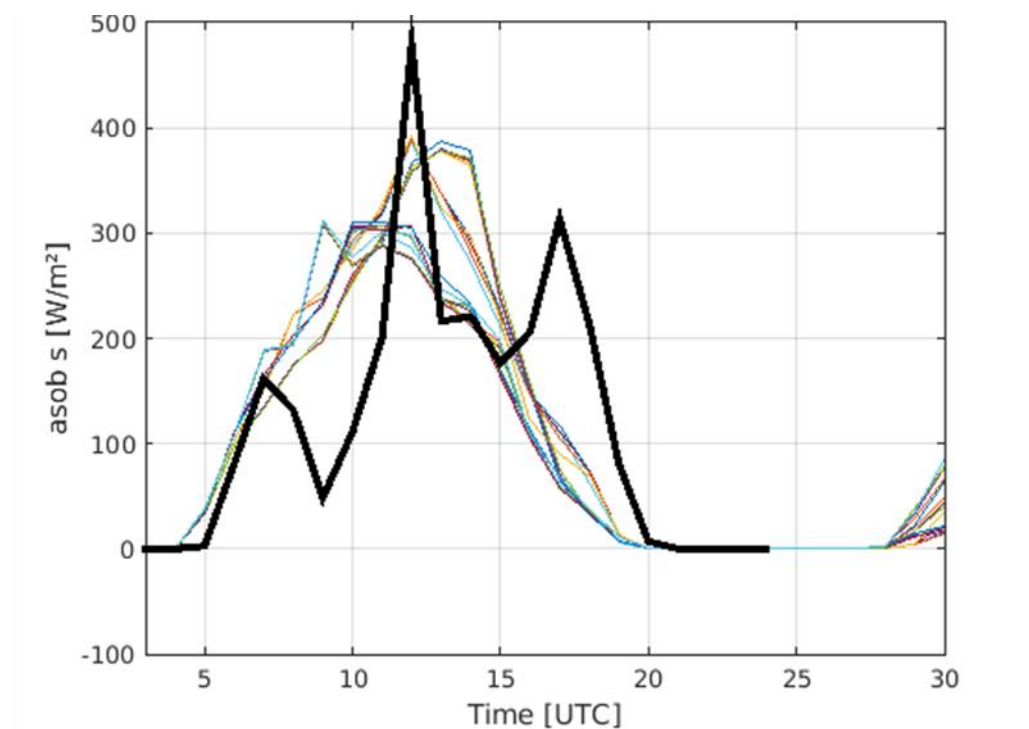


Fig. 7-11: Global irradiance forecast of all 20 ensemble members of COSMO-DE-EPS for Ulm area at 16.05.2013 (run start 03 UTC + 27 h); black line: hourly average of ground measurement at HS Ulm.

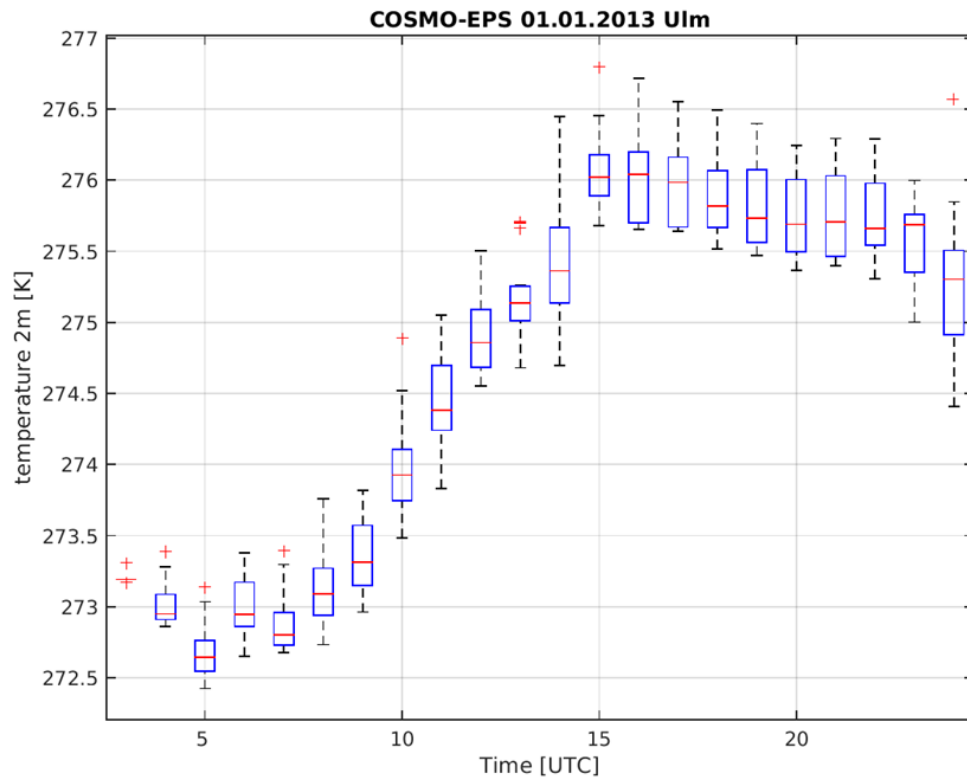


Fig. 7-12: COSMO-DE-EPS boxplot of ensemble forecast of temperature for Ulm area at 16.05.2013 (run start 03 UTC +27 h).

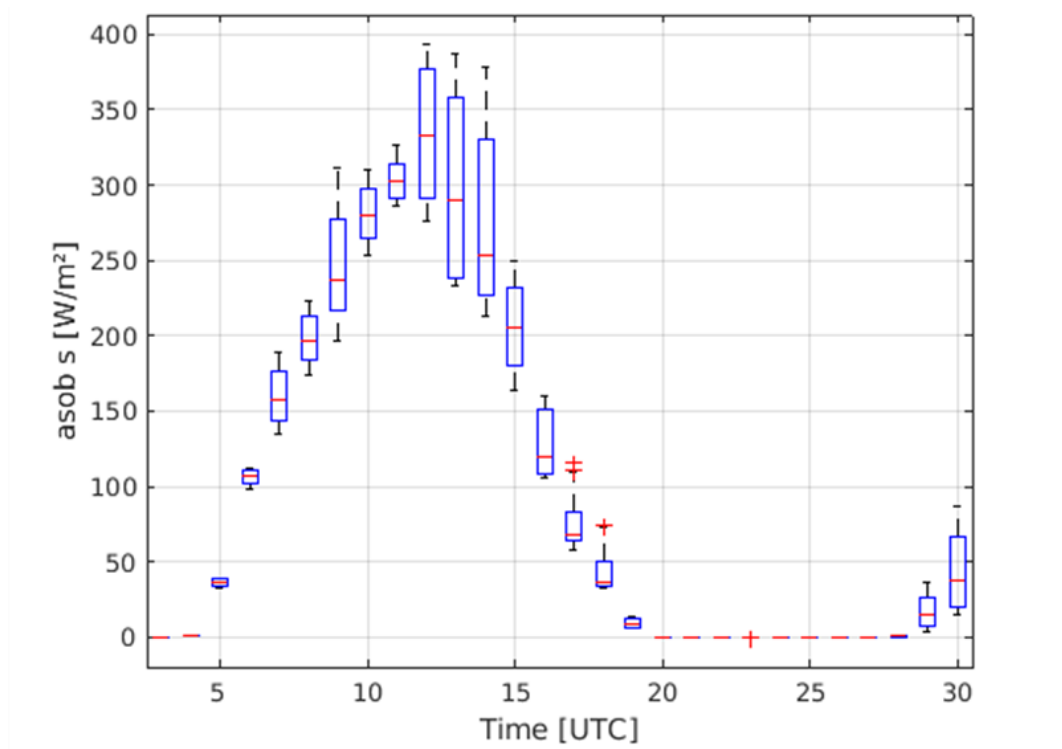


Fig. 7-13: COSMO-DE-EPS rank histogram of ensemble forecast of temperature for DEMMIN area at 01.01.2013 (run start 03 UTC +21 h).

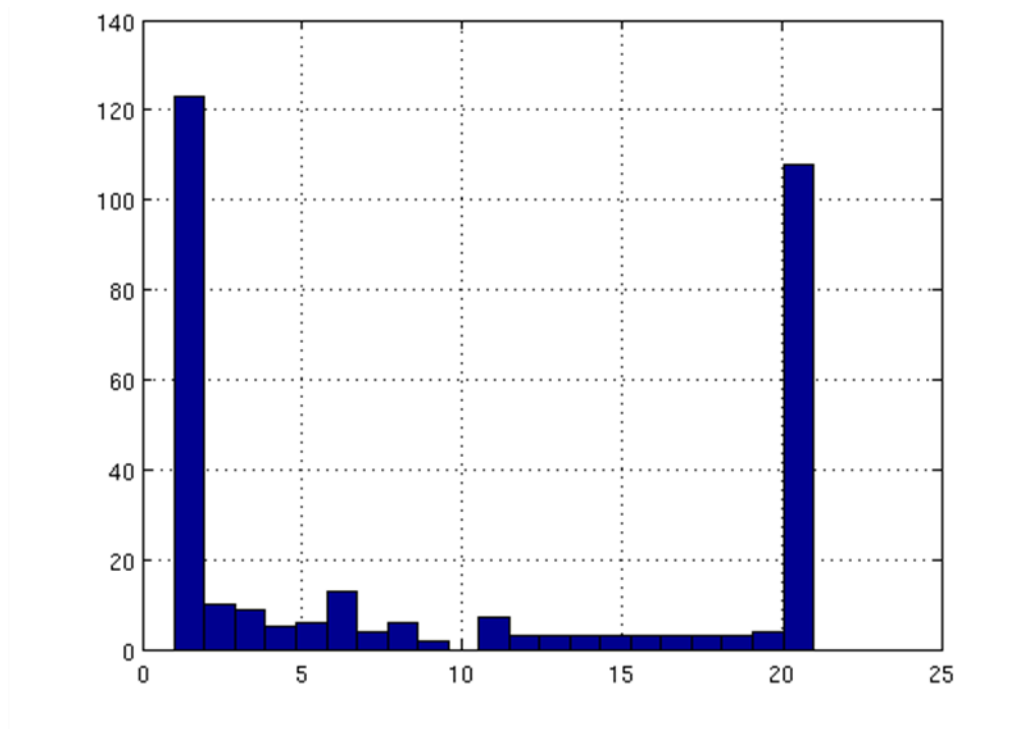


Fig. 7-14: Rank histogram of COSMO ensemble forecast at the HSU observation site for temperature at 2m at 12 UTC (10th time step of forecast, all data of 2013 were used).

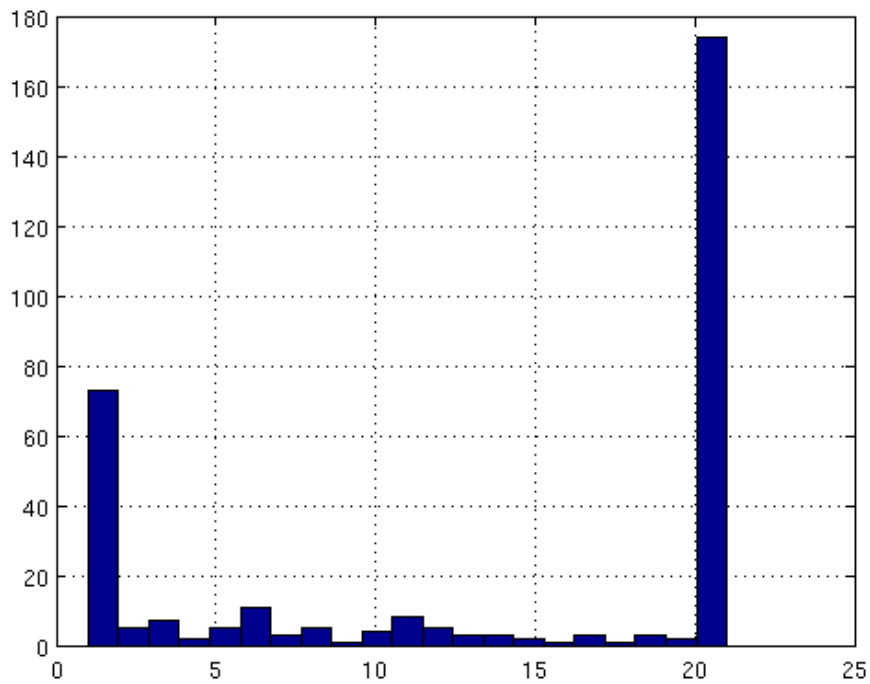


Fig. 7-15: Rank histogram of COSMO ensemble forecast at the HSU observation site for global irradiance at 12 UTC (10th time step of forecast, all data of 2013 were used).

7.2.4.1 Available data for OrPHEuS

The HSU has received from the DWD deterministic and ensemble data with the permission of distribution within the OrPHEuS partners. These data are for better usability analyzed and reprocessed by the DLR.

The ensemble data are available in GRIB format. Each time step and model are saved into a single file. A forecast run of 28 time steps and 20 models yields to 560 files of 24.5 MB. The size of the complete dataset from **1st January 2013 to 9th December 2013** is then approx. 4.3 TB. A dataset of this size needs special handling: The COSMO-DE-EPS is in a special GRIB-format, for which the DLR had to develop a conversion script using GRIB-API and Fortran. This script excerpts meteorological parameters for wished regions (Ulm and DEMMIN) and saves the data into netcdf-files. Thus the data access becomes faster and easier to handle. A detailed description is given in chap. 7.4.2.

7.3 Consultations COSMO-DE-EPS for HSU

The HS Ulm received COSMO-DE-EPS ensemble data from the DWD. The DLR was asked for help with the data as the correct interpretation of ensemble data is no simple task .

Due to some special settings of the headers within the data (GRIB format) it was neither for HS Ulm nor for DLR possible to open and to process the data with the GRIB standard tools (like cdo, nco, panoply).

7.3.1 Data characteristic to be considered

The DLR provided a script to read out the COSMO-DE-EPS-grib files and to save subsets of the data in netcdf format.

As the full dataset with all parameters and the whole COSMO-DE scene demands large storage capacities (more than 4.3 TB), the parameters and regions of interest had first to be extracted with a software script written by the DLR.

Several items had to be taken into account:

API toolbox

The data was only processable using the tool GRIB-API from ECMWF. This toolbox had to be embedded into Fortran code to take advantage of the full complexity of the tools.

Rotated coordinates

The COSMO-DE data are given in rotated coordinates for a better handling of the model. All fields are defined for a spherical grid with „north pole” at 40°N, 170°W. The coordinates of the scene are given in Tab. 4-1. To identify a region of interest within the COSMO-DE scene (e.g. the region around the test site Ulm) it is necessary to convert the rotated coordinates into geographical ones and vice versa.

Tab 7-3: Rotated and geographical coordinates of the corners of the COSMO-DE scene

	Rotated longitude	Rotated latitude	Geographical longitude	Geographical latitude
left upper corner	05.00° W	05.00° S	02.98 °E	44.77° N
right upper corner	05.50° E	05.00° S	17.72 °E	44.72° N
left lower corner	05.00° W	06.50° N	01.04 °E	56.20° N
right lower corner	05.50° E	06.50° N	19.84 °E	56.14° N

Wind components

The wind components (u: zonal and v: meridional) have to be treated with special care:

- They refer to the rotated coordination system, so they have to be rotated into geographical coordinates.
- Also the wind components are given in three different vertical systems: at certain pressure levels, at certain height levels and at 10 m above ground. While the wind components at 10 m and at the pressure levels are already given for the mass grid points, u and v for the height levels are given half a mesh size displaced and need to be interpolated toward the mass grid points.

7.3.2 Content COSMO-DE-EPS subset data

For a better treatment of the large dataset the COSMO-DE-EPS data were splitted into “classical” meteorological parameters (e.g. wind components, temperature, relative humidity) and into “solar” parameters (e.g. net short-wave radiation at surface, albedo, total cloud cover, ...). For a further data reduction only the regions around Ulm and around the DLR test site Demmin are extracted. Thereby is the region extend varies: for the classical meteorological parameters which are given for several height levels only a region of ± 11 pixel ($\cong 64.4$ km x 64.4 km) is saved while the solar information can cover a larger area of $\pm 2^\circ$ ($\cong 450$ km x 450 km) without increasing the data size too much.

Furthermore two additional netcdfs are saved in which the classical / solar data are given only for one pixel of interest.

The contents of the “meteo” and “solar” data listed in table 7-4 and 7-5 respectively.

Tab 7-4: Parameters within COSMO-DE-EPS subset “meteo”

Table of meteo-netcdf			
Shortname	Description	Height level	Unit
dewpoint_temperature_2m	dewpoint temperature	2 m agl	K
geopotential_pl1	geopotential for pressure levels	500, 700, 850, 950, 1000 hPa	m ² /s ²
pressure_hl2	pressure for height levels	500.0, 392.5, 217.9, 150.0, 94.6, 51.4 m agl	Pa
pressure_msl	pressure reduced to MSL	mean sea level	Pa
pressure_surf	pressure at surface	surface	Pa
q_hl2	specific humidity for height levels	500.0, 392.5, 217.9, 150.0, 94.6, 51.4 m agl	kg/kg
relhumidity_2m	relative humidity at 2 m	2 m agl	%
relhumidity_pl1	relative humidity for pressure	500, 700, 850, 950, 1000	%

	levels	hPa	
roughness_surf	surface roughness	surface	m
temperature_2m	temperature at 2 m	2 m agl	K
temperature_hl2	temperature for height levels	500.0, 392.5, 217.9, 150.0, 94.6, 51.4 m agl	K
temperature_of_ground	temperature of ground	surface	K
temperature_pl1	temperature for pressure levels	500, 700, 850, 950, 1000 hPa	K
tmax_2m	maximum temperature at 2m	2 m agl	K
tmin_2m	minimum temperature at 2m	2 m agl	K
u_hl1	u-component (zonal) of wind for height levels	500.0, 392.5, 298.6, 217.9, 150.0, 94.6, 51.4, 20.0, 10.0 m agl	m/s
u_pl1	u-component (zonal) of wind for pressure levels	500, 700, 850, 950, 1000 hPa	m/s
v_hl1	v-component (meridional) of wind for height levels	500.0, 392.5, 298.6, 217.9, 150.0, 94.6, 51.4, 20.0, 10.0 m agl	m/s
v_pl1	v-component (meridional) of wind for pressure levels	500, 700 850, 950, 1000 hPa	m/s
vmax_10m	maximum wind velocity at 10 m	10 m agl	m/s
w_pl2	vertical velocity	500, 700, 850, 950, 975, 1000 hPa	m/s

Tab 7-5: Parameters within COSMO-DE-EPS subset "solar"

Table for solar netcdf			
Shortname	Description	Height level	Unit
alb_rad	albedo	surface	%
clct	total cloud cover	surface	%
clcl	low cloud cover (800 hPa - surface)		%
clcm	medium cloud cover (400 - 800 hPa)		%
clch	high cloud cover (0 - 400 hPa)		%
hbase_sc	cloud base above msl, shallow convection		m
htop_sc	cloud top above msl, shallow convection		m
asob_s	Net short-wave radiation (surface)		W/m ²
athb_s	Net long-wave radiation (surface)		W/m ²

8 Conclusions

Several application areas for meteorological information have been discussed with stakeholders.

When discussing with demo site – related project partners, the focus has been laid on understanding daily life issues as typical problems occurring in today's practices. This project phase was dominated by providing a recommendation how to use additional meteorological information to solve them.

Overall, this work resulted in 6 application areas where we focused on the following activities

- Joint method development for irradiance to voltage modeling for Ulm – with a focus on grid monitoring and planning in highest priority and nowcasting in second priority
- Making meteorological satellite processing schemes available for Ulm
- Providing spatial and temporal variable information in DEMMIN
- Understanding numerical weather prediction quality, but also its typical failure cases in Skellefteå – this includes especially the treatment of ground observations not fulfilling measurement standards in the meteorological sector
- Assessment of nowadays used local meteorological measurements at the demo sites with respect to their usability for the purpose of hybrid grid control, this includes their spatial representativity
- Selection of meteorological forecasts for technical and economic modeling, this includes the handling of forecasts being not exactly provided as wished for or the handling of probabilistic forecasts to allow additional information levels in the modeling

The following findings can be summarized:

- Based in close collaboration with HS Ulm, HS Ulm has now a system being capable to calculate voltage flows at the transformer level based on satellite-based observations or numerical weather predictions.
- The intended use of an existing nowcasting scheme for direct irradiances turned out to be not successful for the Ulm region.
- Variability of clouds and radiation within the DEMMIN region has been quantified. New stations have been implemented at DEMMIN. The DEMMIN facility is now better characterized with respect to the assessment of irradiance structures.
- ECMWF and SMHI based numerical weather prediction of air temperatures in Skellefteå has been evaluated. Strongest error cases have been analysed separately.
- The existing measurement stations in Skellefteå have been evaluated and their pro's and con's have been described.
- The assumed dependence of heat to grid demand vs radiation as control parameter has been investigated and not found in a strong way as assumed by SKR at the beginning of the project.
- A north/south contrast in air temperatures based on different irradiance conditions as supposed to exist due to the Skellefteå orography could not be confirmed in the measurements.
- A number of NWP forecast datasets have been obtained from ECWMF, SMHI and DWD. How-to descriptions are provided for those datasets, where DLR is not allowed to distribute the

data due to the data policy. Characteristics of various NWP schemes – including ensemble predictions – have been described.

- Support to partners has been given to identify meteorological data for the scenario definition in the technical modeling in WP5.

9 Bibliography

Baldauf, M., Seifert, A., Förstner, J., Majewski, D., Raschendorfer, M. and Reinhardt, T. (2011): Operational convective-scale numerical weather prediction with the COSMO model. *Monthly Weather Review* 139, 3887–3905. doi:10.1175/MWR-D-10-05013.1.

Bauer, P., Thorpe, A., Brunet, G., The quiet revolution of numerical weather prediction, *Nature*, 525, 47-55, 2015

Borg, E., Lippert, K., Zabel, E., Löpmeier, F.J., Fichtelmann, B., Jahncke, D., Maass, H. (2009): DEMMIN – Teststandort zur Kalibrierung und Validierung von Fernerkundungsmissionen.- In: 15 Jahre Studiengang Vermessungswesen – Geodätisches Fachforum und Festakt, Neubrandenburg, Eigenverlag (Hrsg.: Rebenstorf, R.W.).- 16.-17.01.2009.- S. 401-419.

Borg, E., Schiller, C., Daedelow, H., Fichtelmann, B., Jahncke, D., Renke, F., Tamm, H-P., Asche, H. (2014): Automated Generation of Value-Added Products for the Validation of Remote Sensing Information Based on In-Situ Data.- (Eds.: Murgante, B. et al.).- ICCSA 2014, Guimarães, Portugal, June 30 - July 3, 2014, Proc. Part I. Vol. 8579 of LNCS (. ISBN: 978-3-642-39642-7), Springer.- 393-407.

Bouallègue, Z.B., Calibration of short-range global radiation ensemble forecasts, ICEM 2015, 2015; http://icem2015.org/wp-content/uploads/2015/07/1150_BenBouallegue.pdf

Breitkreuz, H., Solare Strahlungsvorhersagen für energiewirtschaftliche Anwendungen – Der Einfluss von Aerosolen auf das solare Strahlungsangebot in Europa, DLR Forschungsbericht, 2008-24, 2008

Candille, G., Talagrand, O., Evaluation of probabilistic predicitions systems for a scalar variable, *Q.J.R. Meteorol. Soc.*, 131, pp. 2131-2150, 2005

Driesenaar, T., General Description of the HARMONIE model, <http://hirlam.org/index.php/hirlam-programme-53/general-model-description/mesoscale-harmonie>, 2009a

Driesenaar, T., About GLAMEPS, <http://www.hirlam.org/index.php/hirlam-programme-53/general-model-description/glameps>, 2009b

ECMWF, The ECMWF Re-Analysis (ERA) Project, *ECMWF Newsletter* 73, 1996

ECMWF, ERA-40: ECMWF 45-year reanalysis of the global atmosphere and surface conditions 1957-2002, *ECMWF Newsletter* 101, 2004

ECMWF, ERA-Interim for climate monitoring, *ECMWF Newsletter* 119, 2009a

ECMWF, IFS Documentation, Cy33r1, Part VI: physical processes, 2009b

ECMWF, Atmospheric model identification numbers, http://www.ecmwf.int/products/data/technical/model_id/index.html, 2013

Espinar, B., C. Hoyer-Klick, M. Lefevre, M. Schroedter-Homscheidt, L. Wald, User's Guide to the MACC RAD services on solar energy radiation resources, v3, July 2014, MACC-II project report D122.6, available on <http://www.gmes-atmosphere.eu>

Fouquart, Y., Bonnel, B., Computations of solar heating of the earth's atmosphere: a new parameterization, *Beitr. Phys. Atmosph.*, 53, 35-62, 1980.

Hoyer-Klick, C., Lefèvre, M., Oumbe, A., Schroedter-Homscheidt, M., Wald, L., User's Guide to the SODA and SOLEMI Services, MACC project report D_R-RAD_2.2._1 and _2, version v1.0, public report accessible via <http://www.gmes-atmosphere.eu>, 2010

Jung, Sandra, Variabilität der solaren Einstrahlung in 1-Minuten aufgelösten Strahlungszeitserien. Masterarbeit, Universität Augsburg, 2015

Klüser, L., Killius, N., Gesell, G., APOLLO_NG – a probabilistic interpretation of the APOLLO legacy for AVHRR heritage channels, *Atmos. Meas. Tech.*, 8, 4155-4170, 2015

Køltzow, M. A., Ivarsson, K., Agersten, S. Meuller, L., Bjørge, D., Vignes, O., Eriksen, B., Cahlgren, P., Ridal, M., Rudsar, R., Verification study: HARMONIE AROME compared with HIRLAM, UM and ECMWF, METCOOP MEMO No. 01, 2012,

Kriebel, K.T., R.W. Saunders and G. Gesell, 1989: Optical Properties of Clouds Derived from Fully Cloudy AVHRR Pixels. *Beiträge zur Physik der Atmosphäre*, Vol. 62, No. 3, pp. 165-171, August 1989

Kriebel, K. T., Gesell G., Kästner M., Mannstein H., The cloud analysis tool APOLLO: Improvements and Validation, *Int. J. Rem. Sens.*, 24, 2389-2408, 2003

Morcrette, J.-J., Radiation and Cloud Radiative Properties in the European Centre for Medium Range Weather Forecasts Forecasting System, *Journ. Geophys. Res.*, 96, D5, 9121-9132, 1991

Morcrette, J.-J., chapter on 'Radiation Transfer', Meteorological Training Course Lecture Series of ECMWF, 2002

Morcrette, J.-J., Modzynski, G., Leutbecher, M., A Reduced Radiation Grid for the ECMWF Integrated Forecasting System, *Mon. Weath. Rev.*, 136, 4760-4772, doi:10.1175/2008MWR2590.1, 2008a

Morcrette., J.-J., Barker, H.W., Cole, J.N.S., Iacono, M.J., Pincus, R., Impact of a New Radiation Package, McRad, in the ECMWF Integrated Forecasting System, 136, 4773-4798, doi:10.1175/2008MWR2363.1, 2008b

Morcrette, J.-J., Boucher, O., Jones, L., Salmond, D., Bechtold, P., Beljaars, A., Benedetti, A., Bonet, A., Kaiser, J. W., Razinger, M., Schulz, M., Serrar, S., Simmons, A. J., Sofiev, M., Suttie, M., Tompkins, A. M., Untch, A.: Aerosol analysis and forecast in the ECMWF Integrated Forecast System. Part I: Forward modelling, *J. Geophys. Res.*, 114, D06206, doi:10.1029/2008JD011235, 2009

Nielsen, H. A., Madsen, H., Predicting the heat consumption in district heating systems using meteorological forecasts, in: *Tech. Rep.*, DTU IMM, 2000

Nielsen, H. A., Madsen, H., Modelling the heat consumption in district heating systems using a grey-box approach, *Energy and Buildings* 38 (1) 63-71, 10.1016/j.enbuild.2005.05.002, 2006

Qu, Z., Oumbe, A., Blanc, P., Espinar, B., Gesell, G., Gschwind, B., Klüser, L., Lefèvre, M., Saboret, L., Schroedter-Homscheidt, M., and Wald L.: Fast radiative transfer parameterisation for assessing the surface solar irradiance: The Heliosat-4 method, *Meteorologische Zeitschrift*, submitted, 2016

Ruf, H., D. Funk, D. Stakic, K. Ditz, E. Neuchel, G. Heilscher, M. Schroedter-Homscheidt, F. Schnell, F. Meier, Validation of Metrics for the Comprehension of real-life data with virtual information, Deliverabel D3.4.2, OrPHEuS project

Ruf, H., M. Schroedter-Homscheidt, G. Heilscher, H.-G. Beyer, Quantifying Residential PV feed-in power in low voltage grids based on satellite-derived irradiance data, submitted to *Solar Energy*, 2015b

Schroedter-Homscheidt, M., Jung, S., Report on satellite-based nowcasting methods, chapter 1.3, Deliverable D3.6 in DNICast project, European Commission's 7th Framework Programme project, grant agreement 608623

Theis, S., Gebhardt, C., Ben Bouallègue, Z., Beschreibung des COSMO-DE-EPS und seiner Ausgabe in die Datenbanken des DWD, Version 2.0, 14. Mai 2014

Undén, P., Rontu, L., Järvinen, H., Lynch, P., Calvo, J., Cats, G., Cuxart, J., Eerola, K., Fortelius, C., Garcia-Moya, J. A., Jones, C., Lenderlink, G., McDonald, A., McGrath, R., Navascues, B., Nielsen, N. W., Ødegaard, V., Rodriguez, E., Rummukeinen, M., Rõõm, R., Sattler, K., Hansen Sass, B., Savijärvi, H., Wichers Schreur, B., Sigg, R., The, H., Tijn, A., HIRLAM-5 scientific documentation, http://hirlam.org/index.php/component/docman/doc_download/270-hirlam-scientific-documentation-december-2002?Itemid=70, 2002

Wey, E., M. Schroedter-Homscheidt, APOLLO Cloud Product Statistics. In: *SolarPACES 2013 International Conference*, 49, Seiten 2414-2421. Elsevier. *SolarPACES 2013 International Conference*, 17-20 Sept 2013, Las Vegas, USA. ISSN 1876-6102, 2014

WMO, Guide to meteorological instruments and methods of observation, WMO-NO. 8, ISBN 978-92-63-10008-5, 2008

Wojdyga, K., An influence of weather conditions on heat demand in district heating systems. *Energy and Buildings*, 40(11), 2009-2014, 2008

10 Disclaimer

The OrPHEuS project is co-funded by the European Commission under the 7th Framework Programme “Smart Cities” 2013.

The sole responsibility for the content of this publication lies with the authors. It does not necessarily reflect the opinion of the European Commission.

The European Commission is not responsible for any use that may be made of the information contained therein.

11 Contacts

Project coordinator

Ingrid Weiss & Silvia Caneva @ WIP – Renewable Energies

Sylvensteinstrasse 2, Munich, Germany

Email: Ingrid.weiss@wip-munich.de / Telephone: 0049 (0) 720 12 742

Email: silvia.caneva@wip-munich.de / Telephone: 0049 (0) 720 12 733

Task Leader

Marion Schroedter-Homscheidt @ DLR

Oberpfaffenhofen, 82234 Wessling, Germany

Email: Marion.Schroedter-Homscheidt@dlr.de / Telephone: +49(0) 8153 282896

